Journal of Advanced Ceramics
先进陶瓷
ISSN 2226-4108
CN 10-1154/TQ
清华大学出版社 Tsinghua University Press
SciOpen

J Adv Ceram 2026, **15**: 9221353

https://doi.org/10.26599/JAC.2026.9221353

Review

Rethinking brittleness in ceramics: The emergence of room-temperature plasticity

Zhitong Xu[1], Jie Zhang[1,*], Liran Dong[1,*], Yuanwei Chao[1], Guanghua Liu[2], Kexin Chen[1,3,*]

[1] *Advanced Structural Ceramics Innovation Center, YongJiang Laboratory, Ningbo 315202, China.*

[2] *State Key Laboratory of New Ceramic Materials, School of Materials Science and Engineering, Tsinghua University, Beijing 100084, China*

[3] *State Key Laboratory for Advanced Metals and Materials, University of Science and Technology Beijing, Beijing 100083, China.*

* Corresponding authors.

E-mail: J. Zhang, zjzj0517@gmail.com;
L. Dong, dongliran0602@gmail.com;
K. Chen, kxchen@ustb.edu.cn

Received: May 9, 2026; Revised: July 2, 2026; Accepted: July 19, 2026

Abstract

Ceramics are valued for their high strength, thermal stability, and chemical inertness, but their structural applications are limited by intrinsic room-temperature (RT) brittleness. The stress required for dislocation motion in strongly ionic/covalent ceramics often exceeds their fracture strength, leading to catastrophic failure before plastic deformation occurs. Overcoming this limitation remains a major challenge in materials science. Recent studies have shown that ceramics exhibit RT plasticity through mechanisms including dislocation, phase transformation, and grain boundary sliding (GBS). These findings challenge the conventional view of ceramics as purely brittle materials and suggest that plasticity can be achieved not only in microscale specimens but also in bulk and structurally engineered ceramic systems. Several strategies have been developed to promote RT plasticity. Defect engineering, the controlled introduction and activation of dislocations, is critical for regulating deformation behavior. Structural designs such as coherent interfaces, layered architectures, and amorphous–crystalline composites can reduce dislocation nucleation barriers and improve deformation compatibility. Nanocrystalline structuring and external field regulation further enhance plasticity by altering local stress distributions and diffusion pathways. *in situ* characterization and strain measurement techniques have enabled direct observation and accurate quantification of deformation processes, improving the understanding of the relationship between structure, defects, and mechanical response. Despite these advances, achieving reliable and scalable plasticity in bulk ceramics remains challenging. Future work should focus on intrinsical plastic ceramic systems, scalable fabrications, and integrated multiscale design strategies. These efforts may enable the development of ceramics with improved damage tolerance and deformability for advanced structural and functional applications.

Keywords: ceramics; room-temperature (RT) plasticity; deformation mechanism; structural design; mechanical properties; dislocation engineering.

1. Introduction

Ceramic materials are widely recognized for their outstanding combination of properties, including high hardness [1, 2], excellent wear resistance [3], superior thermal stability [4], and strong resistance to oxidation and corrosion [5, 6]. These characteristics make ceramics indispensable in demanding applications such as cutting tools [7], thermal barrier coatings [8, 9], electronic components [10], and high-temperature structural parts [11]. However, despite these advantages, the widespread structural application of ceramics is severely limited by their inherent brittleness at room temperature (RT), and the lack of macroscopic plastic deformation leads to catastrophic, sudden fracture with little or no prior warning, which significantly restricts their reliability in load-bearing applications [12].

The conventional understanding of ceramic deformation behavior is centered on the stark contrast between high-temperature plasticity and RT brittleness. At elevated temperatures, many ceramic materials can exhibit limited plastic deformation due to enhanced atomic diffusion and thermally activated intragranular mechanisms such as dislocation slip and climb, or intergranular mechanisms such as grain boundary sliding (GBS), and diffusional creep [13-16]. In contrast, at RT, ceramics typically behave as brittle solids, failing via crack propagation rather than plastic flow. A key reason for this behavior lies in the fundamental difficulty of dislocation activity in ceramics. The strong ionic and covalent bonding in ceramics, along with complex crystal structures, makes dislocation nucleation energetically unfavorable and dislocation glide highly restricted. The scarcity of independent slip systems further constrains plastic deformation, leading to a lack of plasticitiy at RT. Consequently, understanding and overcoming these limitations have become central topics in materials science.

From an application perspective, improving the plasticity of ceramics is of critical importance for advanced engineering fields. For example, components in aero-engines, hypersonic vehicles, and nuclear systems are required to maintain structural integrity under extreme conditions such as high temperature, high stresses, and corrosive environments. Enhancing ceramic plasticity could significantly improve their damage tolerance, reliability, and service life in these extreme applications. In recent years, significant progress has been made in addressing the intrinsic brittleness of ceramics, leading to several emerging breakthroughs in ceramic plasticity. One important direction is nanoscale plasticity, where reducing the grain size to the nanometer scale has been shown to activate new deformation mechanisms [17]. At this scale, grain boundary-mediated processes, grain rotation, and partial dislocation activity can contribute to enhanced deformability, allowing ceramics to exhibit measurable plastic strain even at low temperatures. Another notable development is the realization of meso-/macroscale RT plasticity in certain ceramic systems [18, 19]. Through careful control of microstructure, phase composition, and defect distribution, researchers have demonstrated that some ceramics can undergo significant plastic deformation at RT without catastrophic failure. This challenges the traditional view of ceramics as purely brittle materials and opens new avenues for structural applications. Furthermore, defect engineering and structural design have emerged as powerful strategies to tailor the mechanical behavior of ceramics. By introducing controlled defects such as vacancies, dislocations, and interfaces, or by designing hierarchical and composite structures, it is possible to enhance crack deflection, energy dissipation, and plastic deformation mechanisms. These approaches enable the design of ceramics with improved toughness and damage tolerance while retaining their intrinsic advantages.

Recent advances have significantly expanded the landscape of RT plasticity in ceramics. Beyond conventional small-scale deformation studies, bulk twisted-layer boron nitride ceramics have demonstrated high compressive deformability through the combined effects of interlayer sliding and three-dimensional interlocked nanoarchitectures [20]. Meanwhile, defect engineering has emerged as an effective route to activate plastic deformation by introducing dislocations, stacking faults, or twin boundaries before RT loading. Elevated-temperature preloading and mechanically seeded mobile dislocations have both been reported to reduce the barrier for dislocation-mediated deformation and suppress premature brittle fracture [19, 21]. In parallel, nanotwin n and crystalline-amorphous interface engineering have provided additional pathways for coordinating strength, flexibility, and energy dissipation [22, 23]. Recent machine-learning interatomic potentials further enable atomistic investigation of dislocation cores, slip barriers, and plastic deformation in ceramic systems [24]. Nevertheless, direct comparison among these studies requires caution because the reported behaviors span bulk ceramics, micro-scale pillars, coatings, nanofibers, and functional inorganic semiconductors. Therefore, scalable bulk processing, tensile ductility, cyclic stability, and service reliability remain critical challenges for the development of practically useful RT plastically deformable ceramics.

Despite the considerable progress achieved in understanding and improving ceramic plasticity, there still exist significant gaps in the systematic review and comprehensive understanding of this field. In particular, the underlying mechanisms governing plastic deformation in ceramics remain complex and not yet fully unified, especially when multiple deformation modes (e.g., dislocation activity, GBS, phase transformation, and diffusion-mediated processes) operate simultaneously under different length and time scales. A coherent summary of representative plastic ceramic systems is

also lacking, making it difficult to establish clear structure–property relationships and to compare different material design strategies across various ceramic classes.

Moreover, although numerous strategies have been proposed to achieve RT plasticity in ceramics, there is still no unified framework that systematically correlates these strategies with the resulting mechanical performance and underlying deformation mechanisms. At the same time, the development and application of mechanical testing techniques for evaluating plasticity in ceramics, have not been comprehensively summarized in the context of their capabilities, limitations, and applicability to different ceramic systems, such as *in situ* transmission electron microscopy (TEM) [25], nanoindentation [26], micro-pillar compression [27], and advanced synchrotron-based methods.

In addition, the potential engineering applications of plastic ceramics, particularly in extreme environments such as aerospace, energy systems, and protective structures, remain to be fully explored. Critical challenges, including scalability, reliability, and long-term stability under service conditions, still hinder their transition from laboratory research to real-world applications. Looking forward, future research directions in this field are expected to focus on the rational design of ceramics with tailored defect structures, the integration of multi-scale modeling with experimental validation, and the development of new characterization techniques to capture deformation processes in real time.

Therefore, the primary objective of this review is to provide a comprehensive and systematic overview of the plastic deformation mechanisms in ceramics, to summarize representative plastic ceramic systems, and to critically evaluate the strategies for achieving RT plasticity. Furthermore, this review aims to highlight the state-of-the-art mechanical testing techniques used to probe ceramic plasticity, and to discuss the current challenges, engineering prospects, and future research directions in this rapidly evolving field. By addressing these key aspects, this work seeks to fill the existing

knowledge gaps and provide a coherent framework to guide future research and development in plastic ceramics.

2. Basic theory of plasticity in ceramics

2.1 The nature of ceramic brittleness

In most ceramics, the Peierls stress required for dislocation nucleation and motion is exceptionally higher than the fracture stress due to their strong, directional ionic and/or covalent bonding within their rigidly ordered crystalline structures [28, 29], which creates a highly resistant lattice with narrow dislocation cores, making dislocation movement require breaking and reforming many strong bonds simultaneously, whereas fracture only involves breaking bonds along a crack plane. As a result, it is energetically and mechanically easier for cracks to propagate than for dislocation to move, leading ceramics to fail by brittle fracture before any significant plastic deformation can occur [30]. Consequently, conventional ceramic materials typically exhibit limited deformability and inherent brittleness, which significantly restricts their utility in advanced technological applications requiring resilience against mechanical shocks and vibrations [31]. This fundamental characteristic necessitates high energy input to break and reform atomic bonds for macroscopic shape changes, making plastic deformation by conventional means challenging [28]. This leads to catastrophic failure under tensile loading rather than ductile yielding, a behavior exacerbated by the highly directional nature of covalent bonds and ionic bonds [32]. Therefore, pillars experienced brittle failure at small strain accompanied by the propagation of cracks under compression, such as the single crystal TiO_2 and Al_2O_3, see **Fig. 1**.

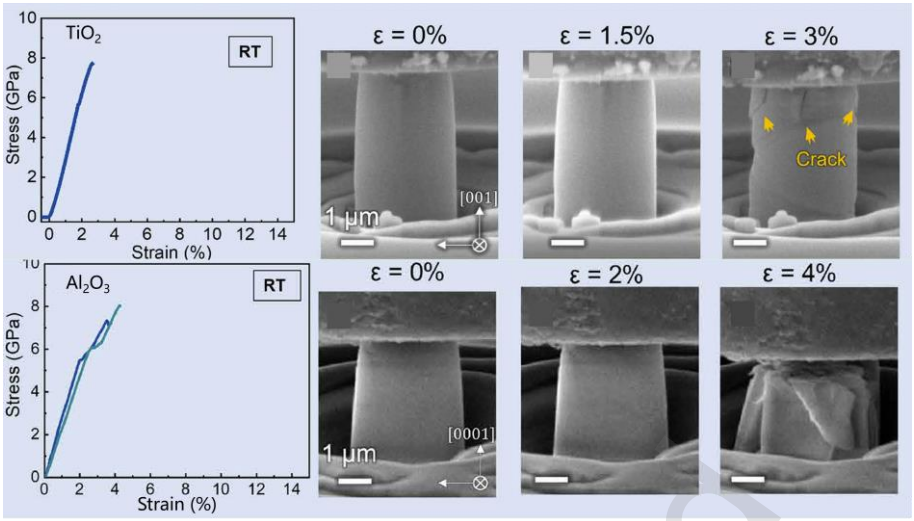

Fig. 1 Representative stress-strain curves of single crystal TiO_2 and Al_2O_3 tested at RT. Reproduced with permission from Ref. [21], © AAAS, 2024.

Despite their high strength and thermal stability, the propensity of ceramics like silicon carbide (SiC) to undergo catastrophic brittle fracture under various loading conditions, particularly at RT, remains a significant impediment to their broader engineering implementation [33]. This behavior is primarily attributed to the inherent difficulty in activating dislocation slip systems due to strong interatomic bonds and a low ratio of tensile strength to shear strength, leading to stress release predominantly via crack propagation rather than plastic deformation [34]. For instance, highly directional covalent bonds between Si and C atoms in SiC fundamentally restrict dislocation-based deformation, leading to trans-granular fracture along grain boundaries rather than ductile yielding [35]. Similarly, boron carbide (B_4C), despite being one of the hardest materials, experiences anomalous failure under hypervelocity impact due to the formation of higher-density amorphous bands and subsequent cavitation, rather than dislocation-mediated plasticity [36]. This phenomenon, where intrinsic factors like the high ratio of critical shear stress to critical normal fracture stress influence fracture behavior, is further complicated by internal defects such as pores that reduce critical normal fracture stress [37]. This inherent limitation has historically constrained the widespread

application of ceramics in scenarios demanding robust mechanical performance, such as aerospace components or flexible electronic devices [38]. Overcoming this intrinsic brittleness to achieve RT plasticity in ceramics is therefore a critical area of research, with recent efforts focusing on alternative deformation mechanisms like bond switching at coherent interfaces [31], or the introduction of mechanically seeded mobile dislocations [19]. However, the development of strategies to overcome this fundamental challenge holds the potential to unlock new frontiers in ceramic engineering, enabling the design of materials with enhanced plasticity and fracture toughness [19, 39].

2.2 Distinction between toughness, plasticity, and ductility

For brittle ceramics, it is essential to distinguish clearly among toughness, plasticity, and ductility, as these terms describe different aspects of mechanical response. Fracture toughness refers to the resistance of a material containing a pre-existing crack to crack initiation and/or crack propagation. Depending on the constitutive response and testing configuration, it may be quantified by fracture-mechanics parameters such as the plane-strain fracture toughness K_{IC}, the critical J-integral J_{IC}, the critical energy-release rate G_{IC}, or crack growth resistance curves (R-curves) [40, 41]. For advanced ceramics at RT, reliable fracture-toughness assessment requires a sharp and well-defined crack together with an appropriate fracture-mechanics test method.

In contrast, plasticity denotes irreversible deformation under mechanical loading before catastrophic fracture. In the present review, a claim of RT plasticity requires direct experimental evidence, for example, a detectable yield event, measurable residual strain after unloading that cannot be explained solely by crack-induced damage, accumulated plastic strain, or a verified irreversible deformation mechanism. Hence, nonlinear stress–strain behavior should not be equated with

plasticity, as it may also result from damage buildup, microcracking, interfacial debonding, crack closure and other fracture-related phenomena.

Moreover, Intrinsic plasticity denotes permanent deformation generated within the crystal lattice or within the load-bearing ceramic phase itself. It is governed by crystal-internal deformation mechanisms, including dislocation plasticity, deformation twinning, and irreversible stress-induced structural rearrangement. Therefore, intrinsic plasticity is primarily determined by the bonding character, crystal structure, available deformation modes, defect population, and mobility of lattice defects in the ceramic phase. By contrast, extrinsic plasticity denotes permanent deformation generated primarily through microstructural features external to the crystal lattice of the load-bearing phase. Such deformation is mediated by grain boundaries, phase boundaries, interfaces, secondary phases, pores, or architected structural units. Representative mechanisms include grain-boundary sliding, interface sliding, interphase shear, particle rearrangement, and so on. Thus, extrinsic plasticity depends predominantly on microstructural architecture, interface characteristics, grain size, phase distribution, and structural connectivity. Accordingly, the essential distinction is the origin of irreversible strain: intrinsic plasticity originates from crystal-internal deformation of the ceramic phase, whereas extrinsic plasticity originates from the relative displacement, rearrangement, or sliding of microstructural constituents outside the crystal lattice.

Traditional ceramic toughening primarily aims to increase resistance to crack initiation and/or propagation. Typical intrinsic and extrinsic crack-resistance mechanisms include transformation toughening, microcracking, crack deflection, crack bridging, grain interlocking, and fiber or whisker pull-out [41-44]. These mechanisms can increase K_{IC}, J_{IC}, G_{IC}, or the rising-R-curve response by shielding the crack tip, extending the fracture path, or dissipating energy during crack extension.

Importantly, however, a substantial improvement in fracture toughness does not necessarily imply appreciable macroscopic plastic deformation. Conversely, the detection of plastic deformation at RT cannot be taken as direct evidence for improved fracture toughness. In addition, the term ductility is used only when tensile deformation or a clearly defined tensile elongation-to-failure is reported. Compressive plastic strain, flexural nonlinearity, or damage-assisted pseudo-ductile behavior should not, by themselves, be interpreted as tensile ductility.

2.3 Fundamental mechanisms of ceramic plastic deformation

Ceramic plasticity originates from several fundamental deformation mechanisms that accommodate irreversible strain under mechanical loading. These mechanisms including dislocation-mediated plasticity, GBS, twinning, phase transformation, amorphous flow, and interface sliding. The current section focuses on the intrinsic physical nature of these deformation modes, namely how plastic strain is generated and accommodated in ceramic materials. The discussion emphasizes the elementary carriers of plastic deformation, their activation conditions, and their contribution to strain accommodation. In contrast, material-design approaches that deliberately activate, enhance, or combine these mechanisms to achieve RT plasticity are discussed separately in **Section 4**.

2.3.1 Dislocation plasticity

Dislocation slip constitutes one of the primary and most thoroughly documented mechanisms of plastic deformation in ceramic materials, which are classically considered brittle at RT owing to their high Peierls stress, limited slip-system multiplicity for cleavage fracture. In contrast to metals, where five independent slip systems readily satisfy the von Mises criterion for general ductility [45], most ceramics possess insufficient independent systems or high lattice friction that confines

dislocation motion until elevated temperatures [18]. Nevertheless, under conditions of high crystallographic symmetry, weak interplanar bonding, or reduced sample dimensions that suppress cracking, dislocation glide can prevail and give considerable plastic strains (e.g., 5-20%) in the absence of macroscopic crack propagation [21]. This intrinsic dislocation-mediated plasticity has been conclusively demonstrated through a combination of macroscopic compression, micro-pillar compression, nanoindentation, and TEM across several model ceramic families.

Frisch *et al.* [18] presented a comprehensive overview of RT dislocation-mediated plasticity in ceramics, elucidating the fundamental mechanisms that enable irreversible deformation in typically brittle materials, see **Fig. 2**. They summarized a list of 44 ceramics compounds grouped by crystal structure as rock-salt, perovskite, sphalerite, wurtzite, fluorite, cesium chloride, and spinel structures, which have been reported to exhibit dislocation plasticity at ambient conditions in the millimeter range. They demonstrated that, contrary to conventional expectations, dislocation slip can be activated at RT in selected ceramics with lower lattice resistance when subjected to sufficiently stress states induced by various deformation methods (e.g., indentation, scratch, uniaxial bulk compression, surface grinding/polishing, sand blasting, and shot peening) or preparations (e.g., high-pressure high-temperature sintering, flash sintering, bi-crystal bonding, thin film growth, high-pressure torsion HPT, and irradiation). Plastic deformation is governed by the dislocation nucleation, motion, glide, and interaction, with processes such as partial dislocation emission, stacking fault formation, and dislocation multiplication playing central roles.

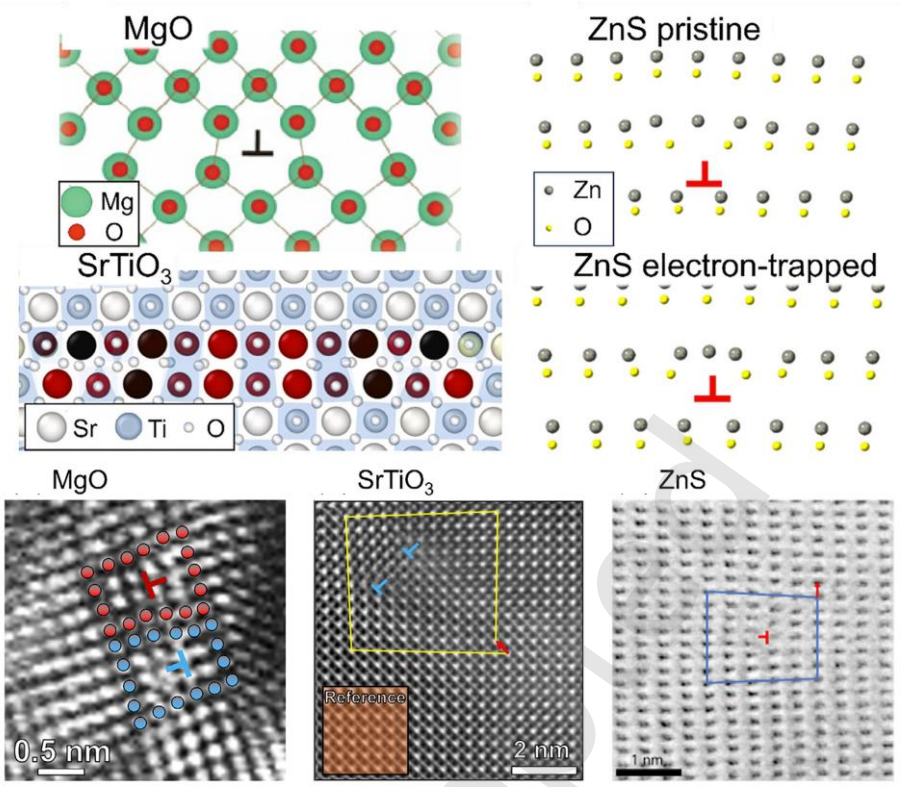

Fig. 2 Representative research results on dislocation plasticity of typical ceramics. Reproduced with permission from Ref. [18], © The American Ceramic Society, 2025.

Rock-salt structure ceramics, exemplified by Magnesium oxide (MgO), lithium fluoride(LiF), Sodium chloride (NaCl), and silver chloride (AgCl) single crystals, serve as the archetypal model materials for dislocation slip in ceramics. Their high-symmetry cubic lattice (space group $Fm\bar{3}m$) provide at least 12 equivalent $\{110\}<110>$ slip systems (and occasionally secondary $\{100\}<100>$), easily satisfying the von Mises criterion. Gilman and Johnston [46, 47] revealed well-defined glide bands on LiF via etch-pit techniques, demonstrating that dislocations move readily on $\{110\}$ planes at RT under modest stresses. Subsequent micro-compression and indentation studies confirm that these crystals exhibit pronounced plastic zones devoid of cracks, and plastic strains routinely exceed 10% under uniaxial compression along soft orientations (e.g., <100>).

Meanwhile, Amodeo *et al.* [48] reviewed that MgO, as an archetype ionic ceramics with the rock-salt structure, serves as a model crystal in which plasticity is primarily governed by soft $\frac{1}{2}\{110\}<110>$ and hard $\frac{1}{2}\{100\}<110>$ slip systems, constrained by electrostatic considerations that forbid glide on densely packed $\{111\}$ planes. The plastic response is strongly temperature-dependent: at low to intermediate temperatures, deformation is controlled by thermally activated dislocation glide overcoming lattice friction (Peierls mechanism), while at higher temperatures, dislocation interactions and climb processes dominate, leading to an athermal, viscous-like regime. They outlined the dislocation core modeling, including cluster-based embedded model, periodic dipole model, and semi-continuum Peierls–Nabarro model, see **Fig. 3**. Dislocation mobility is largely dictated by kink-pair nucleation for screw dislocations, with edge dislocations exhibiting higher mobility. The critical resolved shear stress (CRSS) reflects these mechanisms, showing strong sensitivity to temperature, impurities, and heat treatment, the latter influencing dislocation pinning through point defect distributions. Additionally, strain hardening arises from dislocation interactions such as junction formation and dipole creation, while high-temperature creep is governed by dislocation glide-assisted climb, consistent with power-law creep behavior. Overall, the study demonstrates that dislocation core structure, mobility, and interactions across multiple length scales collectively control plasticity in MgO, providing a fundamental framework applicable to other ionic and structural ceramics.

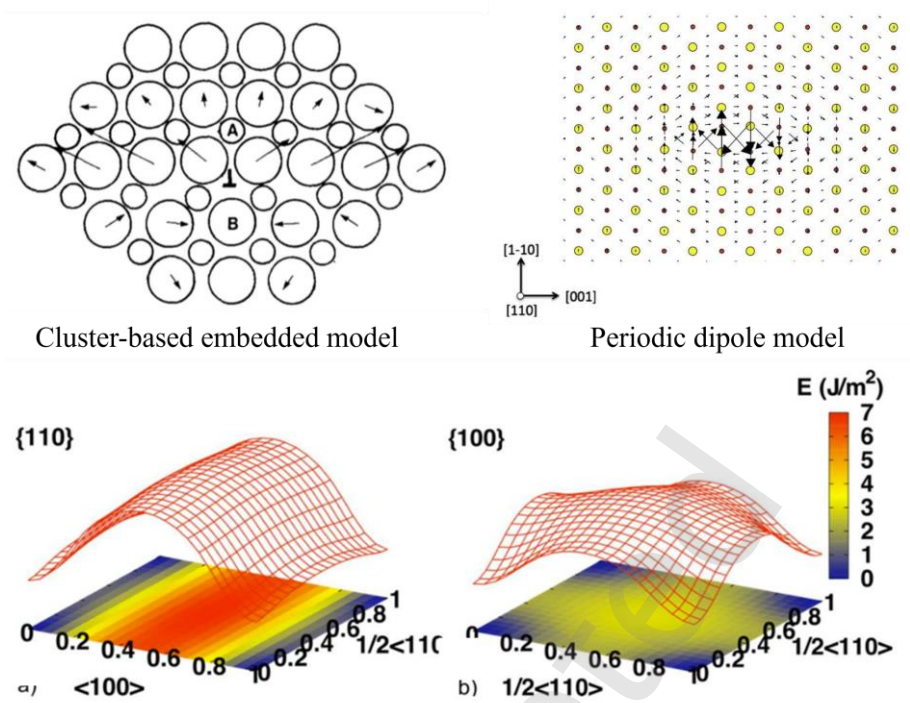

Fig. 3 Representative dislocation core modeling of MgO. Reproduced with permission from Ref. [48], © MDPI, 2018.

Cubic perovskites, prototypically $SrTiO_3$, exhibit RT dislocation plasticity when tested in single-crystal form, particularly at micro- or meso-scales. The structure (space group $Pm\bar{3}m$) activates the $\{110\}\langle 1\bar{1}0\rangle$ slip system, which provides sufficient independent systems for plasticity. Bulk compression along [001] produces clear yield points followed by plastic flow to strains of 5-15%, with prominent slip bands visible on the surface [18, 19, 49]. Micro-pillar compression further accentuates this behavior: dislocation glide dominates, as evidenced by TEM showing straight screw dislocations and occasional cross-slip. Recent studies demonstrate that pre-introducing dislocations (via HT pre-straining or scratching) dramatically enhances subsequent RT plasticity by lowering the effective CRSS through multiplication and source activation. While polycrystalline $SrTiO_3$ remains macroscopically brittle due to grain-boundary constraints, the single-crystal response unambiguously

establishes dislocation slip as the operative mechanism. Oxygen-vacancy engineering has also been shown to reduce Peierls stress, further facilitating glide [50].

Fluorite (CaF_2-type) single crystals (e.g., CaF_2, BaF_2 and CdF_2) possess a cubic structure (space group $Fm\bar{3}m$) with facile slip on $\{001\}<110>$ systems. RT indentation produces extensive, crack-free plastic zones surrounded by well-defined slip traces [51, 52]. The ionic character and relatively open lattice permit low Peierls resistance, and dislocation nucleate and glide readily, forming pile-ups and networks without triggering cleavage on $\{111\}$ planes. Microstructural analysis confirms that plastic flow is entirely dislocation-mediated, rendering these materials excellent optical ceramics with intrinsic RT plasticity under localized loading.

Even highly covalent NaCl-type transition metal nitrides exhibit clear dislocation-mediated plasticity when dimensions are reduced to the micro- or nanoscale dimensions, such as titanium nitride (TiN) [53], zirconium nitride (ZrN) [54], and vanadium nitride (VN) [55]. Micro-pillar compression or nanoindentation reveals plastic strains > 5% at RT, directly correlated with observable slip bands and dislocation motion in TEM. Although bulk polycrystalline forms remain brittle (owing to high Peierls stress from directional bonding), the size effect suppresses cleavage, allowing dislocation nucleation and glide to dominate. These observations extend the dislocation-plasticity paradigm to refractory ceramics and underscore the universal role of sample size in activating slip before fracture.

In summary, the examples above establish dislocation slip as the typical mechanism of plastic deformation in ceramics whenever sufficient slip systems, low-to-moderate lattice friction, and/or microstructural confinement are present. High crystallographic symmetry (rock-salt, perovskite, fluorite) or layered anisotropy (MAX phases) minimizes the Peierls barrier, while microscale testing

circumvents crack nucleation. These findings not only overturn the traditional brittleness dogmas, but also provide rational design guidelines for plastic and dislocation-resistant ceramics through compositional adjustments, defect engineering, or dimensional control, which can be applied to structural, functional, and energy conversion technologies.

2.3.2 Grain boundary sliding (GBS)

GBS is a well-established deformation mechanism in polycrystalline ceramics, primarily effective at high temperature (typically > 0.5-0.7 T_m) rather than at RT. It enables significant plastic strain (including super-plasticity with elongations exceeding 100-800%) under conditions where diffusional accommodation prevents intergranular cavitation. In this process, grains slide relative to one another along their boundaries, contributing the majority of the total strain, while accommodation occurs via grain-boundary diffusion, viscous flow through intergranular glassy phases, limited dislocation activity, or grain rotation [56]. GBS is particularly prominent in fine-grained ceramics at homologous temperatures $T/T_m > 0.4$ (where T_m is the melting temperature) and low strain rates ($< 10^{-4}$ s^{-1}), as these conditions promote boundary mobility and suppress dislocation creep or cracking. Unlike metals, ceramics often require a thin intergranular glassy or amorphous phase to lower the sliding resistance and facilitate coordination. This mechanism has been extensively documented in both single-phase oxides and composites, with seminal demonstrations in yttria-stabilized tetragonal zirconia polycrystals (Y-TZP) [57, 58]. Ceramics exhibiting GBS-dominated plasticity/creep are typically classified into three categories based on composition and microstructure: classic single-phase oxides, oxide-based composites, and non-oxides/special ceramics. All share the requirement

for ultrafine grains with the grain size smaller than 1 μm, ideally 0.2-0.5 μm or nanocrystalline, which to meet the sufficient grain-boundary area and sliding paths.

The classic single-phase oxide ceramics systems represent foundational models for GBS studies, where fine grains and minor glassy phases at boundaries enable sliding as the rate-controlling process, often coordinated by Coble creep (a form of diffusion creep, as a mechanism for deformation of crystalline solids [59]) or interface-reaction diffusion. Y-TZP (e.g., 3Y-TZP, 2Y-TZP, and Ce-TZP) with grain sizes < 1 μm (typically 0.2 -0.5 μm) are the archetype of ceramic super-plasticity. GBS, accommodated primarily by grain-boundary diffusion of Zr^{4+} cations and influenced by dopant segregation, dominates at 1200-1500 ℃ and low strain rates. Thin SiO_2-rich glassy phases at boundaries act as lubricants, enabling elongations > 100% with minimal cavitation. Wakai *et al.* [57] established this behavior, with subsequent studies confirming stress exponents ≈ 2 and activation energies consistent with boundary diffusion.

Coarse-grained pure alumina (Al_2O_3) deforms primarily by dislocation creep, but fine-grained (< 1 μm) variants doped with MgO, SiO_2, or CaO (forming intergranular glassy phases) shift the mechanism to GBS-dominated plasticity at 1400-1700 ℃. Sliding is accommodated by boundary diffusion or limited dislocation motion at triple junctions, with MgO additions promoting spinel phases that enhance boundary mobility [60]. MgO has long served as a model material for studying GBS mechanism. Fine-grained pure or lightly doped MgO with grain size < 5 μm exhibits GBS as the dominant creep mechanism at 1300-1600 ℃. Thin non-crystalline boundary layers facilitate easy sliding, though this often leads to intergranular fracture without sufficient accommodation.

Both mullite ($3Al_2O_3 \cdot 2SiO_2$) and spinel ($MgAl_2O_4$) display GBS-controlled creep in fine-grained forms with glassy boundary phases at 1400-1600 ℃ [56, 61]. Mullite benefits particularly

from inherent SiO_2-rich glassy phases, promoting easier sliding compared to spinel. Second-phase additions refine and stabilize grain size through pinning and Zener drag, enhancing GBS by increasing the fraction of dissimilar-phase boundaries to promote slide while suppressing cavitation. All boundaries (same-phase or dissimilar) contribute significantly to total strain. The benchmark system (e.g., Al_2O_3-20 vol% 3Y-TZP), feature fine interlocked dual-phase microstructures and glassy-phase lubrication. At 1400-1600 ℃ and low strain rates, coordinated GBS (accommodated by diffusion and minor grain rotation) yields elongations of 200-800% without significant cavitation, making it a reference for ceramic superplastic forming [62]. Three-phase fine-grained structures (e.g., 40 vol% Al_2O_3-30 vol% ZrO_2-30 vol% mullite) with uniform glassy-phase distribution enable fully accommodated GBS at 1400-1700 ℃. Atomic force microscopy (AFM) and scanning electron microscope (SEM) characterizations confirmed that all boundary types (e.g., Al_2O_3/Al_2O_3, ZrO_2/ZrO_2, mullite/mullite, and mixed) contribute substantially to strain, with no systematic preference for dissimilar interfaces [56]. Nanophase additions, such as SiC particles in ZrO_2-Al_2O_3-SiC composites, similarly enhance GBS by boundary pinning at 1300-1500 ℃, combining high strength with super-plasticity [62].

Non-oxide and specialty ceramics rely on analogous GBS strategies but demand deliberate introduction of intergranular phases. Silicon nitride (Si_3N_4) and silicon carbide (SiC) exhibit GBS-controlled creep only when sintered with additives (e.g., Y_2O_3-Al_2O_3) that form persistent glassy boundary films, under which conditions, sliding accommodated by diffusion through the viscous phase dominates at 1600-1900 ℃ (Si_3N_4) or 1800-2100 ℃ (SiC) and low strain rates, whereas pure crystalline coarse-grained variants revert to diffusion or dislocation creep. B_4C and aluminum nitride (AlN) achieve GBS dominance in nanocrystalline forms with non-stoichiometric or thin amorphous

boundaries under high-pressure high temperature processing. Other oxides such as TiO_2, SnO_2, and functional ceramics like $LiNbO_3$ follow the same fine-grain, high temperature paradigm, where GBS emerges as a key contributor to plasticity/creep [63]. Nano-SiC particles pin boundaries to maintain ultrafine grains, enabling GBS dominance at 1300-1500°C while retaining high strength alongside super-plasticity. Must incorporate intergranular glassy phases (e.g., from Y_2O_3-Al_2O_3 sintering aids). Fine-grained Si_3N_4 deforms by GBS-accommodated creep at 1600-1900 ℃ and SiC at 1800-2100°C. Pure crystalline coarse-grained forms revert to diffusion or dislocation creep [63].

Across all systems, four interdependent conditions are indispensable for GBS to govern deformation: (1) ultrafine or fine grains (typically <1 μm, ideally nanocrystalline) to maximize boundary fraction and sliding pathways; (2) grain-boundary engineering via thin amorphous/glassy phases or defect-rich interfaces that lower viscosity and enable diffusional accommodation; (3) homologous temperatures > 0.4 T_m to activate atomic mobility; (4) low strain rate (< 10^{-4} s^{-1}) to allow sufficient time for stress relaxation without cavitation. These criteria form the basis for the transition from brittle to superplastic response and guide the design of advanced HT forming processes for ceramics. While recent advances have begun exploring GBS contributions at lower temperatures through extreme grain refinement or boundary modifications, the mechanism remains typically HT in conventional ceramic systems [64]. GBS at RT lacks diffusional accommodation, leading to stress concentrations and cracking unless grains are extremely (< ~100 nm) or boundaries are engineered (e.g., non-stoichiometric or glassy phases) [65]. Then, polycrystals need about 5 independent slip systems for compatible deformation, while ceramics have few at RM, so GBS become crack nucleation sites unless dislocations multiply profusely inside grains [18]. Moreover, plasticity arises from pre-existing mobile defects lowering the CRSS for glide, not from sliding per se. GBS, when

present, assists in polycrystals by relieving local stresses or enabling grain rotation alongside dislocation slip [21].

2.3.3 Twinning

Deformation twinning is a high-CRSS, crystallographically distinct mode of plastic deformation in crystalline materials, characterized by uniform shear across a twin plane, resulting in a mirror-symmetric orientation between the deformed twin region and the undeformed matrix (parent lattice), while preserving the underlying crystal structure [66, 67]. Twinning has emerged as critical mechanism enabling plastic deformation under specific conditions, such as high stress, elevated temperatures, nanoscale structuring, or tailored microstructures. In contrast to metals, where twinning typically supplements dislocation glide at low temperatures or high strain rates, twinning in ceramics often activates when conventional slip is inhibited by high Peierls barriers, providing an alternative shear accommodation mode that can lead to either strain hardening (via twin boundary-dislocation interactions) or enhanced plasticity through twin-mediated slip or detwinning processes. Twin boundaries act as both obstacles and sources for partial dislocations, leading to complex hardening/softening competition that is highly dependent on twin spacing, orientation, and material class [68].

This mechanism spans diverse ceramic families, highlighting its broad relevance to the design of plastic or damage-tolerant ceramics. In oxide ceramics, rhombohedral and basal twinning are well-documented in Al_2O_3, where deformation twins form readily under compression along the c-axis at moderate temperatures (350-1100 ℃), often nucleating at surface defects or grain boundaries and contributing to localized plasticity when prismatic or basal slip is restricted [69]. Similar twinning-

assisted deformation occurs in ZrO_2-based systems, including yttria-stabilized zirconia and shape-memory variants such as (Zr, Hf)O_4-(Y, Ta)O_4 solid solutions, where deformation twinning enables pseudoplastic strain exceeding 5% and couples with martensitic transformations for enhanced toughness [70]. Perovskite oxides like $SrTiO_3$ and garnets as $Y_3Al_5O_{12}$ (YAG) also exhibit twinning under indentation or high-pressure conditions, facilitating stress relaxation and limited plastic flow [71]. Plastic deformation in cubic boron nitride (cBN) can be achieved primarily through deformation twinning rather than dislocation slip: with the high energy barrier for dislocation motion, applied high pressure and stress activate partial dislocations that generate nanoscale twins, which accommodate strain and enable limited plasticity in this otherwise brittle material [27].

Non-oxide ceramics demonstrate even more striking twinning-induced plasticity, particularly when engineered at the nanoscale. In nitrides, nano-twinned cubic boron nitride (NT-cBN) displays pronounced size-dependent hardening and complex plastic flow under nanoindentation, governed by dislocation blockage, absorption, dislocation, and re-nucleation at twin boundaries [72]. Moreover, the competitive interplay between hardening (slip transfer and dislocation plie-ups) and softening (twin boundary destruction) yields exceptional hardness while accommodating strain. Remarkably, nano-twinned chromium nitride (NT-CrN) achieves simultaneous super hardness (> 36 GPa) and RT plasticity, sustaining >40% compressive strain without catastrophic fracture, see **Fig. 4** [22]. Here, high-density nanotwin boundaries ($\approx 9.0\times10^{15}$ m^{-2}) enable a unique "polyhedron-twisting" slip mode along Cr-(111) and N-$\{111\}$ planes without bond breakage, accompanied by twin proliferation ,fusion, and partial dislocation-mediated detwinning that dissipates energy effectively. Layered MAX-phase ceramics (e.g., Ti_2AlN) further illustrate deformation twinning under localized loading such as nanoindentation, where twin formation within the nano-laminated structure augments

basal slip and confers machinability-like plasticity uncommon in conventional carbides or nitrides [73].

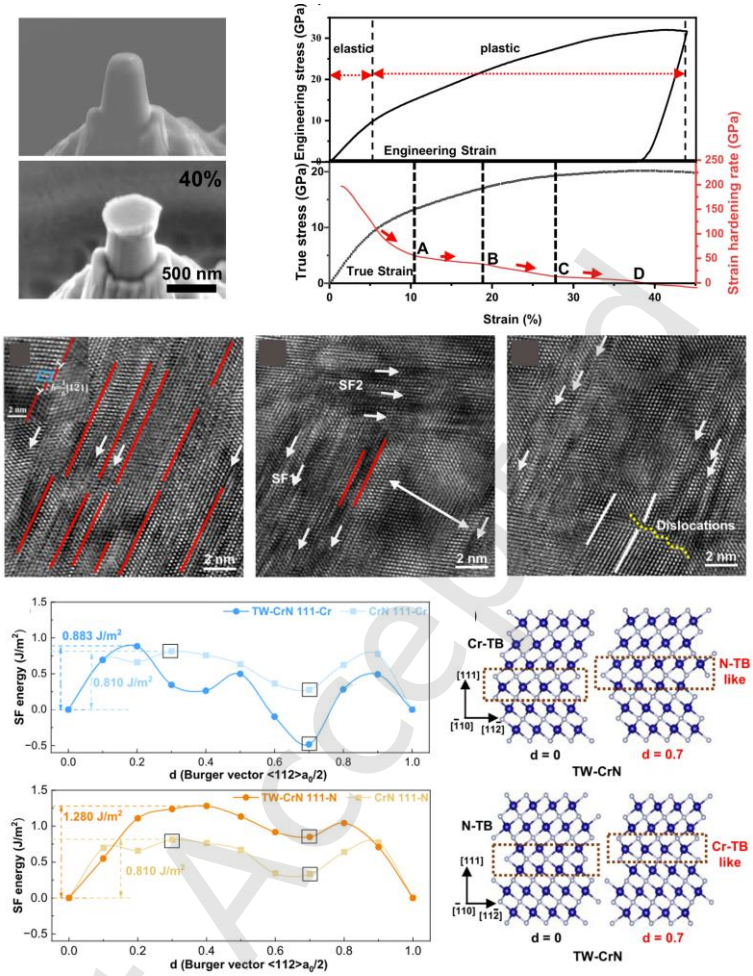

Fig. 4 Nano-twinned CrN ceramics with enhanced plasticity. Reproduced with permission from Ref. [22], © Springer Nature, 2025.

Collectively, these examples-from simple oxides (e.g., Al_2O_3, ZrO_2) and perovskites to superhard nitrides (e.g., cBN, and CrN) and layered MAX phases-underscore twining' versatility as plasticity enabler across ceramic chemistries and crystal structures. Advances in processing (e.g., high-power impulse magnetron sputtering for dense nanotwins or HPT for severe deformation) are now unlocking RT plasticity in otherwise brittle ceramics, paving the way for next-generation structural components that combine high hardness with damage tolerance. Future work will likely

focus on twin-density optimization and twin-slip interactions to tailor the strength-plasticity balance in a wider range of covalent and ionic ceramics [74].

2.3.4 Phase transformation

One of the most effective mechanisms enabling plastic deformation in otherwise brittle ceramics is stress- or strain-induced phase transformation, which provides an alternative pathway for strain accommodation without relying on conventional dislocation slip systems. In ceramics, limited active slip systems at RT typically lead to catastrophic brittle failure, while certain polymorphic transformations-particularly those involving significant shear and dilatational strains-can dissipate energy and accommodate permanent deformation through a transformation induced plasticity (TRIP) effect analogous to that observed in metastable austenitic steels [75]. This mechanism is most prominently exemplified in ZrO_2-based ceramics, where the metastable tetragonal (*t*) phase transforms martensitically to the monoclinic (*m*) phase under applied stress. $t \rightarrow m$ transformation is accompanied by a volume expansion of ~3-5% and shear strain of ~14-15%, generating compressive stresses that shield cracks and enable macroscopic plastic strain prior to fracture. Garvie *et al.* [76] first highlighted this phenomenon in metastable ZrO_2 to describe the resulting combination of high strength and toughness.

In Y-TZP or Ce-TZP, careful control of stabilizer content, grain size, and microstructure allow the critical stress for $t \rightarrow m$ transformation to be tuned such that transformation bands or zones form progressively during loading. Recent advances in ceria-stabilized zirconia composites, such as 10.5-11 mol% Ce-TZP reinforced with 8 vol% Al_2O_3 and 8 vol% $SrAl_{12}O_{19}$, demonstrate pronounced TRIP behavior with plastic strains up to ~0.38% in bending without detectable damage (i.e., no

measurable drop in Young's modulus or extensive microcracking) [77]. The transformation occurs in localized bands on the tensile surface, with monoclinic fractions reaching 20-45 vol% inside the bands, confirming that the plasticity arises purely from the reversible or irreversible phase change rather than microcrack coalescence. Grain-boundary segregation of divalent cations (e.g., Mg^{2+}, or Ca^{2+} at 0.1-0.4 mol%) in monolithic 10Ce-TZP further optimizes transformability, yielding damage-tolerant ceramics with biaxial strengths > 1200 MPa, fracture toughness >10 $MPa \cdot m^{1/2}$, and high Weibull moduli while still exhibiting inelastic deformation zones ahead of cracks. These materials also display shape-memory or super-elastic responses when the transformation is made reversible through doping and thermal control, expanding their utility beyond conventional toughening [78].

Beyond oxide systems, phase-transformation plasticity has extended to covalent ceramics such as Si_3N_4. In dual-phase α/β- Si_3N_4 nanostructures featuring coherent interfaces, compressive loading triggers a stress-induced $\beta \rightarrow \alpha$ phase transformation via successive bond switching and interface sliding [31]. This process enables substantial plastic bond rupture, achieving plasticity that is otherwise unattainable in monolithic covalent ceramics. Similar transformation-assisted plasticity under severe plastic deformation (e.g., HPT) has been reported in other ceramics, including TiO_2, $BaTiO_3$, and high-entropy oxides, where pressure- and shear-induced polymorph changes refine microstructures and introduce defects that further enhance deformability. Transformation super-plasticity during thermal cycling through allotropic transitions has also been demonstrated in ZrO_2 and related systems, allowing large elongations without fracture when fine grain sizes are maintained.

Moreover, Li *et al.* [79] introduced a ceramic self-toughening strategy that triggers twin-assisted martensitic transformations via slip bands or stacking faults in titania-doped $(Hf,Zr)O_2$ layers formed on (Hf-Zr-Ti)C coatings, enhancing both plasticity and thermal-shock resistance for improved

cyclic ablation tolerance in ultra-high-temperature ceramics above 2000 ℃, see **Fig. 5**. By engineering metastability (through doping, grain-size control, or coherent multi-phase architectures), ceramics, spanning ionic (ZrO_2-based) to covalent (Si_3N_4) bonding types can exhibit measurable plastic strain, improved damage tolerance, and even functional responses such as shape memory. Ongoing research focuses on scaling these mechanisms to bulk components while preserving strength and reliability, positioning transformation-plastic ceramics as promising candidates for structural, biomedical ,and energy applications.

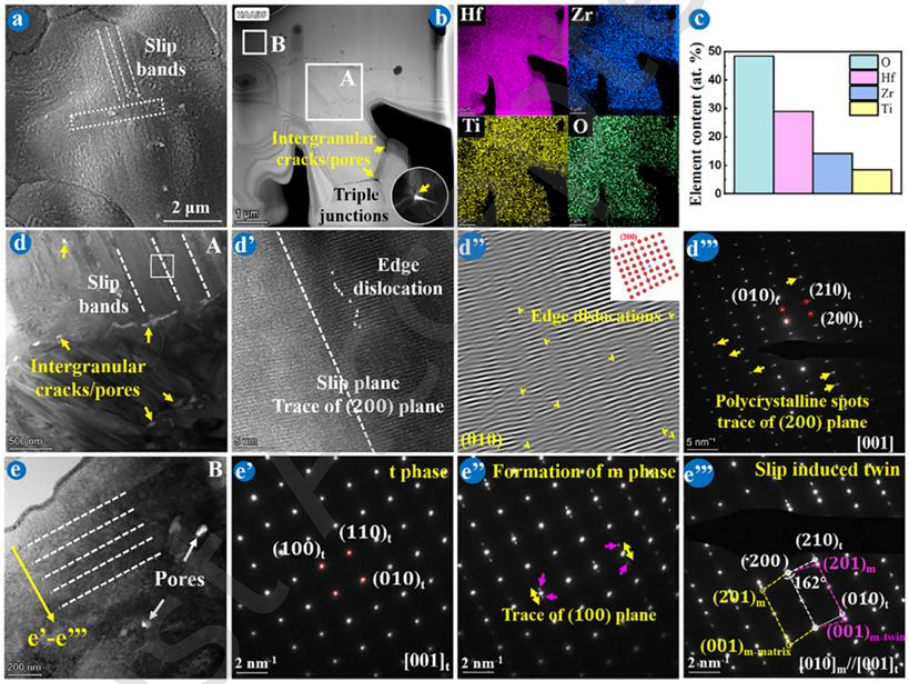

Fig. 5 Self-toughening strategy that triggers twin-assisted martensitic transformations via slip bands or stacking faults in titania-doped (Hf, Zr)O_2 layers formed on (Hf-Zr-Ti)C coatings. Reproduced with permission from Ref. [79], © Wiley, 2025.

2.3.5 Amorphous flow

In amorphous ceramics, plastic deformation is fundamentally governed by amorphous/viscous flow, a mechanism distinct from the dislocation-mediated slip that dominates plasticity in crystalline ceramics [80]. The process relies on localized, cooperative atomic rearrangements-often

conceptualized as shear transformation zones (STZs)-that enable irreversible shear strain under applied stress, particularly when thermal activation allows the material to behave as supercooled liquid above its glass transition temperature (T_g) [81]. At ultrahigh temperature, homogeneous viscous flow becomes Newtonian, permitting large-scale plastic strains without fracture; deviations toward non-Newtonian behavior occur at high strain rates or stresses due to structural relaxation or shearing thinning. SiO_2 glasses, such as fused silica or vitreous silica, exemplify this behavior. Their fully polymerized network undergoes anomalous densification-driven deformation at RT (via compaction of ring structures) and transitions to pronounced viscous flow at elevated temperatures, enabling micropillar compression tests to reveal permanent plastic strains exceeding 10-20% through shear banding and volume-conserving flow [82].

Borosilicate glasses, including commercial formulations such as Borofloat® 33 (low-alkali) and N-BK7® (soda-borosilicate), exhibit similar yet composition-dependent plasticity [83]. Low-alkali variants display anomalous densification akin to pure silica, while higher modifier contents promote shear-driven flow via bond switching and non-bridging oxygen (NBO) formation. Uniaxial tension and compression experiments, supported by molecular dynamics simulations, demonstrate that plastic response arises from increasing NBO production rates, yielding measurable ductility even under tensile loading. Thermal history (cooling rate and melting temperature) further modulates connectivity between borate and silicate domains, shifting deformation from densification-dominated to shear-dominated modes [84]. Other silicate glasses, such as soda-lime-silica compositions, follow analogous trends but display more pronounced non-Newtonian viscous flow at high stresses, with viscosity reductions facilitating processing and deformation [85].

Beyond traditional oxide glasses, nanostructured amorphous ceramics-such as Al_2O_3-ZrO_2 (La_2O_3) or precursor-derived Si-C-N systems-extend amorphous flow mechanisms through hierarchical shear bands originating at nanoscale amorphous interfaces or free-volume-rich regions [86, 87]. These materials achieve permanent plastic strains (up to ~15%) via interface-induced STZ activation, even under medium-derived ceramics similarly exploit supercooled-liquid viscous flow for shaping at moderate temperatures (~645 °C). Collectively, these examples illustrate that amorphous flow not only confers intrinsic plasticity to otherwise brittle ceramics but also underpins advanced processing routes (e.g., flashing sintering) and toughness enhancements in plastic ceramic design, with deformation modes tunable via composition, scale, and thermomechanical history.

A recent study on amorphous oxide glasses further expands the concept of RT plasticity in nominally brittle ceramic systems by introducing paracrystallization as an atomic-scale structural design strategy. Tang *et al.* [88] demonstrated that high-pressure/high-temperature treatment can generate uniformly distributed crystal-like medium-range-order clusters within aluminosilicate glass, producing a paracrystalline state without forming conventional coarse crystalline phases. Under mechanical loading, these paracrystalline regions undergo a stress-induced inverse transformation back to the amorphous state, which activates multiple shear bands and dissipates fracture energy at the crack tip. This mechanism differs from dislocation-mediated plasticity in crystalline ceramics and from conventional crack-deflection or bridging toughening in glass-ceramics. Instead, it represents a transformation-assisted plastic deformation mode based on reversible local ordering–disordering of the atomic structure. As a result, paracrystallized oxide glass exhibits markedly enhanced damage tolerance and fracture toughness, highlighting atomic-level structural modulation as a promising route for designing plastically deformable and tougher amorphous ceramic materials.

2.3.6 Phase interface sliding

MAX phases with general chemical formula $M_{n+1}AX_n$ (M is the early transition metal, A is the A-group element, X is either element C or N, and n is an integer typically ranging from 1 to 4) such as Ti_3SiC_2, Ti_3AlC_2, Ti_2AlC, and Cr_2AlC possess a hexagonal layered structure (space group $P6_3/mmc$) with strongly bonded M-X slabs separated by weakly bonded A layers. This anisotropy confines primary slip to the basal (0001) plane along $<11\bar{2}0>$ directions. RT compression of polycrystalline or single-crystal MAX phases yields plastic strains of 5-20%, accompanied by pronounced surface slip bands, dislocation cells, and extensive tangling without crack extension [89-91]. **Fig. 6** depicts the kink band of MAX. Deformation proceeds via the formation of dislocation arrays and kink bands: basal dislocations pile up, create low-angle boundaries, and induce local buckling that accommodates strain while dissipating stress concentrations [89]. The weak interlaminar bonding lowers the Peierls stress for basal glide, and the layered architecture inherently suppresses cleavage perpendicular to the basal planes. Importantly, cyclic loading experiments demonstrate fully reversible deformation up to ~1 GPa, confirming that plasticity is dislocation-based rather than microcrack-mediated. MAX phases therefore represent an intrinsic, bulk-scale example of ceramic dislocation plasticity driven by structural anisotropy.

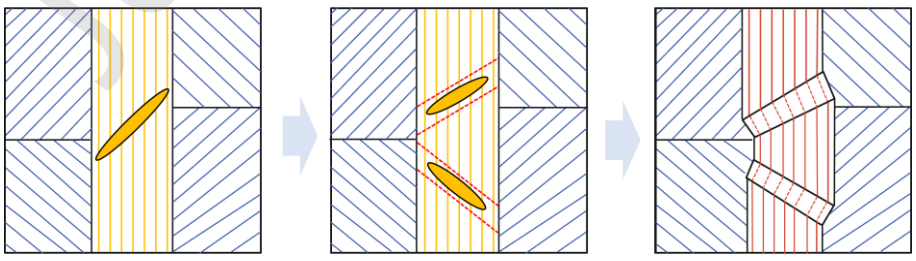

Fig. 6 schematical diagram of kink-band formation in MAX phases.

These mechanisms differ significantly in their underlying physics, activation conditions, and material dependencies, and their relative contributions to RT plasticity are strongly shaped by the

crystal structure, bonding type, grain size, and microstructural design of ceramics. The intrinsic crystalline mechanisms, including dislocation plasticity and twinning, are governed by the inherent resistance of lattice to shear deformation. Dislocation plasticity, the dominant mode of plasticity in metals, is severely limited in most ceramics at RT due to strong directional bonding, high lattice friction (Peierls stress), and a scarcity of independent slip systems required for homogeneous plastic flow. Even in ceramics with active slip systems, dislocation motion is often accompanied by stress concentration at grain boundaries, leading to premature fracture before significant macroscopic strain can be achieved. Twinning, by contrast, offers an alternative shear path in materials with restricted slip, but it typically operates at high stresses and produces localized, rather than bulk, deformation. Nanoscale twin boundaries can mitigate this limitation by acting as both deformation carriers and crack blunting sites, but this requires precise microstructural engineering. Intergranular and interphase mechanisms, such as GBS and interface sliding, rely on motion along disordered or structurally mismatched boundaries. At RT, these mechanisms are kinetically constrained: GBS in conventional polycrystalline ceramics is accompanied by void nucleation and crack formation rather than plastic accommodation, unless combined with nanocrystalline microstructures or amorphous grain boundary phases that enable stress relaxation. Interface sliding, most relevant in composite or multiphase ceramics, similarly requires a delicate balance: weak interfaces can slide to relieve stress concentrations, but excessive debonding degrades load-bearing capacity, making this mechanism a secondary contributor to plasticity rather than a primary source of plasticity.

Microstructure-dependent mechanisms, including amorphous flow and transformation plasticity, are uniquely tied to specific material features. Amorphous flow in glassy grain boundaries or fully amorphous ceramics is suppressed below the glass transition temperature at RT, but residual

glassy phases can still accommodate small strains via local atomic rearrangements, improving toughness without enabling bulk plasticity. Transformation plasticity, the most successful route to RT plasticity in commercial ceramics, leverages stress-induced phase transitions to dissipate energy via volume and shear strain changes. Unlike true plastic flow, this mechanism is a stress-triggered structural transition, and its effectiveness depends on the metastability of the high-temperature phase and the ability of the transformation to absorb strain without initiating catastrophic crack growth.

These differences explain why bulk RT plasticity remains elusive in conventional ceramics. Dislocation plasticity and twinning are too limited by lattice constraints, while boundary-based mechanisms lead to fracture rather than flow. Only transformation plasticity, nanotwin-assisted deformation, and carefully engineered amorphous or nanocrystalline microstructures enable measurable plasticity, highlighting that RT plasticity in ceramics is rarely the result of a single mechanism but rather the synergistic interaction of multiple processes. This complexity underscores the critical role of microstructural design in tailoring ceramic deformation behavior, and it continues to drive research into novel processing routes to unlock new plasticity mechanisms in these inherently brittle materials.

To facilitate comparison among the deformation mechanisms mentioned above, **Table 1** summarizes their representative strain levels, physical principles, operating conditions, advantages, and limitations. It should be noted that the reported strain level is not intrinsic material constant. Instead, it depends strongly on specimen size, loading mode, strain rate, stress state, microstructure, defect density, temperature, and the criterion used to distinguish irreversible deformation from damage-induced nonlinearity. Therefore, the values and ranges listed in **Table 1** should be interpreted as representative literature-reported levels under specific conditions rather than as a direct ranking of

the 6 mechanisms. In addition, the mechanisms listed in **Table 1** are basic but non-exclusive deformation modes. In practical ceramic systems, one mechanism may act as the dominant strain carrier, whereas others provide strain accommodation, reduce activation barriers, or suppress crack initiation. For example, interface-mediated deformation can involve dislocation transmission, interfacial shear, or local atomic rearrangement; phase transformation may be accompanied by twin formation, dislocation activity, and transformation-strain accommodation at interfaces.

Table 1 Comparison of fundamental mechanisms governing plastic deformation in ceramics.

Deformation mechanism	Strain level	Fundamental principle	Operating conditions	Material systems	Advantages	Limitations
Dislocation	Low-moderate	Glide of lattice dislocations	High resolved shear stress; suitable crystal orientation, small dimensions, or confining pressure.	Ceramics compounds grouped by crystal structure as rock-salt, perovskite, sphalerite, wurtzite, fluorite, cesium chloride, and spinel structures	Intrinsic crystallographic plasticity; does not require a second phase.	High Peierls stress and limited slip systems; fracture often competes with slip in polycrystals
Grain boundary sliding	High; may exceed 100% in superplastic ceramics	Relative sliding of fine equiaxed grains, accommodated by diffusion, interface reactions, or intragranular deformation	Fine grains, usually <1 μm; high homologous temperature; moderate stress and controlled strain rate	Y-TZP, Al_2O_3-ZrO_2 composites, fine-grained Si_3N_4 and SiC	Enables superplastic forming and near-net-shape processing	Requires high temperature/low strain rate; prone to cavitation, grain growth, and post-deformation strength loss
Twinning	Low-moderate; localized	Cooperative lattice shear produces a crystallographically reoriented twin domain.	High resolved shear stress; often promoted at low/intermediate temperature, high strain rate, or under shock loading	α-Al_2O_3, selected carbides and borides	Rapid strain accommodation when slip is restricted; may reorient grains favorably	Limited twinning systems and finite twin volume; strong anisotropy and possible crack initiation at twin boundaries
Phase transformation	Low-moderate; limited by transformation fraction	Diffusionless transformation generates transformation shear and volumetric strain	Metastable parent phase; applied stress or crack-tip stress above the transformation threshold; composition and grain size must be controlled	ZrO_2-based ceramics	Provides transformation strain and crack-tip shielding; improves toughness and damage tolerance	Limited transformable phase fraction; may cause residual stress, microcracking, and hydrothermal/thermal degradation
Amorphous flow	Moderate-high	Viscous or non-Newtonian shear flow of an amorphous matrix or intergranular film	At or above the glass-transition/softening range; sufficient glassy-phase continuity and viscosity control	Oxide glasses, nanostructured amorphous ceramics	Reduces flow stress and accommodates grain rearrangement/GBS	Degrades high-temperature creep resistance; may induce cavitation, devitrification, oxidation sensitivity, and reduced RT stiffness
Interface sliding	Moderate; architecture-dependent	Shear displacement after debonding, yielding, or bond switching at heterophase/coherent interfaces	Weak or compliant interfaces; interface shear stress above the sliding threshold; strongly dependent on interface chemistry and architecture	MAX phase	Enables load redistribution, crack deflection, bridging, and non-catastrophic deformation	Not intrinsic bulk plasticity; interface wear, oxidation, debonding, and reduced stiffness/strength may occur

2.4 Coupled and competitive deformation mechanisms

The deformation mechanisms discussed above should be regarded as basic but non-exclusive deformation modes. In practical ceramic systems, irreversible deformation rarely proceeds through only one isolated mechanism. Instead, the observed mechanical response is commonly determined by the coupled activation, accommodation, and competition of multiple mechanisms at atomic, interfacial, grain, and microstructural length scales [78, 92].

Accordingly, the 6 mechanisms are classified here according to their functional roles during deformation. First, primary strain-carrying mechanisms directly contribute to irreversible strain, including dislocation slip, GBS, interface sliding, amorphous flow, twinning, and irreversible phase transformation. Second, accommodation mechanisms reduce local stress concentration or maintain strain compatibility among neighboring regions. These include dislocation transmission across interfaces, twin-boundary migration, detwinning, diffusion-assisted grain-boundary accommodation, transformation-strain relaxation, and local atomic rearrangement within amorphous regions. Third, regulatory factors determine which mechanism becomes dominant, including grain size, phase/interface spacing, interface coherency, crystallographic orientation, defect density, local chemical non-stoichiometry, temperature, strain rate, confining pressure, and loading mode. Therefore, the total irreversible deformation should not be interpreted as a simple linear superposition of independent strain contributions. Rather, the contribution of each mechanism depends on whether other mechanisms reduce its activation barrier, supply compatible strain, relax stress concentration, or suppress its propagation.

2.4.1 Dislocation-interface coupling

Interfaces are not merely geometric boundaries between phases or grains; they may act as dislocation sources, barriers, sinks, or transmission pathways. Whether an interface promotes or suppresses plasticity depends on its coherency, crystallographic orientation relationship, elastic and shear-modulus mismatch, interfacial chemistry, defect structure, and spacing.

A representative example is the borrowed-dislocations strategy, in which a designed metal/ceramic interface enables mobile dislocations to transfer from the metal into the ceramic phase, thereby reducing the difficulty of dislocation nucleation in the ceramic and enabling tensile ductility [25]. Similarly, in refined Al_2O_3-$GdAlO_3$ eutectic ceramics, submicron-scale interphase boundaries promote the activation of prismatic and basal slip systems in the Al_2O_3 phase that are normally difficult to activate at RT [93]. These studies indicate that interface engineering can alter the activation sequence of dislocation-mediated deformation rather than simply serving as a passive obstacle to dislocation motion.

2.4.2 Dislocation-twinning coupling

Dislocation and twinning activity are closely associated but should not be treated as identical mechanisms. Dislocation slip contributes strain through the motion of lattice dislocations, whereas twinning contributes strain through crystallographic reorientation and twin-boundary migration. Their interaction may be synergistic when twin boundaries lower the barrier for localized slip, promote localized dislocation activity, or accommodate strain through twin proliferation, migration, and detwinning.

For example, in nano-twinned CrN, partial , partial dislocations nucleate and glide near twin boundaries during the early deformation stage, while subsequent twin-boundary evolution and detwinning provide additional strain accommodation and energy dissipation [22]. A recent study further demonstrated that coherent twin-boundary migration-driven detwinning can serve as a direct route to high plasticity in hard ceramics [94]. In nano-twinned 3C-SiC, atomistic simulations also revealed the concurrent operation of twin-boundary-associated deformation, dislocation activity, and phase transformation during ductile-mode cutting [95]. Therefore, the contribution of twinning should be interpreted together with local dislocation processes and twin-boundary mobility, rather than as an isolated deformation mode. The twin boundaries are not only structural features but also active participants in the deformation process. However, twins may also suppress conventional dislocation motion when they act as strong barriers or when the stress state is insufficient to activate twin-boundary migration. Thus, twinning and dislocation slip may exhibit either synergy or competition depending on the local energy barriers and stress distribution.

2.4.3 Grain-boundary diffusion, grain-boundary sliding, and defect-mediated coupling

GBS is frequently coupled with grain-boundary diffusion, local boundary disorder, grain rotation, and interface accommodation. In fine-grained ceramics, the activation of GBS is strongly influenced by grain-boundary chemistry and diffusivity. Xu *et al.* [78] demonstrated that boundary non-stoichiometry in high-pressure-sintered B_4C promotes grain-boundary diffusion and lowers the temperature required for plastic deformation, with GBS becoming the dominant deformation mechanism. This example also highlighted the competitive nature of mechanism coupling. Although twins and other defects may coexist with grain-boundary sliding, they do not necessarily provide the

primary deformation path. In B_4C, the introduced twin structures were not identified as the dominant origin of lower-temperature plasticity, whereas grain-boundary diffusion-assisted sliding was responsible for the observed deformation response. Therefore, coexistence of defects, twins, and grain-boundary activity should not be interpreted automatically as a synergistic mechanism without direct evidence of causal interaction.

2.4.4 Crystalline/amorphous-interface coupling

In ceramic systems containing crystalline and amorphous domains, local deformation can involve stress redistribution between the two phases, interfacial strain accommodation, nanocrystal rotation, amorphous shear flow, and defect-mediated structural rearrangement. The relative contribution of these processes is controlled by phase fraction, interface density, nanocrystal size, defect population, and loading geometry. Recent work on crystalline/amorphous dual-phase TiO_2 ceramic nanofibers showed that high strength, flexibility, and RT plasticity can be achieved by increasing internal interfaces, reducing nanocrystal aggregation, and minimizing fiber-scale defects [38]. The dual-phase architecture was reported to activate multiple deformation mechanisms rather than relying on a single deformation carrier. This finding suggests that amorphous flow and interface-mediated accommodation should be discussed together when interpreting deformation in dual-phase ceramics.

2.4.5 Phase transformation, twinning, and interfacial accommodation

Phase transformation is often accompanied by large local shear and volume strains. Its contribution to irreversible deformation therefore depends on how transformation strain is accommodated by neighboring grains, interfaces, dislocations, transformation variants, or twin-like

interfaces. Consequently, phase transformation should not be considered fully independent from twinning or interface-mediated deformation.

For transformable zirconia-based ceramics, stress-induced martensitic transformation is strongly affected by mechanical confinement, interfacial load transfer, and the ability of adjacent phases to accommodate transformation strain [78]. In ceramic-containing composites, robust interfaces and a deformable surrounding phase can suppress premature fracture while enabling transformation-induced strain accommodation. More generally, a transformation mechanism should be identified separately from twinning unless crystallographic analysis directly confirms the formation and migration of deformation twins or transformation twins. This distinction avoids assigning all transformation-mediated deformation to twinning.

2.4.6 Design rules for synergistic and competitive mechanism coupling

The above examples suggest several general principles for designing coupled deformation mechanisms in ceramics. Synergy is favored when adjacent phases, grains, or interfaces can accommodate the shape strain generated by dislocation slip, twinning, phase transformation, grain-boundary sliding, or amorphous flow. Otherwise, local incompatibility promotes crack initiation. A secondary mechanism can enhance plasticity only when its activation stress is comparable to or lower than the stress required for catastrophic fracture. For example, interfaces may promote dislocation transfer only when the transmission barrier is sufficiently low, while twin boundaries enhance plasticity only when migration or detwinning can occur before cracking. Characteristic length scales must be matched. Fine grain size and high interface density may promote grain-boundary or interface-mediated deformation, whereas excessively small dimensions can suppress dislocation storage or

induce premature interface-dominated failure. The optimum microstructure therefore depends on the relevant deformation carrier and loading condition. A defect that assists one deformation mode may suppress another. For example, grain-boundary diffusion can promote grain-boundary sliding, whereas twin boundaries may either facilitate localized slip or obstruct dislocation propagation. Mechanistic interpretation should therefore identify the dominant carrier of irreversible strain rather than merely list all observed structural features. The presence of dislocations near an interface, twins near a transformed region, or amorphous domains near a crack does not by itself demonstrate a coupled mechanism. Reliable identification requires correlated mechanical and structural evidence, such as *in-situ* TEM, *in-situ* synchrotron diffraction, load-unload experiments, residual-strain measurements, post-deformation orientation mapping, or validated atomistic and multiscale simulations [18, 24, 74].

Overall, the 6 deformation mechanisms mentioned in **Section 2.3** should be understood as interconnected elements of a hierarchical framework. Dislocation slip, GBS, twinning, amorphous flow, phase transformation, and interface sliding may act as primary carriers, accommodation processes, or competing pathways depending on the material architecture and loading environment. Such a coupling-based framework provides a more unified basis for designing RT plastically deformable ceramics.

2.5 Multiple origins of plasticity in ceramics

The origin of plasticity in ceramics remains an open and material-specific issue, and different mechanisms have been proposed even for well-studied ceramic systems. For example, in $SrTiO_3$, RT plasticity has been directly associated with dislocation nucleation and glide during nanoindentation

and compression, while defect chemistry, especially oxygen-vacancy-related effects, has been shown to regulate dislocation nucleation, mobility, and Peierls resistance [30, 50, 96, 97]. In addition, stress-induced ferroelectric phase transitions have also been reported in $SrTiO_3$-related perovskite systems. Uniaxial stress applied normal to the (100) or (110) plane can induce a ferroelectric phase transition in otherwise quantum- paraelectric $SrTiO_3$, accompanied by pronounced changes in the ferroelectric soft mode, which indicates that is $SrTiO_3$ highly susceptible to stress-driven polar structural instability. From the viewpoint of plastic deformation, such stress-induced ferroelectric transformation may provide an additional strain-accommodation pathway under highly localized stress fields, such as indentation or compression. The associated lattice distortion, domain formation, and local symmetry change may interact with dislocation nucleation and motion, suggesting that transformation-assisted plasticity could contribute to the apparent plastic response of $SrTiO_3$ under certain loading and temperature conditions.

In Al_2O_3, high-temperature plasticity has been interpreted in terms of dislocation slip and creep in sapphire (α-Al_2O_3), whereas fine-grained polycrystalline Al_2O_3 is often discussed in terms of GBS, coble-type diffusion creep, and GBS accommodated by slip or diffusion [14, 98-100]. In B_4C, several mechanisms have been proposed, including mobile dislocation activity, shock- or shear-induced amorphization, dislocation-mediated shear amorphization, and nanotwin/planar-defect-assisted deformation [101-104]. In SiC, plastic deformation has been linked to basal dislocation glide, diffusion-accommodated grain-boundary sliding coupled with dislocation glide, grain ration, and stress-induce polytype transformation under indentation [105-107]. In ZrO_2-based ceramics, the plastic response may arise from stress-induced tetragonal-to-monoclinic transformation, dislocation

activity, ferroelastic/domain switching, or a combination of them, depending on the temperature, grain size, dopant content, and crystallographic orientation [77, 108-110].

These examples indicate that ceramic plasticity should not be assigned to a single universal mechanism. In the present study, the predominance of dislocation-mediated plasticity is supported by the direct observation of dislocation-related deformation features and the absence of clear evidence for alternative mechanisms, such as deformation-induced amorphization, stress-induced phase transformation, or extensive grain-boundary sliding. These observations indicate that plastic strain is primarily accommodated through the nucleation, multiplication, and glide of lattice dislocations under the applied stress field. Neverthe8less, considering the complexity of ceramic deformation and the limited spatial and temporal resolution of the current characterization techniques, secondary contributions from phase-transformation-assisted deformation, grain-boundary-mediated processes, or defect-assisted mechanisms cannot be completely ruled out.

2.6 Size effect plasticity

In particular, nanocrystalline ceramics or small-scale mechanical testing have revealed measurable plastic deformation. This size-dependent behavior, often termed the “smaller is stronger and more ductile” phenomenon, see **Fig. 7**(a). The mechanical response of ceramic micro- and nanopillars is strongly size dependent because the dominant deformation and failure mechanisms evolve with specimen dimension. At relatively larger micron-scale dimensions, failure is generally governed by pre-existing cracks, pores, surface damage, or other critical defects. As the pillar diameter decreases, the probability of containing a critical flaw is reduced; consequently, the apparent fracture strength increases, giving rise to the commonly observed “smaller is stronger” behavior. This

regime is therefore referred to as flaw-limited deformation or fracture. When the sample dimension is reduced further, the influence of pre-existing flaws becomes less dominant. In this ultrasmall-size regime, plastic deformation is increasingly controlled by the nucleation of dislocations, often from free surfaces or interfaces, rather than by the propagation of an existing crack. The activation of such dislocation-mediated processes can delay catastrophic fracture and increase the attainable plastic strain, leading to the "smaller is more ductile" behavior. **Fig. 7**(b) schematically summarizes the transition from flaw-limited fracture to dislocation-nucleation-limited deformation in ceramics.

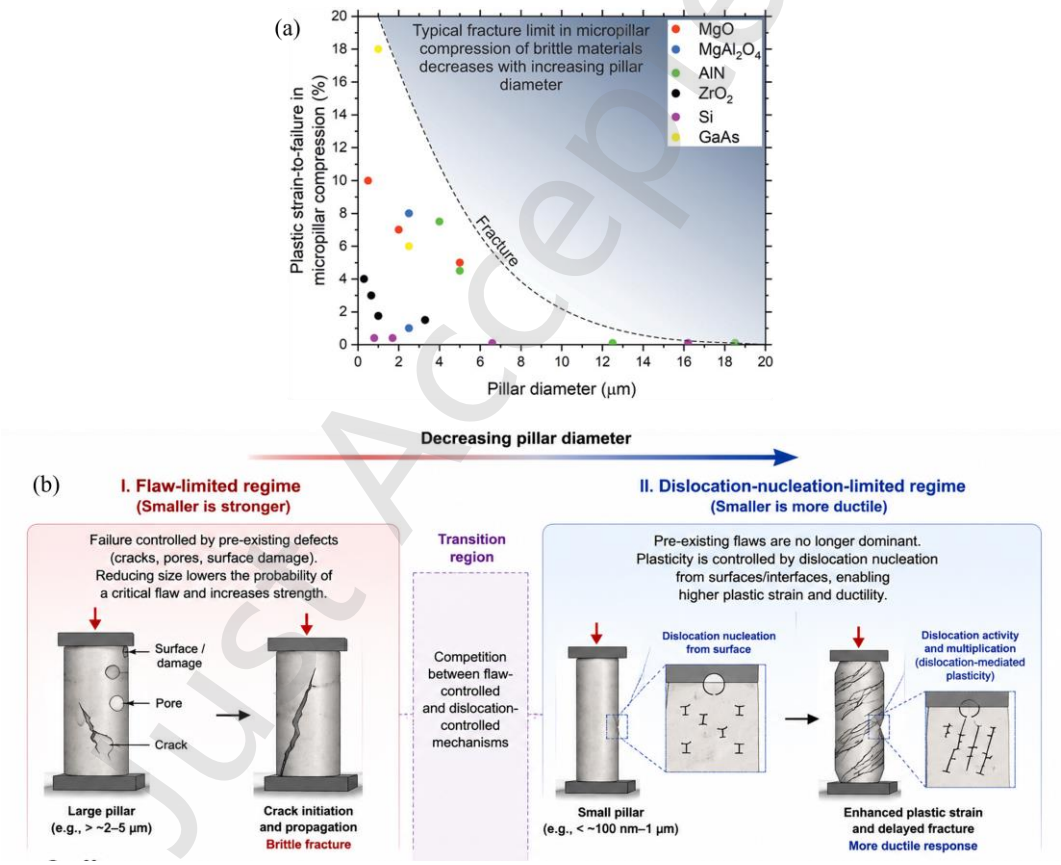

Fig. 7 (a) Reported plastic strain-to-failure in micropillar compression of crystalline ceramics and semiconductor materials at RT. Reproduced with permission from Ref. [111], © Wiley 2023. (b) Schematic illustration of the size-dependent mechanical response of ceramic micro- and nanopillars.

micro-pillar compression studies at RT indicated that the amount of plastic strain-to-failure reached in brittle ceramic, and decreased towards zero when increasing the pillar diameter towards bulkier samples. For metallic, the size effect arises primarily from the suppression of flaw statistics and the transition from source-limited to nucleation-controlled deformation mechanisms when the deformed volume is confined to the micro- or nanoscale for metallic samples [112]. Therefore, the classical Hall-Petch relationship provides a useful conceptual baseline, where strength increases with decreasing grain size due to dislocation-grain boundary interactions [113, 114]. While this relationship is well established in metals, its direct applicability to ceramics is fundamentally limited, and has been widely observed in the hardness of layered ceramics (i.e., cubic BN [115]).

The emergence of plasticity in ceramics at reduced length scales has challenged the conventional view of these materials as inherently brittle at RT. At RT, most ceramics exhibit restricted dislocation mobility due to their strong ionic/covalent bonding and high lattice resistance, thereby suppressing the classical dislocation pile-up mechanism underlying Hall-Petch strengthening [18]. Nevertheless, numerous studies have reported Hall-Petch-like scaling in ceramics, particularly in nanocrystalline systems [116]. This apparent similarity arises not from conventional dislocation activity, but from a combination of alternative mechanisms. First, grain refinement constrains the size of critical flaws, effectively increasing strength through a Griffith-type fracture-controlled mechanism, and grain boundaries can act as barriers to crack propagation, promoting crack deflection and energy dissipation. Moreover, at sufficiently small grain sizes or under high local stresses, limited dislocation activity or grain-boundary-mediated plasticity (e.g., sliding or amorphization) may occur, contributing to deformation [18].

Therefore, it is important to distinguish between intrinsic grain-size strengthening and extrinsic size effects associated with sample dimensions. While the former is often described using a Hall-Petch-like relationship, the latter (commonly observed in micropillar compression or thin films) reflects source-limited plasticity and the "smaller is stronger" paradigm. In ceramics, these effects can coexist and interact, forming a complex size-dependent plasticity landscape. At extremely small grain sizes, deviations from classical Hall-Petch behavior, including inverse Hall-Petch softening, have also been observed [116]. Such behavior is typically attributed to the increasing dominance of grain-boundary-mediated mechanisms, including diffusion and sliding, which reduce the resistance to deformation.

Moreover, Zhou *et al.* [117] demonstrated that a size-dependent transition in deformation mechanisms in nanocrystalline Cr_2AlC MAX phase enables the simultaneous enhancement of hardness and toughness. With decreasing grain size, the dominant deformation mode shifts from dislocation-mediated lamellar slip to grain boundary-mediated and more homogeneous plastic deformation. This transition promotes a more uniform stress distribution and mitigates stress concentration, thereby suppressing crack initiation and propagation. The observed mechanical synergy is attributed to the combined effects of grain refinement strengthening and enhanced energy dissipation via cooperative deformation at grain boundaries. Yuan *et al.* [118] reported that in nanocrystalline Cr_2AlC, Hall-Petch strengthening arises from the high density of grain boundaries that hinder dislocation motion as grain size decreases, while the layered structure further impedes slip yet permits interlayer shear, enabling a combination of ultrahigh strength and retained plasticity. These findings provide a viable pathway for optimizing the mechanical performance of MAX phase materials through microstructural design.

Although the Hall-Petch law cannot be directly applied to ceramics in the same manner as in metals, it remains a valuable reference framework. The observed size effect plasticity in ceramics is better understood as a Hall-Petch-like relationship arising from the interplay of flaw size limitation, grain boundary effects, and emerging plasticity mechanisms at reduced length scales. Amodeo *et al.* [48] summarized in the review further demonstrate that plasticity in MgO (by extension ionic ceramics) exhibits pronounced size effects when deformation is confined to small volumes. At the micro- and nano-scale, mechanical response deviates significantly from bulk behavior, primarily due to the scarcity of pre-existing dislocation sources and the increasing importance of dislocation nucleation and surface-controlled mechanisms. Nano-indentation and micro-compression experiments revealed that plastic deformation often initiates through homogeneous or surface-assisted dislocation nucleation under high local stresses, rather than by activation of pre-existing dislocation networks. As a consequence, the measured strength increases markedly with decreasing sample size.

This size-dependent strengthening is further amplified by limited dislocation storage capacity, enhanced dislocation escape to free surfaces, and reduced probability of junction formation and forest interactions that typically govern strain hardening in bulk crystals. In confined volumes, deformation is frequently dominated by discrete dislocation events, such as the nucleation and propagation of individual loops, leading to intermittent plasticity and strain bursts. Moreover, high local stresses beneath nano-indenters can activate otherwise unfavorable slip systems or promote cross-slip and non-conventional glide planes. These observations highlight that size effects in ceramic plasticity are intrinsically linked to the transition from collective dislocation behavior in bulk to source-limited,

nucleation-controlled mechanisms at small scales, providing critical insights for the design of ultra-hard and damage-tolerant ceramic materials.

Fundamentally, In bulk form, ceramics typically fail catastrophically at stresses well below their theoretical shear strength because critical flaws trigger crack propagation before significant dislocation activity can occur. However, when specimen dimensions or contact are reduced, the probability of containing critical defects decreases dramatically ,enabling stresses to approach the ideal strength required for homogeneous dislocation nucleation or activation of alternative deformation modes such as twinning and stress-induced phase transformations [119].

Two principal experimental approaches have quantified this size effect. First, in spherical nanoindentation, the yield pressure P_y (mean contact pressure at the first pop-in event marking the onset of plasticity) increases markedly with decreasing indenter radius R or contact radius a, following the scaling relations $P_y \propto R^{-1/3}$ or equivalently $P_y \propto a^{-1/2}$ [120]. This size effect at yield initiation reflects a source-starved regime: the highly stressed volume beneath the indenter becomes too small to harbor pre-existing dislocation sources, necessitating higher stresses for nucleation from the free surface or homogeneous mechanisms. The effect is distinct from the more familiar indentation size effect in hardness observed with pyramidal indenters and has been systematically demonstrated across a wide range of ceramics, confirming that plasticity initiation is governed by the stressed volume rather than indentation depth per se.

Advanced experimental approaches, including micro-/nano-compression and *in-situ* TEM, reveal that reducing sample size effectively suppresses pre-existing flaw populations and enables the attainment of near-ideal strength, thereby facilitating dislocation activity before fracture [18]. A more dramatic manifestation occurs in micropillar compression testing, where focused-ion-beam-milled

pillars (diameters typically 0.3-5 μm) of nominally brittle ceramics sustain several percent plastic strain before failure. Compressive strength rises sharply with decreasing pillar diameter d, often following a power-law relation of the form $\sigma_p/\mu = A(d/b)^n$, where μ is the shear modulus, b is the Burgers vector, and the exponent n is smaller in ceramics with high lattice friction than in ductile metals [121].

Failure strains can exceed 7%, accompanied by clear evidence of dislocation glide, twinning, or phase transformations, the behaviors inaccessible in macroscopic samples. In polycrystalline 3Y-TZP, for instance, micropillars exhibit compressive strengths of 6.5-9.3 GPa (versus 3.5-4.3 GPa in bulk) and pronounced plastic barreling; the dominant mechanism is TRIP via the stress-activated tetragonal-to-monoclinic phase change, which is itself size-dependent owing to the reduced flaw population and enhanced transformability at small scales. SEM characterizations of such pillars reveal surface transformation bands and irreversible shape changes in sub-micron specimens, while larger pillars or bulk material remain essentially elastic until catastrophic fracture [119].

Similar size-enabled plasticity has been achieved in other oxides through defect-engineering strategies. In single-crystal TiO_2 and α-Al_2O_3, pristine micropillars remain brittle at RT; however, preloading at elevated temperatures (≈ 600-740 °C) injects high densities of dislocations, stacking faults, and twins that persist upon cooling. Subsequent RT compression then yields 6-10% plastic strain, demonstrating that artificially introduced defects can "import" the small-scale plasticity benefit to otherwise brittle ceramics [21]. Across systems, the governing mechanisms include dislocation starvation (mobile dislocations escape free surfaces faster than they multiply), activation of secondary slip or twinning systems once the CRSS is reached, and reduction of grain-boundary in polycrystalline materials constraints when pillar diameter approaches single-grain dimensions.

These observations collectively establish that the brittle-to-ductile transition in ceramics is not an intrinsic material limitation but a length-scale phenomenon. By confining deformation volume, flaw-controlled fracture is suppressed and dislocation-based or transformation-mediated plasticity is unlocked, opening pathways to ductile-regime machining, nanolattice architectures, and defect-engineered bulk ceramics with improved toughness and formability.

3. Room-temperature plastic ceramic material system

3.1 Oxide ceramics

Oxide ceramics represent one of the most extensively studied classes for RT plastic deformation, primarily through dislocation-mediated mechanisms, though intrinsic plasticity varies significantly across systems such as ZrO_2-based, Al_2O_3, and perovskites (e.g., $SrTiO_3$, $KNbO_3$, and $KTaO_3$) [18]. Perovskite oxides exhibit intrinsic RT bulk plasticity via dislocation glide on the $\{110\}<110>$ slip system, facilitated by a relatively low Peierls barrier, kink-pair formation for dislocation motion, and heterogeneous nucleation from pre-existing defects or seeded dislocation. Moreover, partial dissociation into stacking faults further aids mobility but limits cross-slip, enabling plastic strains up to several percent in bulk compression while coupling with functional properties like ferroelectricity. In contrast, rock-salt oxides such as MgO (often grouped with perovskites in comparisons) share the $\{110\}<110>$ system but feature extended, charge-neutral dislocation cores stabilized electrostatically, allowing Frank-Read multiplication and work hardening with lower CRSS.

ZrO_2-based systems, including Y-TZP or alumina-toughened zirconia (ATZ), typically rely on transformation-induced plasticity (tetragonal-to-monoclinic phase) or doping (e.g., Ti co-doping) to induce localized plastic flow and enhanced toughness at RT, rather than pure dislocation slip [122].

This mechanism provides strain accommodation via volume expansion but is less ductile than perovskites and often requires microstructural tailoring for noticeable yielding. α-Al_2O_3 and rutile TiO_2, conventionally brittle at RT due to high lattice friction, achieve substantial plasticity (6-10% strain in micropillar compression) only through defect-engineering strategies such as elevated-temperature preloading, which injects high densities of mobile dislocations, stacking faults, and twins [21]. Then, subsequent RT deformation proceeds via stacking faults/twin boundary migration and dislocation interactions leading to work hardening, mechanisms absent in pristine crystals but analogous to metallic behavior once defects are pre-introduced. Overall, perovskites and MgO-like oxides demonstrate intrinsic, dislocation-core-governed plasticity with low slip resistance, while ZrO_2 leverages phase transformations, and Al_2O_3 and TiO_2 depend on extrinsic defect populations, highlighting the role of bonding ionicity/covalency and defect engineering in enabling RT plasticity across oxides. Zhang *et al.* [123] introduced 1D prismatic dislocation loop array in wurtzite zinc oxide (ZnO) using nanoindentation not only advances the understanding of dislocation-based plasticity but also provides a strategy for the controlled formation of highly ordered PDL arrays in ceramics.

3.2 Non-oxide ceramics

Non-oxide ceramics, exemplified by Si_3N_4, BN, and SiC, achieve RT plasticity through mechanisms distinct from dislocation slip in oxides, often exploiting covalent bonding, phase interfaces, or layered architectures in dual-phase or nanostructured forms. Si_3N_4 is generally regarded as a brittle structural ceramic because of its strong covalent Si-N bonding. However, recent small-scale experiments demonstrate that β-Si_3N_4 single crystals can undergo measurable RT plastic deformation under sufficiently high local stresses [124-126]. Nanoindentation reveals pronounced

crystallographic anisotropy, with hardness increasing from basal to prismatic orientations, whereas the indentation modulus shows the opposite trend, consistent with orientation-dependent slip activation [125]. Plasticity is dominated by prism $\langle c \rangle$ slip, i.e., $\{10\bar{1}0\}\langle 0001 \rangle$, through the nucleation and glide of [0001] dislocations [124-126]. Micropillar compression and microcantilever bending measurements reported critical resolved shear stresses of approximately 1.34-1.66 GPa, confirming that dislocation-mediated plasticity can occur at RT before fracture [124, 126]. Nevertheless, the deformation remains highly anisotropic and limited by a high Peierls barrier for screw [0001] dislocations[124, 126].

BN, particularly in twisted-layer bulk ceramics, displays exceptional compressibility (up to 14% strain) and permanent plasticity (~8%) via kinking, delamination, and ripplocations within interlocked nanoplates; twisted interfaces drastically reduce interlayer shear modulus and sliding energy barriers (by ~2 orders of magnitude), promoting omnidirectional kink formation and energy dissipation far superior to conventional h-BN, with minimal reliance on dislocations [20, 127].

SiC shows RT plasticity primarily at small scales (e.g., nanowires achieving large strains near RT [128]), attributed to size-dependent dislocation activity or confined deformation, though bulk examples are less common and often require HPT or dual-phase designs analogous to Si_3N_4. Comparing these, Si_3N_4 relies on coherent-interface bond switching for phase-enabled flow, BN on van der Waals (vdW)-enabled interlayer gliding and extrinsic kinking in twisted architectures, and SiC on scale effects or similar interface mechanisms, collectively underscoring that covalent non-oxides achieve plasticity through structural hierarchy or interface engineering rather than the intrinsic low-Peierls dislocation motion prevalent in oxides.

Sulfide ceramics, including rock-salt types (e.g., PbS, and SmS) and wurtzite/sphalerite structures (e.g., ZnS, CdS, and CdSe), demonstrate RT plasticity predominantly via dislocation-mediated glide, with notable sensitivity to electronic effect. Rock-salt sulfides such as SmS and PbS deform on $\{110\}<110>$ or $\{100\}<110>$ systems through kink-pair mechanisms con compact or extended cores, similar to oxide rock-salt analogs but with enhanced mobility due to lower ionicity. Wurtzite sulfides (CdS, ZnO-analogous) and sphalerite ZnS activate basal/prismatic $\{0001\}<1120>$ or $\{110\}<110>$ slips with extensive partial dislocation dissociation (low stacking-fault energy), enabling individual partial motion and large plastic strains. A hallmark is photo-plasticity, where illumination alters core reconstruction and charge-carrier trapping [129], dramatically reducing plasticity (e.g., see **Fig. 8**, ZnS fractures at ~2% strain under UV but reaches ~45% in darkness [130]). Across sulfides, mechanisms converge on dislocation core structure governing mobility (partial vs. compact) and electronic modulation (photo-plastic or charge-dislocation effects), contrasting the more ionic, defect-engineered plasticity in oxides and interface-driven modes in non-oxides, which allows intrinsic bulk in many sulfides without extensive preprocessing. Bismuth chalcogenides exhibit stress-temperature-induced plasticizing (>50% strain) or high-pressure cold-pressing effects that promote local plastic flow via grain elongation and low-angle boundary formation [131].

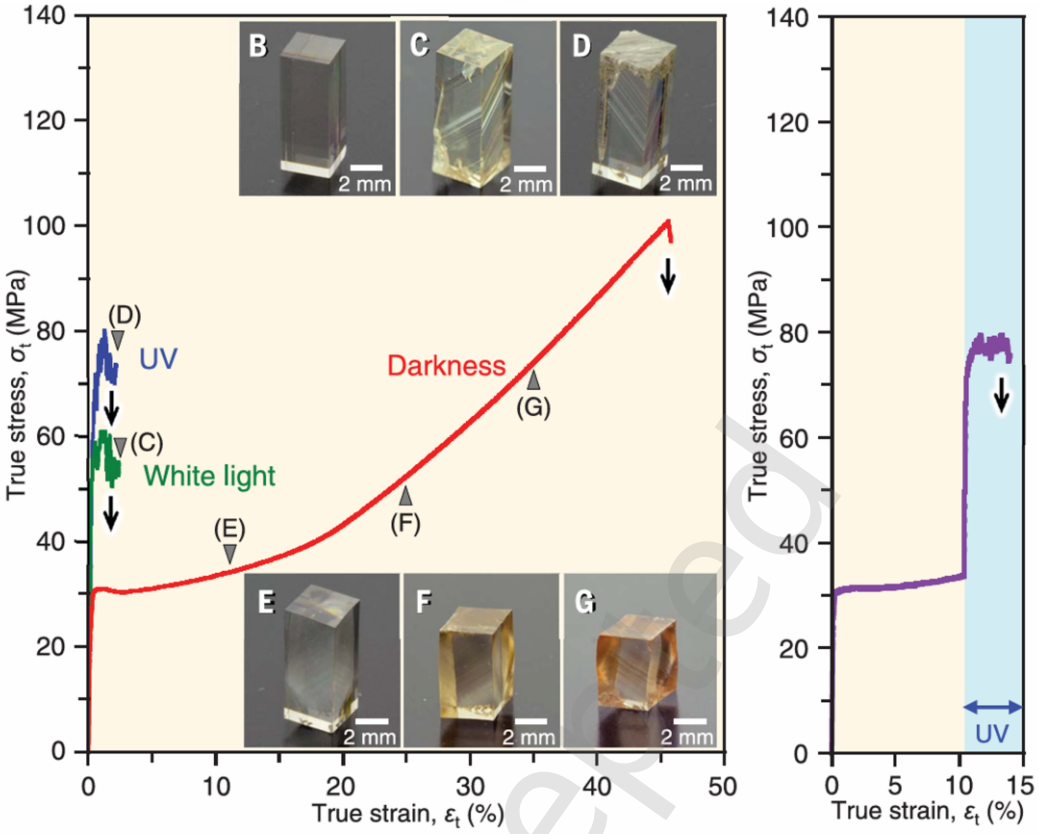

Fig. 8 Characterizations of plastic deformation of single crystal ZnS at RT under white or UV light or in complete darkness. Reproduced with permission from Ref. [130], © AAAS 2018.

3.3 Inorganic thermoelectric materials

Inorganic plastic thermoelectric materials overcome the intrinsic brittleness of traditional inorganic thermoelectric compounds and the inferior electrical transport properties of organic thermoelectric materials, achieving exceptional RT deformability and superior thermoelectric properties, which endows them with promising application potential of thermoelectric technology in solid cooling, power generation and flexible electronics. The conventional perception that inorganic semiconductors are intrinsically brittle was first overturned by the pioneering work by Lidong Chen and co-works, see **Fig. 9**. Their research established a new class of plastic inorganic thermoelectric materials, which exhibit metal-like deformability at or near RT while retaining favorable thermoelectric performance.

The initial breakthrough emerged from the discovery of RT plasticity in silver chalcogenides, particularly α-Ag_2S-based compounds, which established the foundation for the field of plastic inorganic semiconductors [132]. This discovery demonstrated that certain inorganic compounds can sustain large plastic deformation via dislocation motion rather than brittle fracture. Then, a notable advancement was reported that where bulk single-crystalline InSe exhibited extraordinary plastic deformability [133]. This unusual behavior originates from its layered structure, where weak interlayer vdW interactions enable facile slip, while strong intralayer bonding preserves structural integrity. Subsequent work further revealed that such plasticity can be associated with unconventional mechanisms such as martensitic transformation-induced plasticity [134], providing new insights into deformation pathways beyond traditional dislocation-mediated processes. Building on these insights, they extended the concept to broader material systems and dimensionalities. For example, they demonstrated that layered 2D materials can simultaneously achieve high thermoelectric performance and mechanical flexibility [135]. Importantly, the concept of plasticity has been successfully translated into device level application, plastic inorganic semiconductors were directly integrated into flexible thermoelectric devices, demonstrating stable performance under bending and mechanical deformation [136].

Pristine Bi_2Te_3 is brittle, but high-density antisite defects (e.g., via processing) enable plastic deformation by facilitating dislocation glide and microstructural accommodation, yielding high strains while preserving or enhancing thermoelectric performance [137, 138]. A related study further identifies sub-lattice amorphization as a key mechanism enabling plastic deformation in inorganic semiconductors [139]. These findings suggest that local structural disorder can effectively accommodate strain and suppress crack propagation, enabling a brittle-to-ductile transition. Most

recently, a warm metalworking strategy has been introduced to enable plastic forming of brittle semiconductors at intermediate temperatures [140]. Under such conditions, deformation is governed by shear banding, lattice distortion, and cooperative atomic motion, allowing processes such as rolling and forging to be applied to semiconductors. This approach bridges the gap between ceramic processing and metallurgical techniques, establishing a new paradigm for the manufacturing of inorganic functional materials.

Complementarily, high-throughput computational screening further identified a wide range of deformable vdW crystals, suggesting that plasticity is a more universal phenomenon than previously assumed [141]. Another important direction involves phase engineering and compositional tuning. They demonstrated that phase boundaries can significantly influence both mechanical compliance and thermoelectric transport [142]. Similarly, they revealed that alloying strategies can enhance both plasticity and energy conversion efficiency [143].

A major conceptual advance was the identification and realization of p-type plastic thermoelectric materials, as reported [144]. This work resolved a key limitation in device applications by enabling both n-type and p-type legs with mechanical deformability. Moreover, the concept of plastic inorganic thermoelectric materials, including p-type systems, has been proposed and experimentally validated. These materials simultaneously exhibit mechanical deformability and high thermoelectric performance, overcoming the long-standing trade-off between functionality and mechanical robustness. This advancement has also enabled the development of flexible and deformable thermoelectric devices.

More recently, the field has moved toward precise control of deformation mechanisms through phase boundary engineering. For instance, they demonstrated that morphotropic phase

boundaries can simultaneously optimize carrier transport and plastic deformation behavior [145]. A comprehensive perspective summarized the evolution from fundamental discovery to materials design principles, which established a unified understanding that plasticity in inorganic thermoelectric ceramics originates from a combination of the weak or anisotropic chemical bonding, low shear modulus, and accessible slip systems, including interlayer sliding and dislocation-mediated mechanisms [146].

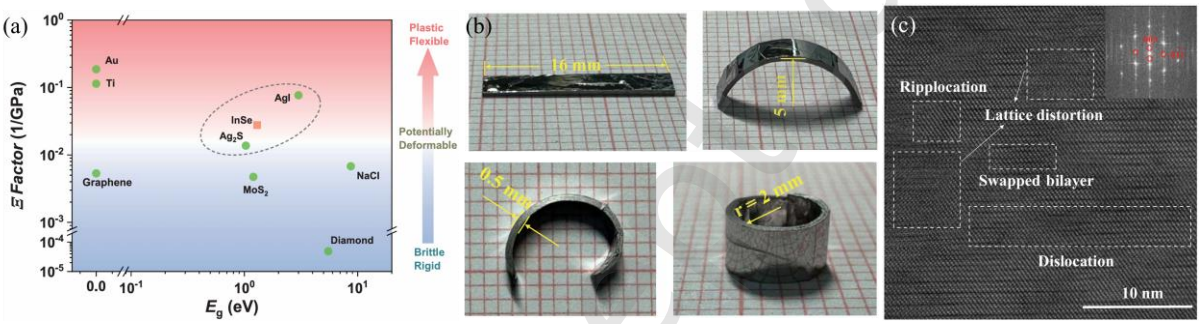

Fig. 9 Representative research results on plastic inorganic thermoelectric materials. (a) Deformation factor (Ξ) and band gap (E_g) of different materials; (b) digital photo of a Te_3Bi_2 sample; (c) defects in the Bi_2Te_3 sample. $\Xi = (E_c/E_s)(1/E_{in})$ as a function of E_g (E_c and E_s are the cleavage energy and slipping energy of the slip system, respectively; E_{in} is the Young's modulus along the slip direction). (a) Reproduced with permission from Ref. [133], © AAAS 2020, (b) and (c) reproduced with permission from Ref. [137], © AAAS 2024.

3.4 Amorphous/high-entropy ceramics

Amorphous ceramics (e.g., amorphous SiO_2, amorphous boron-based ceramics, and glassy oxide/nitride systems) and high-entropy ceramics (HECs, including high-entropy oxides, carbides, nitrides, and borides) represent two emerging classes of materials that challenge the traditional brittle paradigm of ceramics. Although fundamentally different in atomic order, long-range disorder in amorphous ceramics versus chemically complex but crystalline lattices in HECs, both systems exhibit

enhanced RT plasticity through mechanisms that fundamentally deviate from conventional dislocation-mediated deformation.

In amorphous ceramics, the absence of long-range periodicity precludes classical dislocation activity. Instead, plastic deformation is governed by localized shear transformation zones (STZs), which are nanoscale regions where atoms undergo cooperative rearrangement under applied stress. These STZs can percolate into system-spanning shear bands, leading to macroscopic plastic flow [147]. However, due to strain localization, amorphous ceramics often exhibit limited tensile ductility and are prone to catastrophic shear band failure. Plasticity can be improved through structural heterogeneity, such as introducing nanocrystals, compositional modulation, or free-volume engineering, which promotes shear band branching and delays localization. In some glassy ceramics, especially under nanoscale confinement or high pressure, distributed plastic flow rather than single shear banding has been observed, indicating a transition from brittle-like to plastic-like amorphous deformation. Frankberg *et al.* [111] pointed out that amorphous α-Al_2O_3 stands out as a unique diatomic glassy material with prominent nanoscale RT plasticity, see **Fig. 10**. By employing *in-situ* micropillar compression experiments, they verified that the plastic deformation capability of α-Al_2O_3 can be extended from the nanoscale to the microscale even under high strain rates. The α-Al_2O_3 micropillars can sustain compressive strain up to 51% without fracture, governed by the coupled effect of viscous creep and shear band slip propagation. Large-scale molecular dynamics simulations well reproduce the experimental results and further confirm the underlying plastic deformation mechanism at the atomic level.

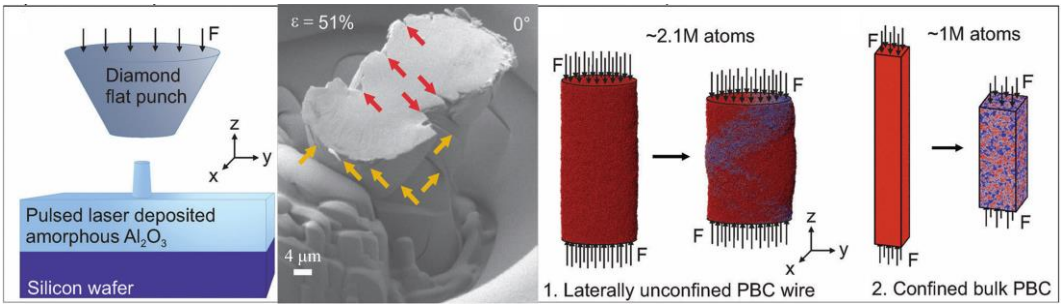

Fig. 10 Experimental and simulated micropillar compression of amorphous α-Al_2O_3 at RT. Reproduced with permission from Ref. [111], © Wiley 2023.

In contrast, HECs possess a crystalline lattice with severe lattice distortion arising from multi-principal element solid solution disorder. This chemical complexity significantly modifies the energy landscape for defect formation and motion. The dominant plasticity mechanism in HECs is still dislocation-mediated slip, but with markedly altered characteristics, such as the lattice distortion increases Peierls stress and inhibits easy dislocation glide, compositional fluctuations create spatially varying energy barriers, leading to heterogeneous dislocation activity, and local chemical disorder promotes dislocation pinning-unpinning processes, resulting in intermittent or avalanche-like plastic flow. Additionally, in some HECs, especially high-entropy carbides, grain-boundary-mediated deformation, including GBS and rotation, becomes increasingly important at nanoscale grain sizes. Csanádi *et al.* [148] investigated the deformation behavior of (Hf-Ta-Zr-Nb)C high-entropy carbides through micropillar compression and demonstrated that these ceramics exhibit enhanced yield strength, strain hardening, and activated slip compared with conventional refractory carbides. Sangiovanni *et al.* [149] showed that the plasticity and fracture resistance of high-entropy carbides can be tailored through the valence electron concentration; compositions with higher valence electron concentrations were found to promote local structural transformations and facilitate dislocation-mediated deformation. In high-entropy oxides, Han *et al.* [150] reported ultra-dense dislocations

stabilized by configurational entropy, suggesting that the high-entropy effect can reduce the energetic instability of dislocations and thereby improve the potential for plastic deformation. Similarly, Wang *et al.* [151] revealed a pronounced grain-size dependence in the RT deformation of (Co,Cu,Mg,Ni,Zn)O high-entropy oxides: micron-sized grains primarily deform through dislocation slip, whereas nanocrystalline materials exhibit GBS and intergranular fracture. In addition, Bian *et al.* [152] explored entropy-boosted amorphous ceramics and proposed a liquefaction-induced plasticity mechanism that enables exceptionally large plastic deformation. More recently, Zhang *et al.* [153] examined the deformation and hardening mechanisms of AlCrNbSiTiN high-entropy nitride nanocomposite coatings, highlighting the importance of nanoscale structural design in improving deformation tolerance. Overall, these studies indicate that the plasticity of HECs can be enhanced through compositional complexity, valence-electron regulation, dislocation stabilization, grain-size control, and amorphous structural design. There is emerging evidence that chemical complexity can stabilize multiple slip systems and enhance strain delocalization, thereby improving damage tolerance compared to conventional single-component ceramics.

Comparatively, amorphous ceramics rely on topological rearrangements without crystalline defects, while high-entropy ceramics deform through defect-mediated processes within a highly disordered crystalline lattice. Both systems achieve enhanced plasticity by introducing structural complexity that suppresses catastrophic crack propagation: amorphous ceramics through distributed STZ activation, and HECs through frustrated dislocation motion and heterogeneous strain partitioning. Despite these advances, both classes still face a common limitation, strain localization (shear banding in amorphous systems and dislocation channeling in HECs), which remains the central challenge for achieving true tensile ductility at RT.

3.5 MAX phases

The MAX phases represent a diverse class of nanolaminate materials with appealing properties that have received incredible global research attention because they bridge the gap between metals and ceramics [154]. As a unique family of ternary layered carbides and nitrides, MAX phases exhibit well-defined chemical composition and nanolaminate structure, which are the fundamental basis for their distinctive combination of metallic and ceramic properties, making them a promising class of materials for various advanced applications [155]. And the highly ordered layered stacking mode determines their physical and mechanical properties.

MAX phases in a hexagonal lattice with space group $P6_3/mmc$ consist of alternating layers of edge-sharing, distorted XM_6 octahedra (the ceramic-like component) and single planar layers of A-group elements (the metallic-like component). The M-X layers are bonded through strong covalent or ionic bonds, which endow MAX phases with ceramic-like advantages such as high elastic modulus, excellent high-temperature resistance, oxidation resistance, and corrosion resistance [156, 157]. In contrast, the A-group element layers are connected to the M-X layers via relatively weak metallic bonds, which grants them metallic characteristics including good electrical and thermal conductivity, plasticity, machinability, and resistance to thermal shock [154]. This layered architecture leads to strong covalent/ionic bonding within the M-X slabs and relatively weaker metallic bonding between M and *A*layers, creating anisotropy in both mechanical and electronic properties [158].

The nano-laminated structure is directly responsible for the unusual mechanical behavior of MAX phases. The layered structure also brings inherent challenges to RT plasticity of MAX phases. Most polycrystalline MAX phases exhibit brittleness at RT, which is primarily attributed to their pronounced plastic anisotropy arising from the high c/a ratio (> 4) and the limited slip systems [159].

It is well established that basal plane dislocations are abundant and mobile in MAX phases at RT [160], but these dislocations are constrained to the basal planes, resulting in fewer slip systems than the five required for polycrystalline plasticity, thus leading to pseudo-plasticity under confined deformations rather than true RT plasticity.

However, several typical MAX phases (e.g., Ti_3SiC_2, Ti_2AlC, and Cr_2AlC) possess exceptional damage tolerance and limited RT plasticity, which originate from their intrinsic layered crystal structures that enable kink band formation, and reversible deformation [117, 161-164]. Under external mechanical loading, deformation can occur via basal plane slip, delamination, and the formation of kink bands, all of which are facilitated by the relatively weak bonding at the M-A interfaces [164-166]. Consistent with these structural advantages, recent experimental investigations have verified that tailored MAX phase microstructures, such as fine-grained and textured architectures, can introduce distinct RT plastic deformation capacity, especially under compressive loading [159]. Such unique mechanical responses of MAX phases, which are rarely observed in traditional brittle ceramics, stem from the synergistic operation of multiple microscopic deformation modes: kink band evolution, basal dislocation glide enabled by weakly bonded A atomic layers, and interfacial crack deflection [155, 158]. *In-situ* mechanical characterization and TEM observations further confirm that the mechanical failure of MAX phases is dominated by reversible and irreversible kinking deformation, rather than the intrinsic brittle fracture that governs conventional structural ceramics [158]. Moreover, Tromas *et al.* [73] reveals a novel plastic deformation behavior of MAX-phase Ti_2AlN under nanoindentation-induced localized high shear stress and hydrostatic pressure suppress basal slip and activate $\{11\bar{2}2\}$ compressive twinning and $\{11\bar{2}1\}$ tensile twinning, see **Fig. 11**. Deformation twinning serves as the primary plastic carrier, accompanied by secondary twinning

structures and minor basal ⟨a⟩ dislocation slip, which provides an alternative strain accommodation strategy and expanding the fundamental understanding of the plastic behaviors of layered MAX phases.

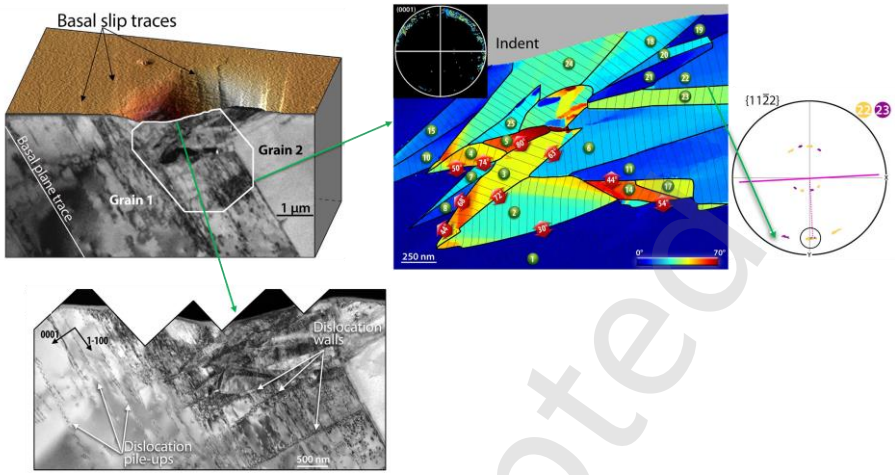

Fig. 11 Nanoindentation-induced deformation twinning in MAX phase Ti_2AlN [73], © Elsevier Ltd., 2022.

4. Material-design strategies for achieving RT plasticity in ceramics

The intrinsic brittleness of ceramics originates primarily from their strong ionic/covalent bonding, high lattice resistance to dislocation motion, limited availability of independent slip systems, and the dominance of flaw-controlled fracture over plastic flow. To overcome these limitations, a variety of material-design strategies have been developed to either activate existing deformation mechanisms mentioned above or introduce new pathways for strain accommodation at RT. A "strategy" refers to a deliberate structural, defect, compositional, or interfacial design approach that reduces the activation barrier for plastic deformation, promotes stable strain accommodate, or suppresses premature catastrophic fracture. These strategies include defect-mediated activation of dislocation plasticity, nanostructure design, coherent interface engineering, layered architectures, multiphase composite design, and so on. Therefore, the emphasis of this section is on how these

fundamental deformation mechanisms can be engineered and combined to improve RT plastic deformability in ceramics.

Recent tribological studies further demonstrate the importance of microstructural design principles. For example, Ti-modified MoS_2 coatings exhibit improved cryogenic wear resistance because local Ti-S coordination and interlayer pinning suppress interlayer sliding, delamination, and stress localization during sliding contact [167]. Similarly, bioinspired graphene/CoCrNi multi-principal element alloy composites with self-assembled lamellar architectures show that well-dispersed graphene and layered interfaces can simultaneously improve wear resistance and reduce friction [168]. These findings illustrate that layered structures and interface-mediated deformation can be used not only to enhance mechanical properties but also to improve tribological reliability. Structural heterogeneity is also highly relevant to amorphous and amorphous/crystalline systems. In Zr-based metallic glasses, cooling-rate-induced nanoscale heterogeneity can substantially regulate nano-wear behavior by modifying the distribution of local soft and hard regions, the susceptibility to shear transformation, and the degree of localized plastic accommodation [169]. Such observations suggest that controlled heterogeneity may provide a useful design strategy for plastic ceramics and ceramic-based composites, particularly where resistance to localized deformation, cracking, and surface damage is required.

4.1 Defect-mediated activation of plasticity

4.1.1 Defect engineering

In defect engineering, oxygen-vacancy regulation is particularly effective in oxide ceramics. Controlled introduction of oxygen vacancies, via doping (e.g., CuO “hard” doping in KNN-based

piezoceramics) or non-equilibrium processing, reduces the Peierls stress and misfit energy for dislocation nucleation, promoting incipient plasticity and creep resistance while simultaneously pinning mobile dislocations for strengthening [170]. In flash-sintered or preloaded oxides such as TiO_2 and Al_2O_3, abundant oxygen vacancies further weaken friction stresses on dislocation cores, enabling RT compressive plasticity exceeding 6-7.5% strain [21]. Dislocation-density regulation, achieved through elevated-temperature preloading, HPT, or cyclic scratching, introduces densities up to 10^{15} m^{-2}; these pre-existing dislocations, stacking faults, and twins persist upon cooling and serve as mobile sources for RT slip, yielding plastic strains of 10-70% in MgO, $SrTiO_3$, and rutile TiO_{2-x}. Lattice-distortion engineering via cation/anion doping (e.g., La^{3+}, Zr^{4+}, Sr^{2+} co-doping in perovskites) induces local structural heterogeneity, activates additional slip systems, and facilitates reversible phase transitions that absorb deformation energy [171].

Wu *et al.* [172] developed a high-entropy 211 MAX phase, $(TiZr_{0.6}NbTa)_2AlC$, by introducing multiple principal transition-metal elements into the M sublattice to deliberately generate local chemical fluctuations within the layered structure. This compositional complexity produces spatial variations in lattice distortion and bonding, which increase lattice friction and impede dislocation glide, thereby providing strong solid-solution strengthening. More importantly, the local chemical fluctuations modify the dislocation-mediated deformation behavior by facilitating dislocation activation, interaction, and multiplication across multiple slip modes, which suppresses strain localization and sustains plastic deformation.

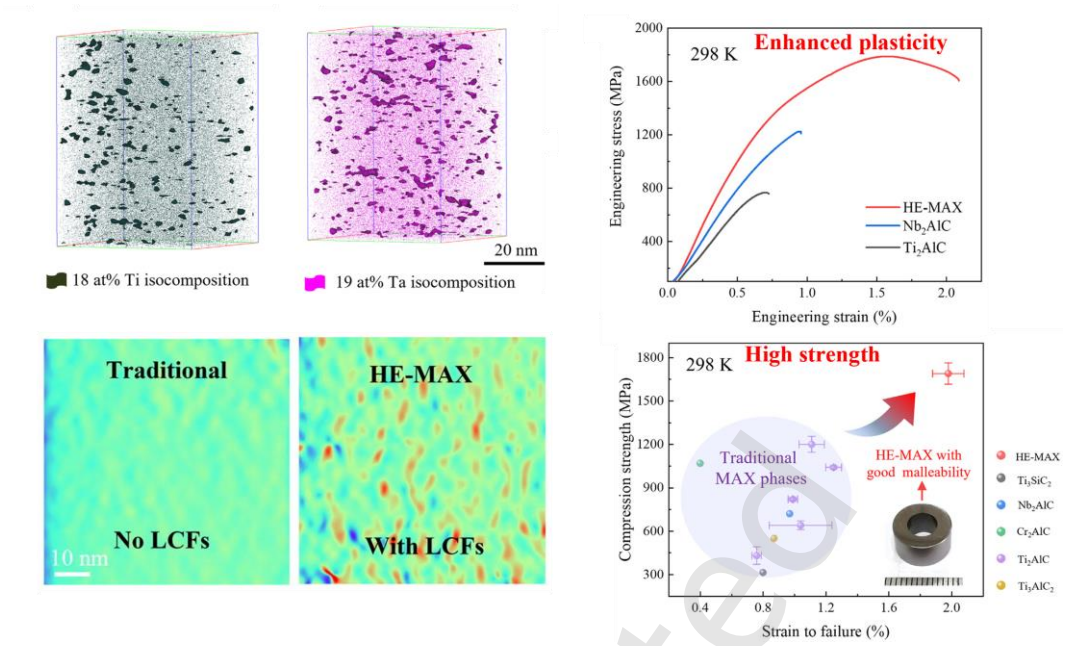

Fig. 12 High-entropy MAX phase with ultrahigh strength and large plasticity mediated by local chemical fluctuations [172], © Elsevier Ltd., 2025.

4.1.2 Dislocation seeding

See **Fig. 13**, a notable strategy to overcome this limitation is the introduction of mechanically seeded dislocations, as demonstrated in recent studies [19]. In this approach, high-density dislocations (~10^{14} m^{-2}) are artificially introduced into the ceramic lattice via mechanical pre-treatment methods such as nanoindentation or micropillar compression. These pre-existing dislocations act as readily available carriers for plastic deformation, bypassing the need for energetically costly dislocation nucleation. Once activated under applied stress, these dislocations can glide, interact, and multiply, giving rise to collective dislocation dynamics analogous to those observed in metals, including cross-slip and dislocation avalanches. This transition enables substantial plastic strain at RT, in some cases exceeding 30%, while simultaneously suppressing catastrophic crack initiation and propagation. The presence of a high initial dislocation density effectively shifts the deformation mechanism from flaw-controlled brittle fracture to dislocation-mediated plastic flow.

This emerging concept of dislocation engineering in ceramics represents a paradigm shift in the design of structural and functional ceramic materials. By tailoring defect populations and their mobility, it becomes possible to achieve a balance between strength and plasticity that was previously inaccessible in these systems. Such advances open new opportunities for the development of damage-tolerant ceramics for applications in extreme environments, microelectronics, and energy systems.

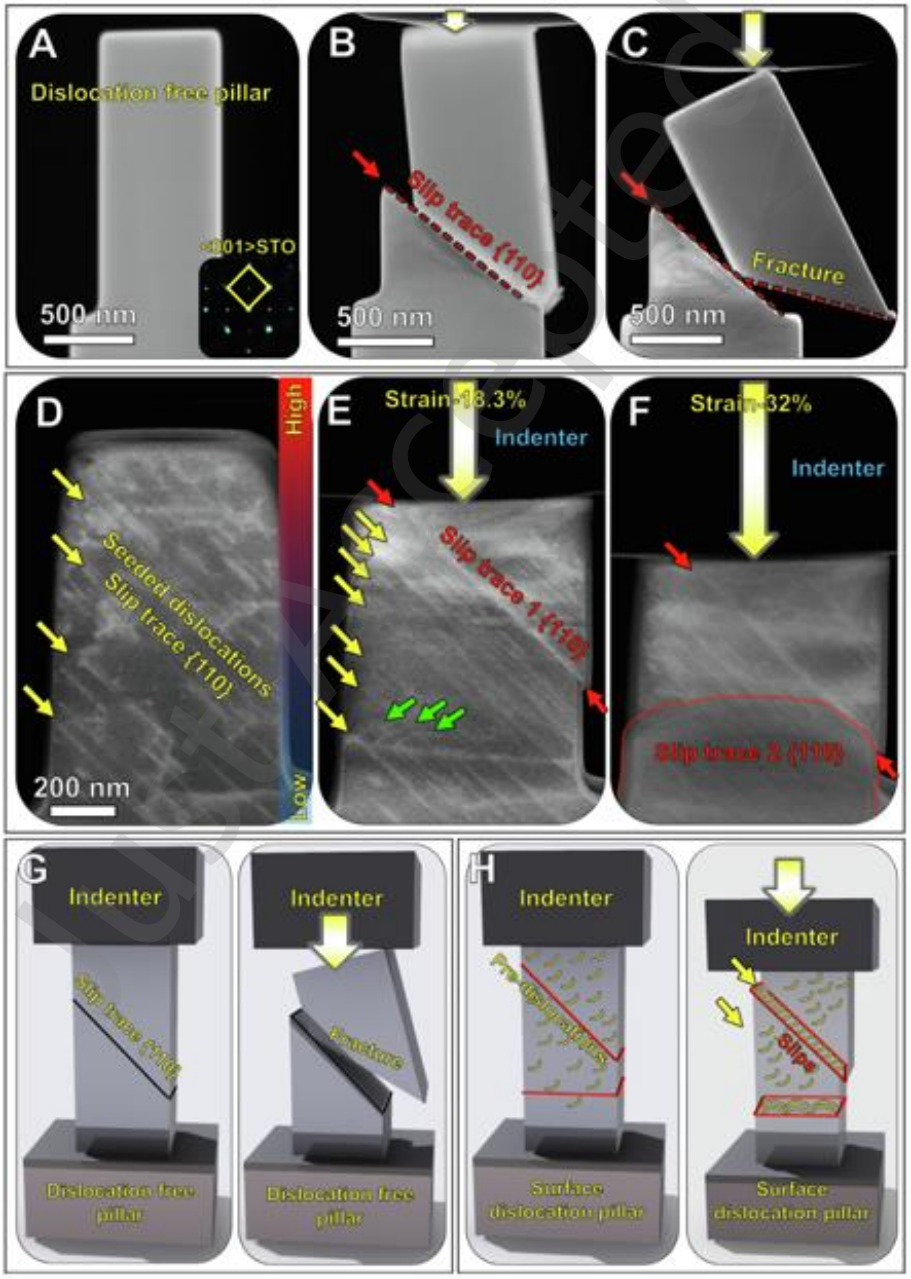

Fig. 13 Mechanically seeded dislocations strategy to achieve RT plasticity in $SrTiO_3$. Reproduced with permission from Ref. [19], © Elsevier Ltd. 2025.

4.1.3 High-temperature preloading

Shen *et al.* [21] established elevated temperature preloading as a robust and generalizable strategy for imparting substantial RT plasticity to inherently brittle single crystal TiO_2, see **Fig. 14**. By deliberately introducing a high density of mobile defects, primarily dislocations, stacking faults, and twins, through controlled plastic deformation at elevated temperatures (e.g., 600 ℃ for TiO_2 and analogous conditions for α-Al_2O_3), the critical barrier to dislocation nucleation at RT is effectively bypassed. Subsequent uniaxial compression of preloaded single-crystal micropillars demonstrates dramatic enhancements in deformability: TiO_2 achieves ~10 % compressive strain with pronounced work hardening, shear-band formation, and crack deflection, while α-Al_2O_3 reaches 6-7.5% strain without immediate catastrophic failure. Detailed TEM reveals that pre-injected defect seeds multiply and interact during RT loading, generating intersecting slip systems, sessile dislocations (such as Lomer locks), and stacking-fault ribbons that simultaneously accommodate plastic strain, promote work hardening, and impede crack propagation.

A comprehensive review of RT dislocation plasticity in ceramics highlights elevated-temperature preloading alongside HPT, irradiation, flash sintering, and interface-mediated strategies as key pathways toward bulk-scale plasticity [18]. The approach is scalable in principle to polycrystalline systems and holds promise for expanding the use of ceramics in structural, electronic, and HT applications where plasticity is a limiting factor. Future efforts should focus on optimizing preloading parameters, validating performance in bulk samples, and incorporating microstructural tuning or alloying to further stabilize and scale the induced plasticity.

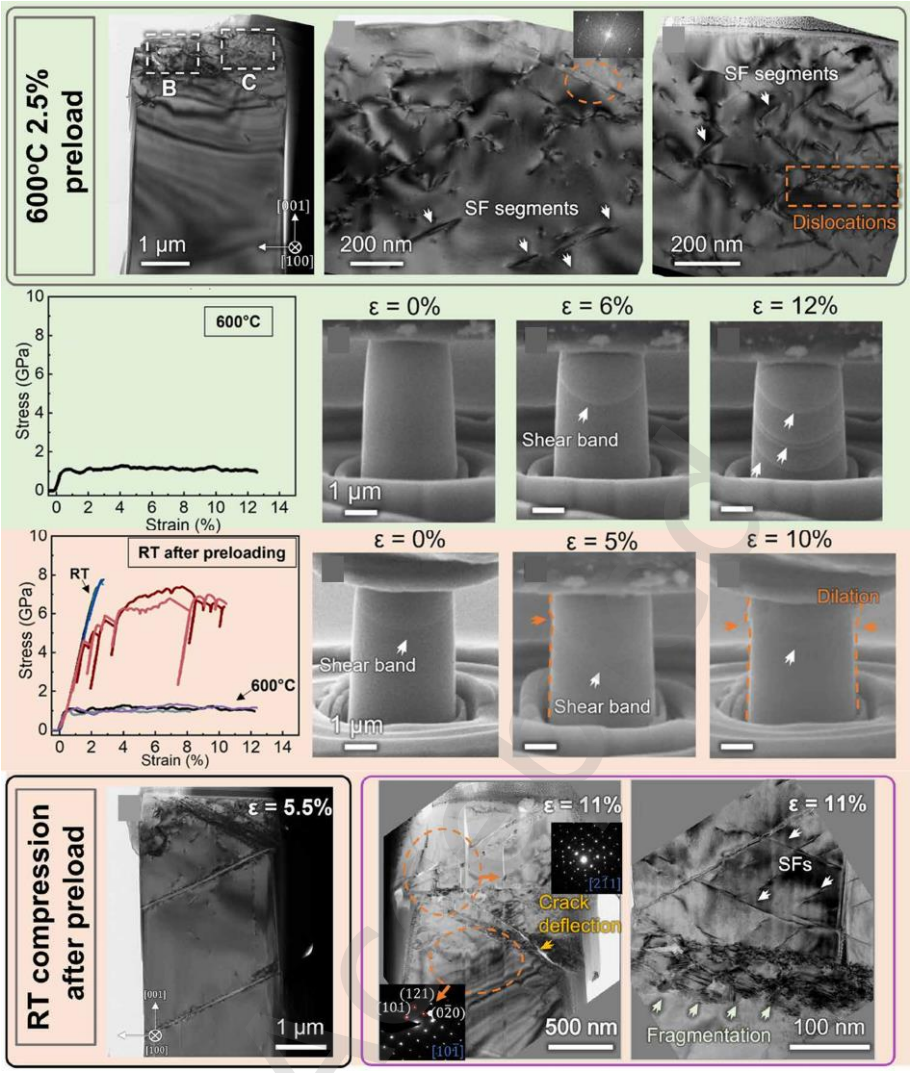

Fig. 14 Uniaxial *in-situ* micro-compression tests on the single crystal TiO_2 through elevated temperature preloading strategy. Reproduced with permission from Ref. [21], © AAAS, 2024.

4.1.4 External field-mediated regulation

External field regulation has emerged as the primary pathway to overcome the intrinsic brittleness of ceramics and enable large plastic deformation, including super-plasticity and even RT plasticity. Rather than altering the strong ionic-covalent bonding inherent to ceramic structures, external fields (e.g., electric/current, temperature, stress, magnetic, ultrasonic, or optical) supply additional energy to lower the activation barriers for dislocation glide, GBS, phase transformations, and diffusion processes. This effectively expands the plastic deformation window from high

temperature regimes (>0.6 T_m) toward intermediate or RT while simultaneously increasing strain rates and suppressing crack initiation and propagation.

The core logic of external-field-mediated plasticity relies on targeted energy input that activates mobile defects without modifying the material's fundamental chemistry. As shown in **Fig. 15**, electric/current fields are the most mature and temperature-reducing approach [173]. The electro-plasticity effect (EPE) arises from localized Joule heating, field-driven ion migration, oxygen-vacancy proliferation, grain-boundary amorphization/softening, and electron-wind forces that reduce dislocation resistance and promote dislocation multiplication [174]. Flash sintering and spark plasma sintering (SPS) further integrate rapid densification with *in-situ* defect introduction, enabling simultaneous sintering and plastic forming. Representative examples include 3Y-TZP zirconia achieving >135% tensile superplastic strain at 1000 °C under DC electric fields (versus >1400 °C conventionally) and SiAlON or Al_2O_3 ceramics undergoing successful plastic forging at 1400-1500 °C via SPS, approximately 300 °C lower than conventional hot pressing. Pulsed electric fields have also dramatically enhanced super-plasticity in Si_3N_4-based ceramics at markedly reduced temperatures and higher strain rates [175].

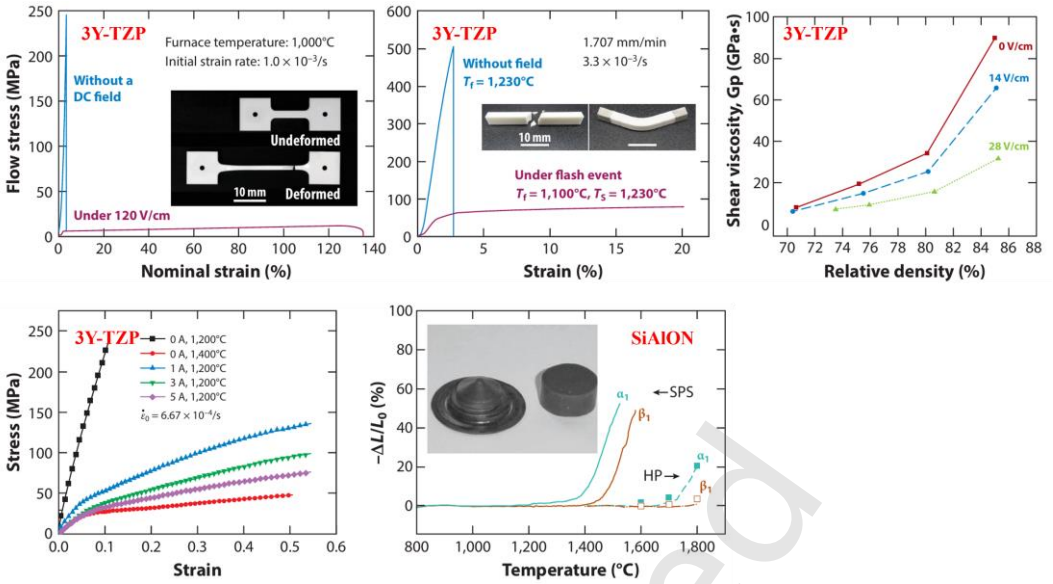

Fig. 15 Electric field-assisted super-plasticity of oxide and non-oxide ceramics [173], © Annual Reviews, 2025.

Temperature fields remain foundational but are typically coupled with other stimuli. Thermal activation unlocks additional slip systems, enhances grain-boundary diffusion and viscous flow (dominant in fine-grained microstructures <1 μm), and enables superplastic elongation exceeding 200% in submicron 3Y-TZP at 1200-1400 °C and strain rates of 10^{-4}-10^{-2} s^{-1}. High temperature preloading introduces high-density dislocations, stacking faults, and twins that persist upon cooling, imparting RT plasticity. Single-crystal TiO_2 and Al_2O_3 have demonstrated compressive strains of ~10% and 6-7.5%, respectively, after such defect engineering [21].

Stress fields provide auxiliary activation and crack suppression. Dynamic loading or ultrasonic vibration lowers yield stress, promotes dislocation motion, refines grains, and heals microcracks, while GPa-level hydrostatic pressure induces beneficial phase transformations (e.g., $t \rightarrow m$ in ZrO_2 or $\beta \rightarrow \alpha$ in Si_3N_4) that create coherent interfaces and layered structures, enabling RT compressive strains of ~20% in dual-phase Si_3N_4 and notable plasticity in BN ceramics [31]. Multi-axial or gradient stress states further prevent localized stress concentrations during near-net-shape

forming. Emerging fields, magnetic (Lorentz-force grain-boundary pinning), ultrasonic (grain-boundary softening), and optical (localized laser heating), offer complementary control over microstructure stability and precision micro-forming.

Edalati *et al.* [74] reviewed the use of HPT as an effective external-field-driven strategy to induce severe plastic deformation in ceramics, thereby overcoming their intrinsic brittleness through dislocation engineering, see **Fig. 16**. Under the combined action of ultrahigh hydrostatic pressure (typically several GPa) and large shear strain ($\gamma > 100$), HPT suppresses crack initiation while activating dislocation motion and accumulation even in otherwise brittle ceramic lattices. This process leads to significant grain refinement down to the nanocrystalline regime (<100 nm) and the introduction of high-density lattice defects, including dislocations and grain boundaries, which collectively facilitate plastic accommodation. As a result, ceramics processed by HPT can exhibit markedly enhanced deformability, with reported plastic strains exceeding several tens of percent in some oxide systems, alongside strength levels maintained in the GPa range. The study highlights that external pressure fields not only inhibit catastrophic fracture but also fundamentally alter deformation mechanisms, enabling dislocation-mediated plasticity and providing a viable pathway for achieving high plasticity in ceramics via severe plastic deformation techniques.

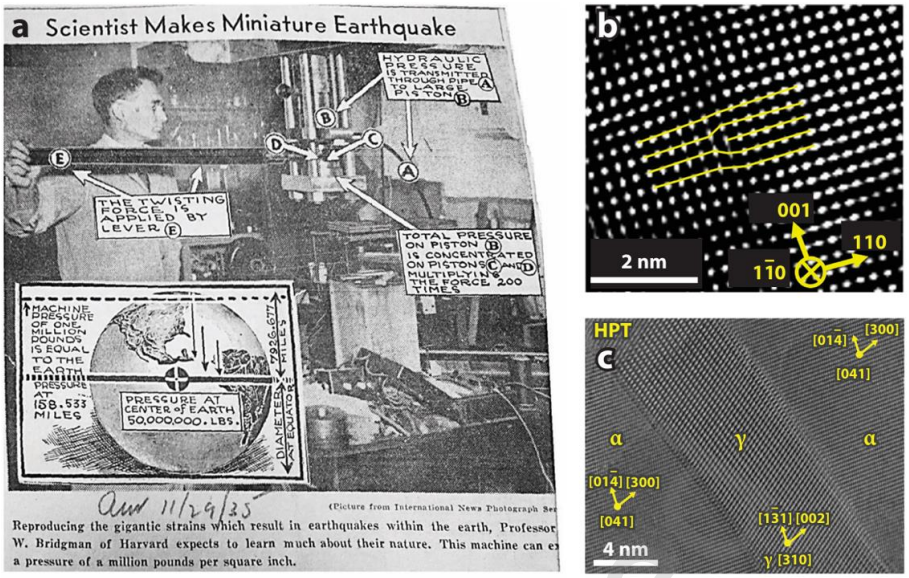

Fig. 16 HPT as an effective external-field-driven strategy to induce severe plastic deformation in ceramics. Reproduced with permission from Ref. [74], © Annual Reviews 2025.

In practice, multi-field coupling (especially thermo-electro-mechanical) delivers the highest efficiency. The synergistic combination of Joule heating, electric-field softening, and stress-driven flow reduces deformation temperatures to 0.3-0.4 T_m, raises strain rates to the 10^{-2} s^{-1} level, achieves >100% strains, and maintains high density while inhibiting grain growth. Key deformation mechanisms activated include GBS (dominant in fine-grained super-plasticity), dislocation glide/climb, stress-induced phase transformations, and transient grain-boundary amorphization/liquid-phase lubrication. These strategies apply across oxide (3Y-TZP, Al_2O_3-ZrO_2), nitride (Si_3N_4, SiAlON), and carbide systems, though covalent ceramics remain more challenging owing to narrower processing windows [176].

Despite remarkable progress, challenges persist: RT plasticity is still limited by necking, electric-field methods risk local overheating and compositional segregation, and scale-up demands improved uniformity and cost-effectiveness. Nevertheless, external-field mediation, particularly thermo-electro-mechanical coupling, constitutes a transformative route for near-net-shape forming of

complex ceramic components, paving the way from laboratory-scale plasticity to industrial manufacture of high-performance structural ceramics.

4.2 Microstructural and interfacial design strategies

4.2.1 Nanocrystalline design

Nanocrystalline ceramics have emerged as a key microstructural strategy to overcome the intrinsic brittleness of ceramics by substantially increasing the grain-boundary volume fraction and thereby activating GBS as the dominant plastic deformation mechanism [56, 177]. When average grain sizes are reduced to the nanoscale regime (typically <100-300 nm), the proportion of atoms located at or near grain boundaries can reach 30-50 vol.%, shifting the balance from limited intragranular dislocation glide to intergranular accommodation processes such as GBS, grain-boundary diffusion, and rotation. This not only lowers the flow stress required for plastic flow but also distributes local stresses across a dense network of boundaries, effectively suppressing crack nucleation and propagation.

The primary fabrication routes focus on producing either monolithic nanocrystalline ceramics or nanocomposite architectures. Monolithic nanocrystalline ceramics are commonly synthesized through chemical co-precipitation, high-energy ball milling, or ultrafast densification techniques such as SPS, which enable full density while preserving nanoscale grains. In recent years, significant progress has been made in the research on realizing and optimizing RT plasticity of MAX phases. With decreasing grain size, the dominant deformation mode of Cr_2AlC shifts from dislocation-mediated lamellar slip to grain boundary-mediated and more homogeneous plastic deformation, which promotes a more uniform stress distribution and mitigates stress concentration, thereby

suppressing crack initiation and propagation [117, 159]. The observed mechanical synergy is attributed to the combined effects of grain refinement strengthening and enhanced energy dissipation via cooperative deformation at grain boundaries. Moreover, Hall-Petch strengthening arises from the high density of grain boundaries that hinder dislocation motion as grain size decreases, while the layered structure further impedes slip yet permits interlayer shear, enabling a combination of ultrahigh strength and retained plasticity [118].

Nanocomposite structures further improve performance by dispersing nano-scale second-phase particles (e.g., zirconia in alumina or mullite in alumina-zirconia systems) that exert Zener pinning on grain boundaries, maintaining microstructural stability during high temperature deformation. Representative examples include nanocrystalline 3Y-TZP, which exhibits markedly accelerated superplastic strain rates with decreasing grain size from 200 nm to 100 nm, and three-phase alumina-zirconia-mullite composites (average grain size ~260 nm) that achieve extensive GBS-dominated super-plasticity under compressive loading [56, 178].

Despite these advantages, the practical implementation of nanocrystalline ceramics faces several hurdles. Firstly, their thermal stability is inherently poor, and exposure to the elevated temperatures required for superplastic forming or service often triggers rapid grain coarsening, which erodes the high grain-boundary fraction essential for GBS and restores brittle behavior [56, 179]. Meanwhile, the preparation of phase-pure nano-powders and their consolidation without excessive grain growth demands sophisticated, energy-intensive processing routes (e.g., wet-chemical synthesis combined with pressure-assisted sintering), resulting in high production costs that hinder large-scale industrial adoption.

In the broader context of plastic ceramics, nanocrystalline engineering and nanocomposite designs serve as complementary pathways to external-field regulation, enabling superplastic elongations >200% in oxide systems and opening avenues for near-net-shape forming of complex components. Continued advances in grain-boundary engineering (e.g., controlled segregation or hybrid nano-/microstructures) will be critical to translating these laboratory-scale achievements into robust, cost-effective structural ceramics.

4.2.2 Coherent interface engineering

Coherent structures, primarily low-energy coherent interfaces and twin boundaries, offer a transformative microstructural approach to overcoming the intrinsic brittleness of ceramics by enabling stress-accommodating atomic rearrangements without catastrophic fracture. In these designs, lattice-matched interfaces (where atomic planes are continuous across phase or twin boundaries) dramatically lower interfacial energy compared with conventional high-angle grain boundaries, allowing successive bond switching, reversible phase transformations, and localized shear that dissipate strain energy plastically. This mechanism shifts deformation from crack-dominated brittle failure to transformation-mediated plasticity, particularly effective in covalently bonded systems where dislocation motion is otherwise severely restricted.

The landmark demonstration is dual-phase α/β- Si_3N_4 ceramics engineered with a high density of coherent α/β interfaces [31]. Under RT compression, stress triggers successive Si-N bond switching at these interfaces, driving a reversible $\beta \rightarrow \alpha$ phase transformation that accommodates plastic strain. Nanopillars with ~32 % coherent interfaces achieve ~20 % engineering plastic strain and fracture strengths exceeding 11 GPa (contrasting sharply with monolithic β-Si_3N_4), which

exhibits purely elastic behavior followed by brittle fracture, see **Fig. 17**. *In-situ* X-ray diffraction (XRD) and molecular dynamics simulations confirm that the coherent geometry enables coordinated bond breaking and reforming while preserving structural integrity, effectively realizing transformation-induced plasticity in a fully covalent ceramic.

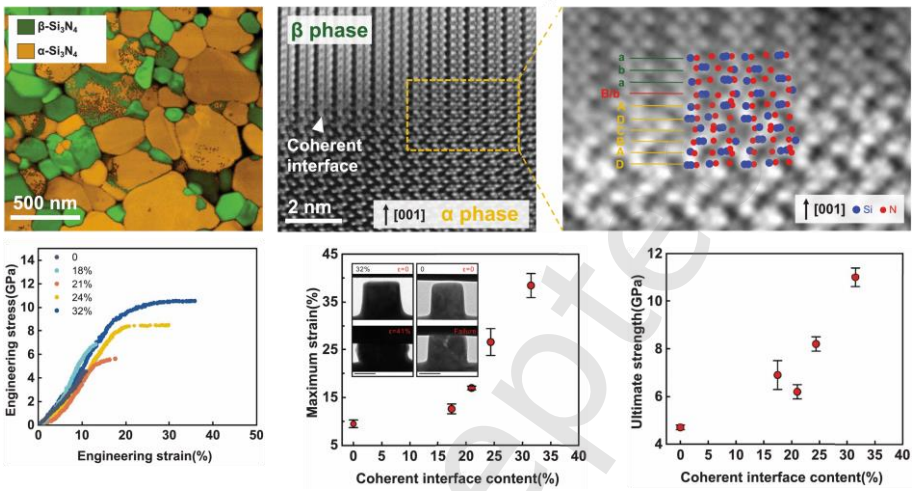

Fig. 17 Dual-phase α/β-Si_3N_4 ceramics engineered with a high density of coherent α/β interfaces with RT plasticity. Reproduced with permission from Ref. [31], © AAAS 2022.

Similar principles underpin plasticity in other systems. Nano-twinned cBN leverages coherent twin boundaries to enhance dislocation transmission and twin boundary migration, yielding size-dependent plasticity and improved toughness [72]. In zirconia-based ceramics, coherent twin domains formed during stress-induced $t \rightarrow m$ phase transformation provide additional strain accommodation [21]. These coherent features also appear in preloaded defect-engineered oxides, where interfacial dislocations at coherent twin boundaries promote twinning/detwinning and further RT deformability.

While coherent-structure engineering has unlocked unprecedented RT compressive plasticity in otherwise intractable covalent ceramics, challenges remain in scaling from nanopillars to bulk components, ensuring long-term interface stability under cyclic loading or elevated temperatures, and

extending the approach beyond specific phase pairs. Nevertheless, when combined with nanocrystalline refinement or external-field assistance, coherent-interface design constitutes a versatile route toward bulk, near-net-shape plastic ceramics for structural applications.

4.2.3 Layered architecture design

Ceramics with a layered atomic structure (vdW between atomic layers), including graphite, MAX phases, and BN might possess a potential in deformation due to various deformation mechanisms, such as basal slip, kink and shear band deformations, and grain delamination. The emergence of plasticity in BN ceramics has recently challenged the long-standing paradigm that ceramics are intrinsically brittle. Prof. Yongjun Tian's research group has conducted impressive systematic explorations and comprehensive investigations on strategies for RT plastic deformation in layered structural ceramics, especially in BN. Early advances, they demonstrated that microstructural design at the nanoscale can fundamentally alter macroscopic mechanical responses [180]. By employing SPS to consolidate either onion-like BN nanoparticles or graphite-like hexagonal BN (hBN) nanosheets, two distinct ceramics were obtained: a three-dimensional interlocked architecture of randomly oriented nanosheets and a pronounced texture perpendicular to the compression axis, both showing measurable plastic deformation with fracture strain of 4.2% and 2.2%, respectively. These results imply the potential plasticity in layered ceramics with proper tailoring microstructure.

Subsequently, they synthesized a bulk BN ceramic featuring a layered building-block architecture with rotational stacking order by exploiting the structural phase transformations of onion-like boron nitride during hot pressing and SPS [20]. Within this ceramic, BN nanosheets form a three-dimensionally interlocked framework. Each nanosheet is constructed from parallel lamellae (ranging

from several to over a dozen atomic layers in thickness) stacked with relative rotational misalignment, serving as the fundamental structural units. Under uniaxial compression, the material achieved an extraordinary fracture strain as high as about 14%, see **Fig. 18**. Simultaneously, its strength increases by 6-10 times compared to conventional h-BN ceramics, while retaining a remarkable permanent plastic strain of ~8% after unloading. This synergistic enhancement of strength and plasticity can be rationalized by synergistic mechanisms operating across multiple length scales. The introduction of rotational stacking order significantly enhances the intrinsic deformability of the material by about two orders of magnitude. And the three-dimensional interlocked microstructure effectively suppresses the propagation of deformation modes such as kinking, delamination, rippling, and dislocation motion, thereby confining deformation within individual nanosheets. This confinement amplifies the contribution of intrinsic deformability while mitigating the detrimental effects of grain boundaries.

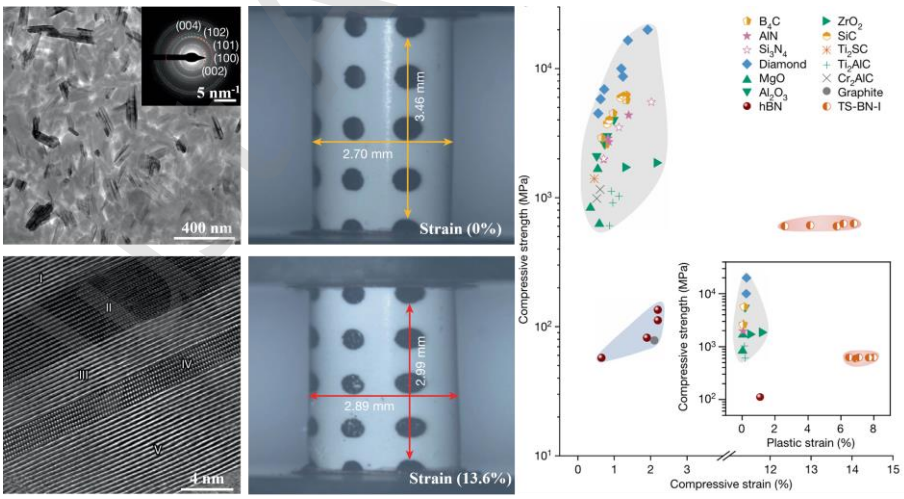

Fig. 18 Microstructure and RT compressive properties of plastic boron nitride (BN) ceramics. Reproduced with permission from Ref. [20], © Springer Nature 2024.

More recent insights, they further revealed that twist-induced lattice frustration gives rise to universal kink-band formation as a dominant deformation mode [127]. Unlike conventional kink

propagation, which often leads to premature failure, these twist-activated kinks are highly stable and reversible at the nanoscale, enabling sustained plastic flow without catastrophic cracking. This mechanism provides a unifying framework to understand how layered ceramics can transition from brittle fracture to ductile-like deformation through controlled structural perturbations. Importantly, such kink-mediated plasticity is not unique to BN but may represent a generalizable principle for a wide class of layered materials.

Beyond their exceptional mechanical performance, twisted-layer BN ceramics also exhibit high energy absorption capacity and superior fatigue resistance, positioning them as promising candidates for advanced engineering applications such as seals, damping components, and protective armor. More broadly, the design principles demonstrated here offer a versatile strategy that can be extended to other layered systems, including graphite and MAX-phase ceramics.

They not only overturn the conventional strength and plasticity trade-off but also establish a coherent mechanistic framework linking nanoscale structural design to macroscopic mechanical performance. The conceptual elegance, experimental rigor, and transformative implications of this body of work place it among the most significant recent advances in the field, opening a compelling pathway toward the rational design of truly damage-tolerant, high-performance ceramic materials.

Beyond its exceptional strength and plasticity, the twist-stacked layered BN ceramic also demonstrates high energy absorption capacity and excellent fatigue resistance, making it a promising candidate for advanced applications such as high-performance seals, damping components, and protective armor. The material design and synthesis strategy reported here can be extended to other layered material systems, including graphite and MAX-phase ceramics, offering a generalizable pathway toward the development of plastically deformable ceramics across diverse material classes.

4.2.4 Multiphase composite design

Multi-phase composite strategies extend plasticity through extrinsic toughening and load-sharing. Metal-ceramic composites exploit the plasticity of a metallic phase (e.g., TRIP-steel matrix reinforced with Mg-PSZ or nacre-like Al_2O_3-metal laminates) to bridge cracks and provide continuous plastic flow, achieving simultaneous high strength and toughness [181]. Layered composites, inspired by nacre, utilize weak interfaces (e.g., Si_3N_4/h-BN or ceramic-metal multilayers) for interface sliding, crack deflection, and delamination, dramatically increasing work-of-fracture while retaining ceramic-level hardness [182]. Particle-dispersion strengthening, realized by uniform nano-scale second-phase particles (e.g., ZrO_2 in Al_2O_3 or Cr in Al_2O_3/Cu), refines grain size, pins boundaries, and creates additional coherent or semi-coherent interfaces that trigger transformation plasticity or local stress redistribution, enhancing both super-plasticity and RT plasticity. Zhang *et al.* [183] enhanced the plasticity of $HfTaC_2$-based ultra-high-temperature ceramics by designing a dual-phase $HfTaC_2$/W microstructure with strong interfacial bonding, which promoted dislocation nucleation, interaction, and motion instead of catastrophic crack propagation. The synergistic effect of interfacial dislocation interactions and dislocation glide inside the W network enabled significant plastic deformation under both compression and tension, leading to simultaneously improved strength and plasticity compared with monolithic $HfTaC_2$ ceramics.

Dong *et al.* [25] proposed a novel "borrowed dislocation" strategy to overcome the intrinsic scarcity of mobile dislocations in ceramics and thereby achieve enhanced plasticity. By introducing a ductile metallic phase or interface that serves as an external dislocation reservoir, dislocations can be generated in the metal and subsequently transmitted across coherent or semi-coherent interfaces into the ceramic phase under applied stress. This mechanism effectively bypasses the high energy

barrier for dislocation nucleation within the ceramic lattice, enabling sustained dislocation activity and plastic deformation. The authors showed that careful interface engineering is critical to facilitate dislocation transfer while maintaining strong interfacial bonding, allowing the ceramic to accommodate strain without premature fracture. As a result, such hybrid systems can exhibit significantly improved tensile strain of about 40% while retaining high strength of 2.3 GPa, see **Fig. 19**. This work highlights an unconventional defect-engineering pathway, where external dislocation sources are leveraged to activate intrinsic plasticity in ceramics, offering a promising route toward quasi-ductile ceramic materials.

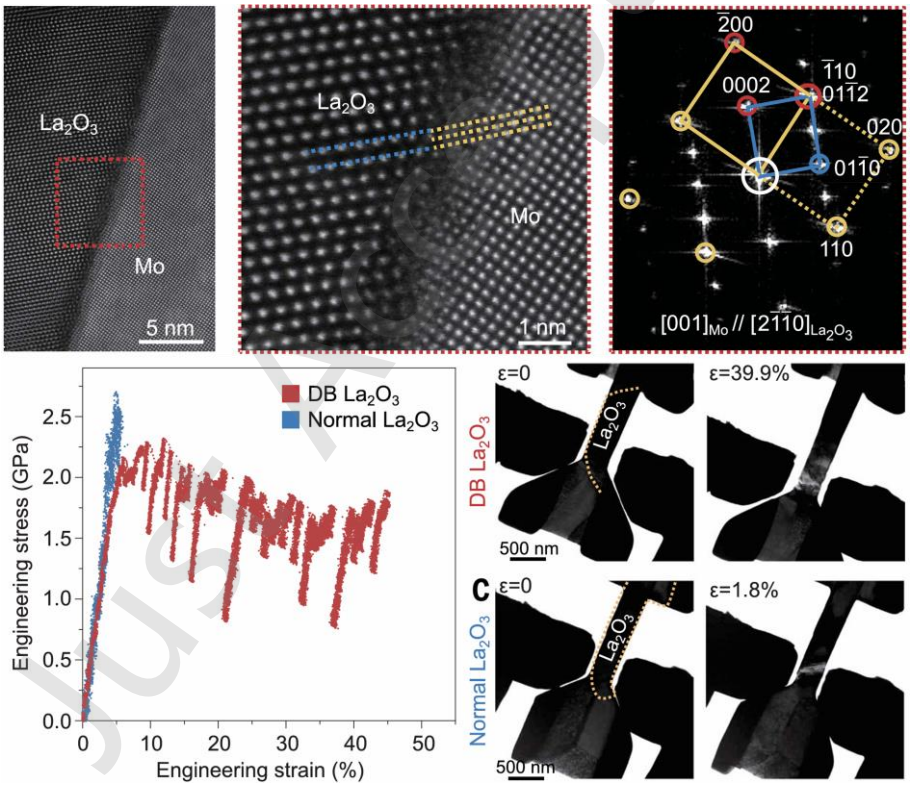

Fig. 19 Microstructure and RT tensile properties of dislocation-borrowed La_2O_3 ceramics. Reproduced with permission from Ref. [25], © AAAS 2024.

Zhu *et al.* [43] reported a bioinspired high-entropy all-ceramic system with a contiguous network structure (i.e., HEC/Cr_7C_3), demonstrating that rational structural design can promote non-

brittle deformation behavior in ceramics, see **Fig. 20**. By constructing an interpenetrating, compositionally complex network, the material enables effective stress redistribution and suppresses localized failure. The heterogeneous lattice distortion inherent to high-entropy phases facilitates dislocation nucleation and impedes their rapid propagation, thereby promoting stable plastic deformation. In addition, the continuous network architecture activates multiple deformation and toughening mechanisms, including crack deflection, bridging, and interface sliding, which collectively delay catastrophic fracture. As a result, the ceramic exhibits a combination of high strength (on the order of ~1-2 GPa) and enhanced strain tolerance, with measurable inelastic deformation reaching ~1% or higher. This work highlights that bioinspired structural design, coupled with high-entropy effects, provides an effective pathway to activate and sustain plasticity in ceramic systems by synergistically integrating dislocation activity and extrinsic toughening mechanisms.

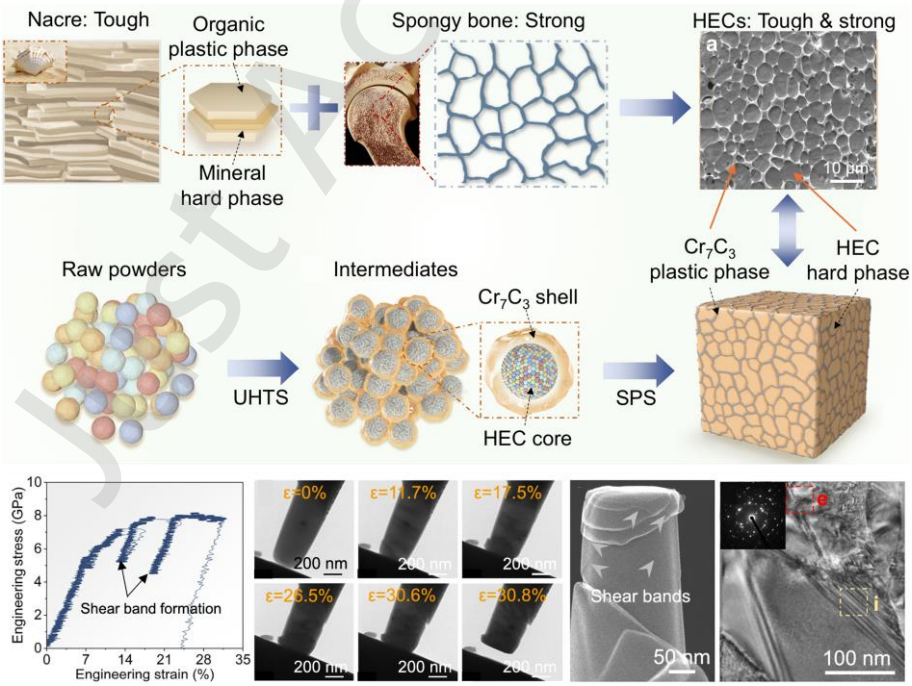

Fig. 20 Tough and strong bioinspired high-entropy all-ceramics with a contiguous network structure. Reproduced with permission from Ref. [43], © Springer Nature 2025.

Awaji *et al.* [184] elucidated that achieving enhanced plasticity in ceramic-based nanocomposites relies critically on nanoscale multiphase design and interface engineering. By introducing finely dispersed second phases (typically at the nanometer scale), these systems generate a high density of interfaces that can effectively impede crack propagation while simultaneously enabling localized inelastic deformation. The authors highlighted that mechanisms such as crack deflection, crack bridging, and pull-out are complemented by interface sliding and constrained dislocation activity within more compliant phases, allowing strain to be accommodated without catastrophic failure. In addition, residual stress fields arising from thermal and elastic mismatch between phases further promote microcrack toughening and stress redistribution. Such nanocomposite architectures can maintain high strength in the GPa range while achieving improved strain tolerance, often approaching ~0.5-1%, demonstrating that nanoscale heterogeneity and strong yet adaptable interfaces are key to activating quasi-plastic deformation in otherwise brittle ceramic systems.

Huang *et al.* [185] demonstrated that tailoring the intrinsic defect energetics, specifically by introducing negative stacking fault energy (SFE), provides a powerful pathway to activate pronounced plasticity in nitride ceramics, see **Fig. 21**. In such systems, negative SFE stabilizes stacking faults and promotes the spontaneous dissociation of full dislocations into partial dislocations, thereby significantly lowering the energy barrier for dislocation nucleation and glide. This facilitates the activation of multiple slip systems and enhances dislocation mobility even at relatively low temperatures, enabling sustained plastic deformation rather than brittle fracture. Moreover, the accumulation and interaction of extended partial dislocations and stacking faults contribute to strain hardening and delay crack initiation. As a result, these nitride ceramics exhibit a combination of high

strength (on the order of several GPa) and markedly improved plastic strain (reaching a few percent), far exceeding conventional ceramics. This work highlights defect engineering, through manipulation of stacking fault energetics, as a fundamentally effective strategy to intrinsically enable dislocation-mediated plasticity in ceramic materials.

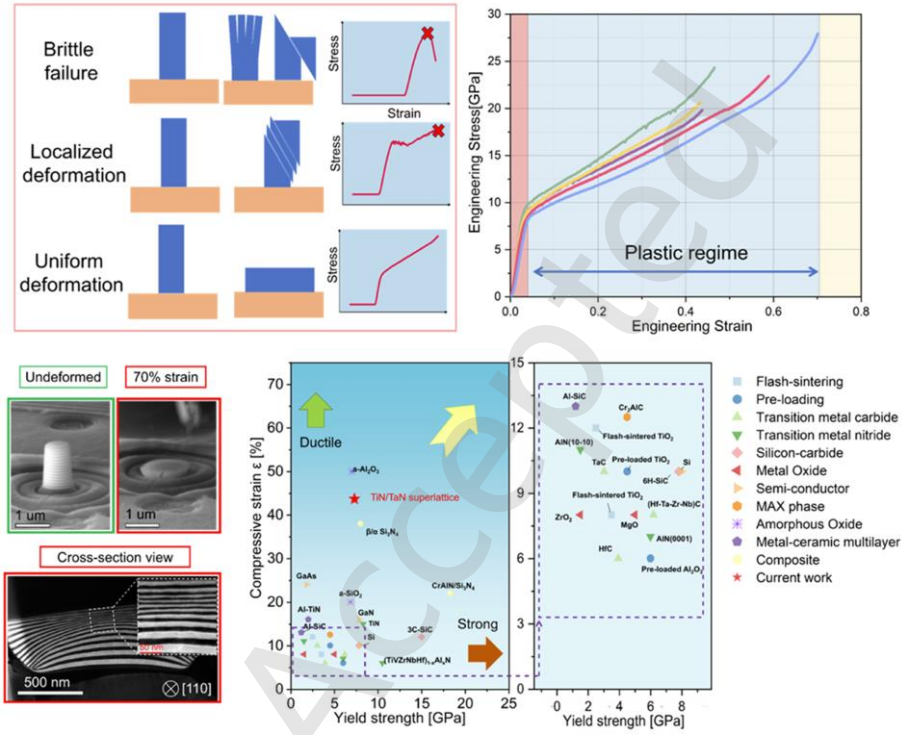

Fig. 21 Introducing SFE to activate pronounced plasticity in nitride ceramics. Reproduced with permission from Ref. [185], © Elsevier Ltd. 2025.

Lorentzon *et al.* [186] constructed ordered point defect superstructures in nitrogen-rich HfN thin films, which effectively activated and modulated the nucleation and glide of dislocations, enabling intrinsically brittle ceramics to exhibit dislocation-dominated large plastic deformation at RT and achieve metal-like plasticity in ceramic materials. When integrated with other plasticity routes, defect-engineered and composite ceramics overcome the narrow processing windows of covalent systems and improve thermal stability of nanostructures. Remaining challenges include long-term defect annihilation at service temperatures, interfacial reaction control in metal-ceramic hybrids, and

scalable, cost-effective fabrication of uniform layered or dispersed architectures. Nevertheless, these strategies provide versatile pathways to transform inherently brittle ceramics into damage-tolerant, plastically formable structural materials suitable for near-net-shape components under complex loading.

Aoki *et al.* [93] demonstrated that the intrinsic brittleness of high-strength Al_2O_3-$GdAlO_3$ eutectic ceramics can be effectively mitigated through the refinement of eutectic microstructures, enabling enhanced plasticity in an otherwise brittle system. By precisely controlling solidification conditions, a highly aligned, interpenetrating lamellar structure with reduced phase spacing can be achieved, which promotes cooperative deformation between the Al_2O_3 and $GdAlO_3$ phases. This refined architecture suppresses catastrophic crack propagation by facilitating crack deflection, bridging, and stress redistribution at phase interfaces, displacing engineering plastic strains of up to 5% at RT. Moreover, the nanoscale lamellar spacing increases the density of interfaces that can accommodate strain through localized shear and dislocation activity, thereby activating non-catastrophic deformation mechanisms.

Gavalda-Diaz *et al.* [41] reviewed how microstructure engineering in ceramics and ceramic composites can be strategically employed to overcome brittleness and promote enhanced plastic deformability. They emphasized that designing multiphase architectures (e.g., lamellar, interpenetrating, and particulate-reinforced systems) enables effective activation of extrinsic deformation mechanisms, including crack deflection, crack bridging, interface sliding, and phase-boundary-mediated stress redistribution. By tailoring grain size, phase distribution, and interface characteristics, these engineered microstructures can delay crack initiation and propagation while allowing localized inelastic deformation to accumulate. In particular, reducing characteristic length

scales to the submicron or nanoscale increases interface density, which facilitates strain accommodation through mechanisms such as GBS and dislocation activity in more deformable phases. The review highlights that such multiphase strategies can achieve a balance between high strength (typically in the GPa range) and improved strain tolerance (approaching ~0.5-2% in optimized systems), demonstrating that controlled microstructural heterogeneity is a key pathway toward realizing quasi-ductile behavior in advanced ceramic materials.

Rahimizadeh *et al.* [187] highlighted that achieving enhanced plasticity in ceramic-based materials can be effectively realized through bioinspired architectured multiphase designs that integrate hard and compliant constituents in hierarchical configurations. By mimicking natural systems such as nacre, these materials employ layered, brick-and-mortar, or interpenetrating architectures that promote progressive deformation rather than abrupt fracture. The authors emphasized that such designs activate multiple extrinsic deformation mechanisms (e.g., crack deflection, crack bridging, interface sliding, and pull-out) while enabling stress delocalization across phases. Crucially, the incorporation of tailored interfaces with controlled bonding strength allows for reversible sliding and energy dissipation, thereby accommodating inelastic strain. When combined with fine microstructural length scales, these architectures can sustain relatively high strengths (typically in the GPa range) alongside improved strain tolerance, often approaching or exceeding ~1%. This work demonstrates that bioinspired multiphase structural engineering provides a robust pathway to achieving quasi-ductile behavior in ceramics by synergistically coupling microstructural hierarchy with interface-mediated plasticity mechanisms.

4.3 Amorphous-crystal composite structure design

Amorphous-crystal composite structures integrate crystalline grains or nanoparticles with an amorphous phase, either as intergranular films, matrix-reinforcement architectures, or crystalline/amorphous dual-phase nanostructures, to overcome the intrinsic brittleness of ceramics. The crystalline component supplies high strength and structural rigidity, while the amorphous phase enables localized shear-band formation, viscous flow, and reversible bond rearrangement that dissipate strain energy and accommodate plastic deformation. Amorphous-crystal interfaces further act as efficient sinks for dislocations and point defects, promote GBS, and blunt crack tips, transforming brittle fracture into stable, distributed plasticity.

The key to this improved plasticity lies in the role of amorphous-crystalline interfaces, which act as both barriers and sources for deformation carriers , enabling a synergistic coupling between dislocation activity in the crystalline phase and shear transformation zones (STZs) in the amorphous phase. According to a comprehensive review [188], dislocations generated in crystalline regions can pile up at interfaces, which in turn trigger localized shear transformations in the amorphous phase. This interaction distributes strain more uniformly across the material, preventing catastrophic failure. Similarly, alternating amorphous and crystalline layers promote cooperative deformation, where each phase compensates for the mechanical limitations of the other [189]. Another critical mechanism is the stabilization of shear bands. In fully amorphous ceramics, deformation tends to localize into a single dominant shear band, leading rapidly to fracture. In contrast, amorphous-crystalline composites disrupt this localization process. Interfaces and embedded nanocrystals deflect and multiply shear bands, allowing for more distributed plastic flow. This phenomenon is demonstrated in both experimental and simulation studies, which highlight how interface density and layer thickness

influence deformation stability [190]. Insights from analogous systems, such as crystalline-amorphous metallic nanolayers, further reinforce the idea that heterointerfaces are central to achieving plasticity in otherwise brittle materials [191].

Typical implementations include crystalline/amorphous dual-phase ceramic nanofibers and self-patterned carbide-amorphous ceramic nanocomposites. In TiO_2-based dual-phase nanofibers engineered via nucleation regulation, the coexistence of crystalline domains and amorphous regions yields an exceptional combination of high tensile strength (~1.06 GPa), large strain limit (~8.44%), superior flexibility, and pronounced RT plastic deformation, the properties unattainable in monolithic crystalline or fully amorphous ceramics [38]. Similarly, see **Fig. 22**, TiC nano-carbides self-patterned within an amorphous Si-O-C ceramic matrix achieve ultra-high compressive strengths (up to 7 GPa at RT) together with uniform plastic strains of 10-18 % across a wide temperature range (up to 700 °C), owing to the synergistic shearing of the amorphous matrix and rotation of the crystalline nano-carbides [23].

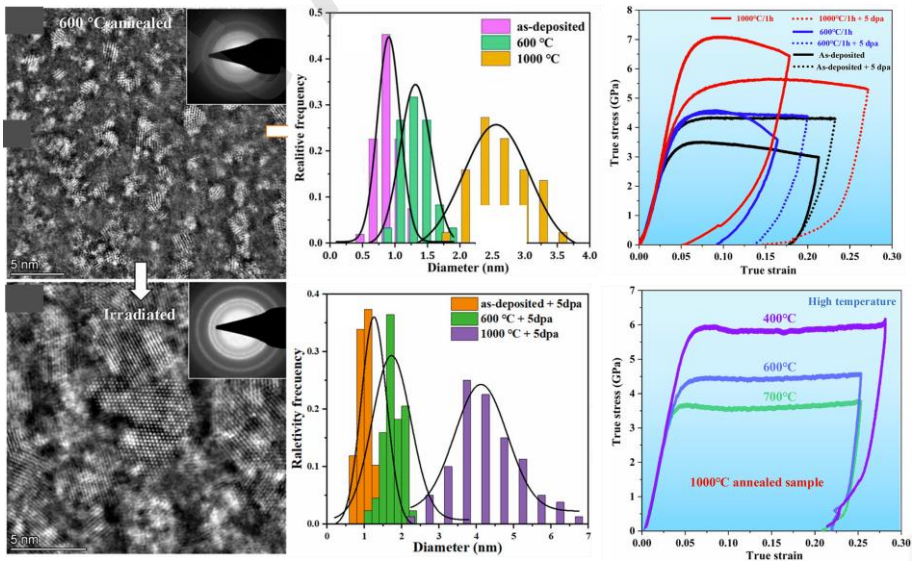

Fig. 22 TiC-SiOC nanostructures (TiC-nanocarbides embedded in amorphous ceramic SiOC) followed by high-temperature annealing and/or irradiation to achieve plasticity at both RT and high temperature. Reproduced with permission from Ref. [23], © Taylor & Francis 2025.

At the grain-boundary level, controlled amorphous intergranular films (equilibrium-thickness glassy phases) in systems such as 3Y-TZP zirconia or Si_3N_4 dramatically enhance super-plasticity by lubricating boundaries and enabling GBS without cavitation [192, 193]. A high-entropy engineering strategy is proposed to balance both by creating a crystalline/amorphous dual-phase microstructure in a single ceramic matrix [194]. The approach leverages spontaneous compositional fluctuations in high-entropy systems to form interpenetrating nanophases: one crystalline (retaining dielectric functionality) and the other amorphous (imparting flexibility). The interconnected amorphous phase enables large viscoelastic deformation and energy dissipation through structural relaxation, while the dispersed nanocrystals preserve functional performance and inhibit catastrophic cracking. As a demonstration, a $Bi_4Ti_3O_{12}$-based dielectric film is developed, which exhibits exceptional flexibility: it withstands ~180° folding, with a bending strain of 4.80% and tensile elongation of 5.29%. It also maintains good dielectric performance: a high permittivity (~35), alongside excellent temperature stability and mechanical durability. This work establishes a scalable, reproducible protocol for tailoring ceramic microstructures with alternating ordered/disordered domains, offering a new pathway to integrate mechanical flexibility and functional properties in next-generation ceramic materials for flexible electronics and related applications.

The design of amorphous-crystalline composite architectures enables ceramics to transition from brittle fracture to quasi-ductile behavior. This is achieved through interface-mediated mechanisms that combine dislocation glide, shear transformation activity, and shear band stabilization. Key design parameters include nanoscale feature size, interface density, and phase distribution, all of which govern the balance between strength and plasticity. As research progresses,

this approach is expected to play a crucial role in developing next-generation structural ceramics with enhanced plasticity and reliability.

5. Experimental characterization methods for RT plasticity

RT plasticity in ceramics has emerged as a vibrant research frontier, driven by the development of advanced experimental characterization techniques that probe plasticity deformation mediated by various mechanisms across multiple length scales. These methods enable the controlled introduction, observation, and quantification of plastic strain in ceramics, overcoming traditional limitations of cracking and premature fracture. The experimental characterization of RT plasticity should distinguish between two related but different questions: whether a ceramic exhibits measurable irreversible mechanical deformation, and which microstructural processes accommodate that deformation. Therefore, this section is organized into two modules: characterization of plastic mechanical behavior and characterization of deformation mechanisms. **Fig. 23** highlights the key features of dislocation mediated plastic deformation introduced by the most common deformation methods, including nanoindentation, Vickers indentation, cyclic Brinell indentation, cyclic Brinell scratching, and uniaxial bulk compression. These methods are arranged by the representative plastic zone size, increasing in the length scale.

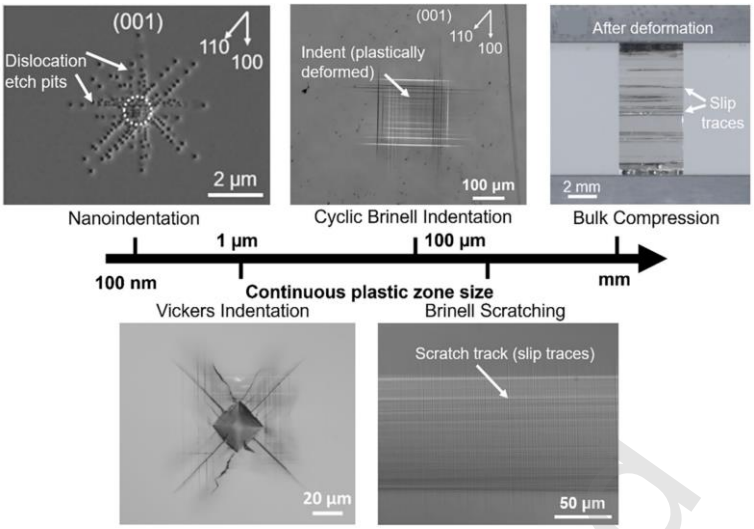

Fig. 23 Methods for mechanically imprinting dislocations through deformation sorted by increasing plastic zone size. Reproduced with permission from Ref. [18], © Wiley 2025.

5.1 Characterization of plastic mechanical behavior

Plastic mechanical behavior refers to irreversible deformation remaining after unloading. A nonlinear load-displacement or stress-strain response alone should not be regarded as sufficient evidence of plasticity, because densification, crack closure, phase transformation, microcracking, and testing-system compliance can also contribute to an apparent nonlinear response.

5.1.1 Macro-mechanical testing with small deformation

Macro-mechanical testing with small-deformation regimes addresses the translation of nanoscale insights to bulk behavior, where precise strain measurements are essential because RT plastic strains in ceramics are often limited (typically <1-5% before cracking) and easily masked by elastic recovery or machine compliance. Techniques such as digital image correlation (DIC), high-resolution extensometers, or strain gauges on bulk single-crystal or polycrystalline samples under uniaxial compression/tension capture subtle yielding, serrated flow, and work hardening while

minimizing flaw-induced premature failure. Bulk RT dislocation plasticity has been documented in perovskites like $SrTiO_3$ (via defect-tuned slip) and other oxides, with cyclic indentation or scratching methods further introducing controlled dislocation densities for subsequent macroscale plasticity [18]. These approaches complement small-scale tests by demonstrating that mechanically seeded dislocations ($\sim 10^{14}$ m^{-2}) or flash-sintering-induced defects can scale RT plasticity to macroscopic levels, enabling applications in near-net-shape forming.

Uniaxial compression is commonly used because it suppresses unstable tensile fracture and permits the determination of yield stress, plastic strain, strain hardening or softening, residual strain after unloading, and fracture strain. Where experimentally feasible, compression results should be complemented by tensile, bending, cyclic loading-unloading, or stress-relaxation tests to distinguish irreversible plastic deformation from damage accumulation. For meaningful comparison among studies, the specimen composition, phase constitution, density, grain size, texture, porosity, residual stress, loading orientation, strain rate, and testing environment should be reported in detail. The stress-strain curves should include the elastic regime, yield criterion, plastic strain, unloading behavior, and failure mode. Repeated tests are necessary to establish reproducibility. Recent demonstrations of enhanced bulk deformability in ceramics further illustrate the importance of combining quantitative macroscopic stress-strain data with detailed structural characterization [20].

Although substantial plastic deformation has been demonstrated in numerous micro- and nanoscale ceramic specimens, the translation of these observations into measurable macroscopic plasticity remains highly challenging. The primary reason lies in the fundamentally different defect statistics governing deformation at different length scales. Small-scale specimens often contain significantly fewer critical flaws, allowing plastic deformation mechanisms to be activated before

catastrophic fracture occurs. In contrast, bulk ceramics inevitably contain pores, microcracks, inclusions, and residual stresses that can trigger premature crack initiation and unstable crack propagation under external loading.

Another important distinction is the competition between strain accommodation and strain localization. In micro-scale specimens, deformation can be relatively homogeneous because of the limited deformation volume and reduced flaw population. However, in bulk materials, local stress concentrations frequently promote crack nucleation before sufficient plastic strain can accumulate. Consequently, many ceramic systems that exhibit significant plasticity under micropillar compression or nanoindentation display only limited irreversible deformation during macroscopic mechanical testing. Therefore, macro-mechanical testing provides a more stringent criterion for evaluating the engineering relevance of RT plasticity. Future studies should place greater emphasis on establishing quantitative relationships between microscale deformation mechanisms and bulk mechanical performance. Such efforts will be essential for bridging the gap between laboratory-scale demonstrations and practical engineering applications of plastically deformable ceramics.

5.1.2 Micro- and nano-mechanical testing

Micro- and nano-mechanical methods, including nanoindentation, micropillar compression, microcantilever bending, microbeam bending, and micro tensile, are particularly useful for identifying the onset of local plasticity and for probing individual grains, phases, interfaces, or selected crystallographic orientations has been instrumental in isolating dislocation nucleation and glide in ceramics at RT by exploiting small deformation volumes (typically sub-micron to a few microns) that statistically exclude critical flaws and generate localized shear stresses approaching the

theoretical strength. In nanoindentation, pop-in events in load-displacement curves signal homogeneous dislocation nucleation, while post-indent slip traces (observed via scanning probe microscopy) confirm plastic flow without cracking; this has been applied to rutile TiO_2 biocrystals, revealing orientation-dependent slip systems such as $\{101\}\langle 101\rangle$ and $\{100\}\langle 010\rangle$ with measurable hardness anisotropy (e.g., ~12-13 GPa on different planes) [195]. Micropillar compression further quantifies stress-strain responses and size effects, where yield strength often follows an inverse power-law dependence on diameter due to source-controlled or stress-assisted dislocation mechanisms. Pioneering work on covalent ceramics has shown exceptional RT plasticity: for instance, single-crystal diamond nanopillars exhibit dislocation-mediated plasticity with direct TEM evidence of glide [195], while B_4C beams achieve ~26.8% tensile ductility via localized amorphization and vacancy-facilitated mechanisms [196], and TiC pillars display size-dependent plasticity mediated by dislocations [197]. Similar micropillar studies on high-purity β-Si_3N_4 single crystals have identified orientation-dependent slip modes and CRSS [126], while pre-deformation strategies (e.g., elevated-temperature preloading of TiO_2 or Al_2O_3 pillars followed by RT testing [21]) seed high-density dislocations and stacking faults [19], enabling up to 10% compressive strain at RT without fracture. These methods highlight how nanoscale confinement suppresses cracking and activates slip systems otherwise inactive in bulk ceramics.

5.1.3 Cross-scale interpretation and reliability of mechanical data

A robust assessment of RT plasticity requires comparison across length scales. Nanoindentation probes a highly confined volume under a complex stress field, whereas micropillar compression and bulk compression sample progressively larger volumes and different populations of

pre-existing defects. Studies on $SrTiO_3$ have demonstrated that the apparent onset of plasticity and its dependence on defect chemistry can differ between nano-, micro-, and bulk-scale measurements [50, 97, 198]. Accordingly, this review recommends reporting the testing scale, stress state, loading rate, specimen geometry, crystallographic orientation, and relevant microstructural variables together with the measured plasticity metrics. Claims of RT plasticity are strongest when irreversible mechanical deformation is reproducible at the largest practicable scale and is supported by complementary microstructural evidence.

5.2 Characterization of deformation mechanisms

The second module identifies the microstructural processes responsible for the measured mechanical response. Potential RT deformation mechanisms in ceramics include dislocation nucleation, multiplication, and glide; stacking-fault formation; deformation twinning; phase transformation; amorphization; grain-boundary processes; and interface-mediated deformation. Because several mechanisms may coexist or compete, mechanism assignment should rely on converging evidence rather than on a single characterization result.

5.2.1 Post-deformation microstructural characterization

Post-deformation characterization establishes the structural signature left by mechanical loading. SEM can reveal surface slip traces, shear bands, crack paths, indentation-induced pile-up, and fracture features. Electron back scatter diffraction (EBSD) can identify grain orientation changes, local lattice rotation, deformation bands, twin boundaries, and spatial heterogeneity in deformation. TEM, high resolution transmission electron microscope (HRTEM), and scanning transmission

electron microscope (STEM) are required when direct evidence of dislocations, stacking faults, nanotwins, interfacial defects, local amorphization, or defect segregation is needed.

Diffraction- and spectroscopy-based methods provide complementary phase-level evidence. XRD can identify phase transformation, lattice-strain evolution, and texture changes, whereas Raman spectroscopy can be useful for detecting local structural transformation, residual stress, or amorphization. For example, nanoscale stacking faults and nanotwins were identified as key deformation features in flash-sintered TiO_2 exhibiting RT plasticity [199]. Therefore, deformation-induced structures should be compared with undeformed reference regions and, whenever possible, quantified in terms of defect density, spatial distribution, orientation relationship, and evolution with applied strain.

5.2.2 In-situ and operando characterization techniques

In-situ characterization techniques, particularly *in-situ* SEM and TEM nanomechanical testing, provide real-time, atomic-scale visualization of deformation dynamics, including dislocation nucleation, glide, multiplication, and interactions with defects, and so on. Advanced holders (e.g., PicoIndenter systems) integrated with SEM/TEM allow simultaneous mechanical loading and imaging, revealing mechanisms such as kink-pair formation in sphalerite structures or shear-band propagation in pre-deformed pillars. Landmark studies using *in-situ* TEM have directly observed RT dislocation plasticity in diamond (dislocation glide without cracking) and B_4C (amorphization-assisted plasticity), while *in-situ* SEM micropillar compression tracks shear-band evolution in TiO_2 and Al_2O_3 under preloading protocols. Pioneering developments in *in-situ* TEM methodologies, building on foundational contributions to nano-mechanics (including early demonstrations of large-

strain plasticity in SiC nanowires at near-RT conditions), have enabled these breakthroughs by correlating stress-strain data with microstructural evolution. Japanese researchers have similarly employed *in-situ* and *ex-situ* electron microscopy to characterize slip in oxides and nitrides. Wang *et al.* [200] has revealed anisotropic tensile super-elasticity in ceramic GeSe driven by reversible shuffle twinning. Unlike martensitic transformation mechanisms in metals, twinning in GeSe enables energy dissipation through bond reconfiguration and is activated only along specific crystallographic directions (e.g., the zigzag direction). Molecular dynamics simulations indicate that both nucleation and propagation of twins occur on the picosecond timescale, consistent with the experimentally observed rapid response. GeSe exhibits a maximum strain of up to 12.8% and demonstrates excellent cyclic stability.

In-situ TEM-based mechanical characterization has emerged as a powerful approach to directly probe the plastic deformation mechanisms of electrode materials during electrochemical cycling at the nanoscale. By integrating a nanoscale electrochemical cell within the TEM, Huang *et al.* [201] visualized the lithiation of a single crystal SnO_2 nanowire in real time and revealed a propagating reaction front accompanied by a high density of continuously nucleated and annihilated dislocations, forming a so-called "Medusa zone", see **Fig. 24**. This observation provides compelling evidence that large lithiation-induced stresses can drive intense dislocation plasticity, which in turn facilitates strain accommodation and promotes solid-state amorphization.

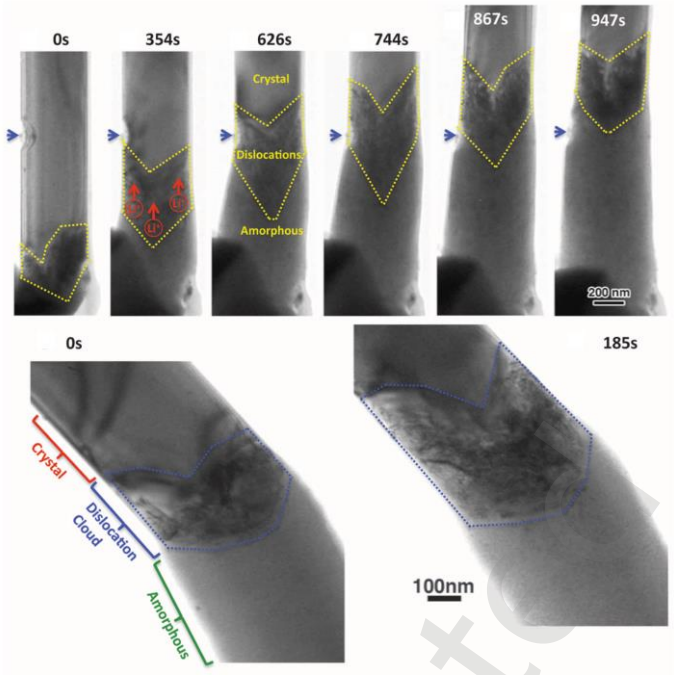

Fig. 24 TEM images revealed a high density of dislocations emerging from the reaction front of a single crystal SnO_2 nanowire. Reproduced with permission from Ref. [201], © AAAS 2010.

Complementarily, Kushima *et al.* [202] developed an *in-situ* TEM tensile testing methodology that enables seamless transition from electrochemical lithiation to mechanical loading, allowing quantitative evaluation of the mechanical properties of lithiated Si nanowires, see **Fig. 25**. Their results show a substantial reduction in tensile strength and elastic modulus upon lithiation, accompanied by large fracture strains (~8-16%) with a dominant plastic component (~70%), indicating that the lithiated Li-Si alloy exhibits pronounced ductility compared to pristine crystalline silicon. Collectively, these studies demonstrate that *in-situ* TEM not only captures dynamic microstructural evolution, such as dislocation activity and phase transformation, but also establishes a direct correlation between electrochemically induced structural changes and mechanical behavior, providing critical insights for constitutive modeling and the design of mechanically robust high-capacity electrode materials.

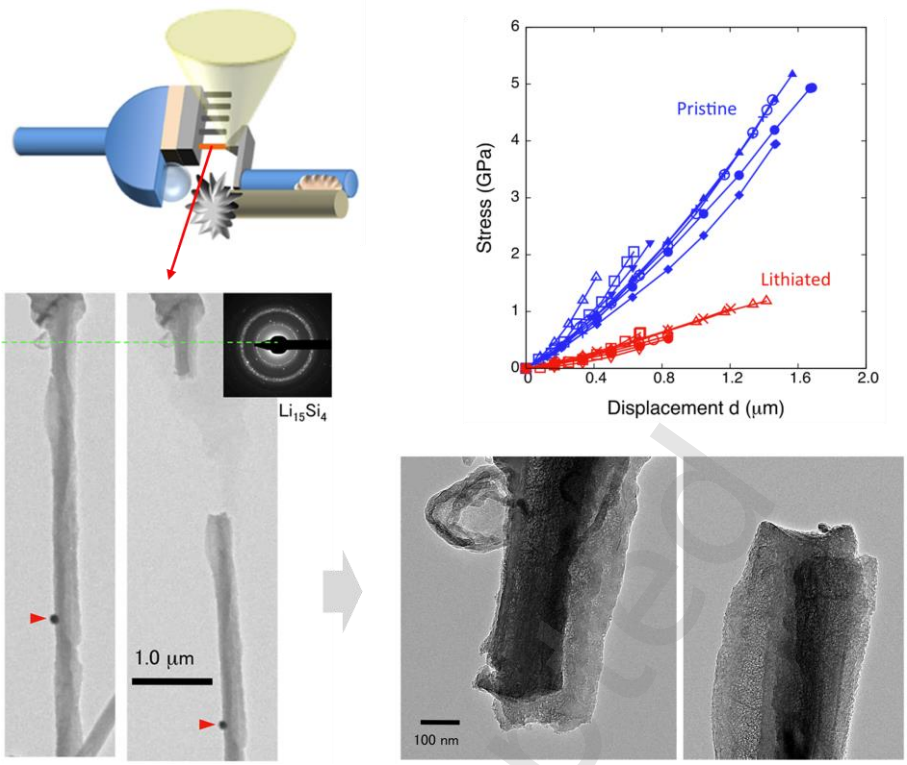

Fig. 25 *In-situ* tensile deformation of the lithiated Si nanowire. Reproduced with permission from Ref. [202], © ACS 2012.

Jian *et al.* [17] investigates the plastic deformation behavior of nanocrystalline titanium nitride (TiN) under ultra-low stress via *in-situ* nanoindentation, see **Fig. 26**. Different from the conventional understanding that ceramic materials are brittle and yield only at extremely high stress, the study revealed that nanocrystalline TiN undergoes obvious inelastic and plastic deformation at stress far below its conventional yield strength. Such low-stress plastic deformation is dominated by GBS and grain rotation, rather than dislocation motion. A clear grain size effect can be observed, which is that finer grains significantly enhance RT plasticity, with smaller nanograins exhibiting more prominent grain boundary activity and plastic flow. The findings overturn the traditional perception of ceramic brittleness, clarify the grain-boundary-dominated plastic mechanism of nanocrystalline TiN at ultra-low stress, and provide fundamental guidance for the toughening and structural design of nanostructured hard ceramics.

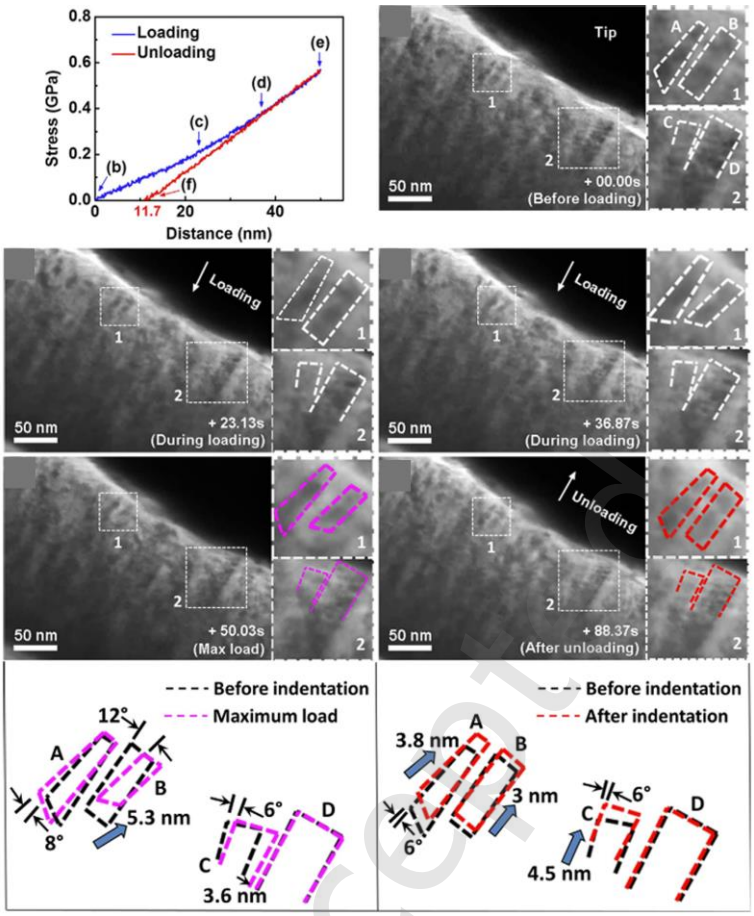

Fig. 26 Plastic deformation of TiN thin film revealed during *in-situ* nanoindentation. Reproduced with permission from Ref. [17], © Elsevier Ltd. 2016.

These methods form a comprehensive toolbox, paving the way for dislocation-engineered ductile ceramics. Ongoing integration (e.g., combining pre-seeding with *in-situ* observation) promises further advances in RT plastic ceramics for structural and functional applications. Nevertheless, *in-situ* TEM results should be interpreted cautiously because thin-foil geometry, free surfaces, electron-beam exposure, and limited deformation volume may alter the activated mechanisms. Therefore, *in-situ* observations should be combined with *ex-situ* TEM/EBSD analysis and with larger-scale mechanical measurements whenever possible. To facilitate a rational selection and interpretation of characterization methods used to investigate RT plasticity in ceramics, **Table 2** summarizes their measurable quantities, applicable specimen-size ranges, dominant stress states, and major limitations.

At the bulk scale, uniaxial compression and tensile testing provide the most direct macroscopic stress-strain response. Compression testing is particularly useful for ceramics that exhibit pressure-sensitive deformation or delayed fracture under compressive loading. However, friction at the specimen-platen interfaces can introduce barreling and stress inhomogeneity, and the resulting behavior cannot be directly extrapolated to tensile loading conditions. Tensile testing offers more direct information on tensile strength and fracture strain, but its application to ceramics is often limited by the difficulty of specimen machining, gripping, alignment, and the high sensitivity of tensile failure to surface flaws. Indentation-based methods are particularly valuable for evaluating local mechanical properties in small volumes, individual grains, multiphase microstructures, and thin films. Conventional indentation can provide hardness, residual deformation features, and indentation-induced crack information, whereas instrumented nanoindentation additionally enables the measurement of reduced modulus, time-dependent displacement, strain-rate sensitivity, and discrete pop-in events. However, the highly confined multiaxial stress field beneath the indenter differs substantially from the stress states encountered in uniaxial tests. Furthermore, indentation size effects, surface roughness, pile-up/sink-in, cracking, and substrate effects can complicate the extraction of intrinsic plastic parameters.

Microscale testing methods, such as micropillar compression and microcantilever bending, bridge the gap between nanoindentation and bulk mechanical tests. Micropillar compression is useful for examining size-dependent strength, intermittent deformation events, and the activation of deformation mechanisms in selected microstructural regions. Microcantilever bending can be used to investigate local fracture resistance and crack initiation behavior. However, both approaches are susceptible to focused-ion-beam-induced damage, specimen geometry effects, residual stresses, and

limited statistical sampling. Consequently, microscale results should be combined with bulk-scale measurements whenever possible.

In-situ characterization techniques, particularly *in-situ* TEM mechanical testing and loading-assisted diffraction or Raman spectroscopy, provide complementary mechanistic information that cannot be obtained from mechanical curves alone. These methods can reveal dislocation activity, phase transformation, lattice strain evolution, shear localization, and crack initiation during deformation. Their main limitations include specialized experimental requirements, small sampling volumes or limited spatial resolution, possible electron-beam effects in TEM, and the challenge of directly correlating local observations with macroscopic mechanical behavior. Therefore, a multi-scale characterization strategy combining bulk, local, and *in-situ* methods is generally required for a reliable assessment of plasticity in ceramics.

Table 2 Comparison of major characterization methods for evaluating plasticity in ceramics.

Characterization method	Measurable physical quantities	Applicable specimen size scale	Dominant stress state	Major limitations
Uniaxial compression	Elastic modulus, compressive yield/proof stress, compressive strength, plastic strain, strain hardening/softening behavior	Bulk specimens; typically, millimeter to centimeter scale	Nominally uniaxial compression	Friction between specimen and platens may cause barreling and non-uniform deformation; tensile failure behavior cannot be directly assessed; accurate strain measurement can be challenging at small strains
Uniaxial tension	Elastic modulus, tensile strength, yield behavior, fracture strain, tensile ductility	Bulk or miniaturized dog-bone specimens; usually millimeter scale or larger	Nominally uniaxial tension	Specimen preparation, gripping, alignment, and strain measurement are difficult for brittle ceramics; premature fracture from surface flaws may obscure intrinsic plasticity
Conventional indentation	Hardness, indentation-induced crack morphology, estimated fracture toughness, residual deformation characteristics	Local regions from tens of micrometers to millimeter-scale surfaces	Highly confined multiaxial contact stress field	Hardness and crack-based toughness values depend on loading history, indenter geometry, surface preparation, pile-up/sink-in, and crack formation; direct conversion to bulk yield properties is not straightforward
Instrumented nanoindentation	Hardness, reduced modulus, creep displacement, strain-rate sensitivity, pop-in events, local deformation resistance	Thin films, grains, phases, and small volumes; typically, nano- to micrometer scale	Highly localized multiaxial contact stress under an indenter	Strong indentation-size effects; substrate effects for thin films; surface roughness and tip calibration errors; local response may not represent bulk behavior
Micropillar compression	Size-dependent yield strength, flow stress, strain bursts, strain hardening/softening, deformation mode	Micropillars with diameters typically from submicrometer to several micrometers	Approximately uniaxial compression	Focused-ion-beam damage, pillar taper, misalignment, and size effects may influence the measured response; limited sampled volume and statistical representativeness
Microcantilever bending	Local flexural strength, fracture resistance, crack initiation and propagation behavior	Micrometer-scale beams or cantilevers	Bending with tensile and compressive stress gradients	Data interpretation depends strongly on beam geometry and notch quality; focused-ion-beam damage and residual stresses can affect results; stress state is not purely uniaxial
In-situ TEM mechanical testing	Direct observation of dislocation motion, phase transformation, shear localization, crack initiation, and nanoscale deformation mechanisms	Nanometer- to submicrometer-scale specimens	Tension, compression, or bending depending on the testing geometry	Electron-beam irradiation, free-surface effects, extremely small sample volumes, and nonrepresentative boundary conditions may alter the observed mechanisms

5.2.3 Correlating mechanical responses with deformation mechanisms

The final step is to quantitatively establish the intrinsic correlation between the characteristic stages of the mechanical response and the corresponding microstructural evolution pathways. Specifically, the onset of yielding can be attributed to the activation of fundamental deformation carriers, such as dislocation nucleation, interface-mediated shear, or grain-boundary sliding; subsequent strain hardening is typically governed by dislocation multiplication, interaction, and accumulation, as well as defect storage and dynamic interactions among multiple deformation modes; whereas strain softening or catastrophic failure is often associated with localized structural instabilities, including amorphization, stress-induced phase transformation, crack initiation and propagation, or interfacial decohesion.

Accordingly, a rigorous identification of deformation mechanisms necessitates the integration of multi-scale and multi-modal evidence, including: macroscopic or localized stress-strain and load-displacement responses; post-deformation microstructural and phase characterization; and, where feasible, real-time *in-situ* observations under applied loading conditions. The establishment of such a comprehensive evidence chain is critical for discriminating intrinsic plastic deformation from apparent deformation dominated by damage-related processes. Furthermore, this integrative framework enables a systematic determination of the dominant deformation carriers, whether governed by dislocation activity, stacking faults and deformation twinning, transformation-induced mechanisms, amorphization, or grain-boundary and interface-mediated processes. Ultimately, this approach provides a robust and scientifically grounded basis for cross-system comparison and for the rational design of ceramic materials with enhanced RT plasticity.

6. Summary of properties of RT plastic ceramics

Another important unresolved issue in ceramic plasticity concerns the apparent discrepancies among deformation data obtained under different experimental conditions. Micropillar compression, nanoindentation, bending, tensile testing, and bulk compression probe different material volumes, stress states, strain gradients, defect populations, and fracture probabilities, and therefore their results cannot be compared in a purely quantitative manner without caution. Small-scale uniaxial testing, such as micropillar compression, has been increasingly used to study plasticity in macroscopically brittle crystals because the reduced specimen volume can suppress fast fracture and expose deformation mechanisms that are inaccessible in bulk tests [203]. However, micropillar compression may introduce its own uncertainties, including specimen-size effects, stochastic dislocation nucleation, pillar taper, focused-ion-beam-induced surface damage, and possible deviations from an ideal uniaxial stress state [204-206]. Therefore, the high apparent yield stresses or enhanced ductility observed in micropillars do not necessarily represent the intrinsic bulk plasticity of ceramics. Nanoindentation provides another powerful but complex approach for probing incipient plasticity in ceramics. The load-displacement response is sensitive to indenter geometry, tip radius, indentation depth, strain gradient, hydrostatic confinement, and local defect density[207, 208]. In oxide ceramics, indentation pop-in events may correspond either to dislocation activation or to crack formation, depending on the indenter tip radius and the competition between local shear stress and tensile fracture stress [209]. Therefore, hardness, pop-in load, and indentation-induced plastic zones should not be directly equated with uniaxial yield stress without considering the indentation size effect and the highly non-uniform stress field beneath the indenter.

By contrast, bending and tensile tests of ceramics are usually governed by flaw-controlled fracture rather than homogeneous plastic flow. Flexural strength is strongly affected by loading configuration, specimen size, surface preparation, test environment, and the size and severity of critical flaws [210]. Similarly, tensile strength depends on the flaw population and may not fully represent the behavior of the full-size component or that under different service environments [211]. Weibull statistics and effective-volume/effective-surface scaling are therefore required when comparing tensile, flexural, and multiaxial strength data of advanced ceramics [212]. These considerations are particularly important because a smaller stressed volume or a more favorable surface condition can lead to apparently higher strength even when the underlying deformation mechanism is unchanged.

Bulk compression provides a closer macroscopic measure of plastic flow but also has limitations. Standardized compression tests for advanced ceramics require careful control of specimen geometry, loading mode, loading rate, allowable bending, and data acquisition [210]. In addition, platen friction, end constraints, alignment errors, pre-existing flaws, and non-uniform slip-band formation may alter the measured stress-strain response. A direct comparison between bulk compression and indentation in $SrTiO_3$ has shown that even when both methods activate dislocation-mediated plasticity, the measured response depends strongly on the loading geometry and probed volume [198]. Thus, apparent contradictions among micropillar compression, nanoindentation, bending, tensile testing, and bulk compression should be interpreted as a combined consequence of intrinsic deformation mechanisms and extrinsic testing conditions.

These issues indicate that the plasticity of ceramics cannot be fully assessed from a single testing method. Instead, scale-bridging studies combining small-scale mechanical testing, bulk

deformation, *in-situ* observation, and post-mortem defect characterization are required. For example, the observed dislocation-related features support dislocation-mediated plasticity as the dominant mechanism under the current specific loading condition in the present work. Nevertheless, direct quantitative comparison with data obtained from different length scales or loading modes should be made cautiously, and unresolved issues related to stress state, defect density, flaw population, and local versus bulk deformation remain important topic for future work.

Table 3 Summary of mechanisms to achieve RT plasticity in ceramics.

Mechanism	Material	Structure	Grain size	Sample form	Loading mode	Strain/loading rate	Plastic strain (%)	Strength (GPa)	Ref.
Dislocation seeding	(001) $SrTiO_3$	Single crystal	-	Micro-pillars (aspect ratio of 2, ~4 μm in diameter)	Uniaxial compression	-	~32	~0.43	[19]
High-temperature preloading	(001) TiO_2	Single crystal	-	Micro-pillars (aspect ratio of 2, ~3 μm in diameter)	Uniaxial compression	5×10^{-3} s^{-1}	10	6.5	[21]
	(0001) Al_2O_3	Single crystal	-	Micro-pillars (aspect ratio of 2, ~3 μm in diameter)	Uniaxial compression	5×10^{-3} s^{-1}	6-7.5	8.0	[21]
Electric field/current-assisted plastic deformation	3Y-TZP	Polycrystal	0.52-0.70 μm	Macro-specimens Rectangular (~30×2×2 mm)	Three- point bending	-	5.5 (setup)	~0.12	[174]
Nanocrystalline	Cr_2AlC	Polycrystal	15.8 nm	Micro-pillars (aspect ratio of 2, ~1 μm in diameter)	Uniaxial compression	2.5×10^{-3} s^{-1}	0.31	12.8	[117]
Bond switching at coherent interfaces	Si_3N_4	Polycrystal	<1 μm	nano-pillars Rectangular (~350×350×250 nm)	Uniaxial compression	1×10^{-3} s^{-1}	32	11.0 ± 0.4	[31]
Twisted-layer interface-induced kink deformation & 3D interlocking	BN	Layer	-	Macro-pillars (~2.70 mm in diameter, ~3.46 mm in height)	Uniaxial compression	1×10^{-4} s^{-1}	14	0.626	[20]
Borrowed dislocations from metal interface	La_2O_3	Polycrystal	-	Tensile micro-sample (~1200×410×135 nm)	Uniaxial tensile	2×10^{-3} s^{-1}	39.9	2.3	[25]
Bioinspired "hard skeleton–plastic network"	(Hf, Zr, Ta, Nb, Ti, Cr)C–Cr_7C_3 high-entropy all-ceramic	Bimodal contiguous network structure	<10 μm	Nano-pillars (aspect ratio of ~3, ~300 nm in diameter)	Uniaxial compression	2 nm/s	30.8	~0.6	[43]
Intrinsic plasticity enabled by SFE	TiN/TaN	Multilayer	-	Micro-pillars (aspect ratio of 1.6, ~800 nm in diameter)	Uniaxial compression	5 nm/s	70	7.79	[185]
Point defect superstructure induced intrinsic plasticity	HfN	Single crystal	-	Nano-pillars (aspect ratio of ~2-3, ~300 nm diameter)	Uniaxial compression	1×10^{-2} s^{-1}	50	>7	[186]
Multi-phase composite	Al_2O_3–$GdAlO_3$	Dual-phase	-	Micro-pillars	Uniaxial compression	1×10^{-3} s^{-1}	5.2	12.3	[93]

				(aspect ratio of 2.5, ~1.02 μm in diameter)					
	$HfTaC_2$-W	Dual-phase	<5 μm	Nano-pillars Rectangular (150×150×300 nm)	Uniaxial compression	2 nm/s	23.8 ± 0.18	7.6 ± 1.2	[183]
				70 nm in thickness	Uniaxial tensile	2 nm/s	6.2	-	
Crystalline/amorphous dual phase	TiO_2	Crystalline/amorphous dual phase	-	Nanofiber (aspect ratio of 13, ~20 nm in diameter)	Uniaxial tensile	5 nm/s	~8.44	~1.06	[38]
	$Bi_4Ti_3O_{12}$	Crystalline/amorphous dual phase	0.1μm	Film (50 μm×8 μm×400 nm)	Bending	-	4.80	-	[194]
				Film (1.2 μm×700 nm×400 for tensile)	Uniaxial tensile	3×10^{11} s^{-1}	5.29	-	

7. Engineering application prospects and future research directions

7.1 Engineering application prospects

Plastic ceramics capable of significant plastic deformation without catastrophic fracture, mark a transformative advancement in materials science by overcoming the inherent brittleness o conventional ceramics through mechanisms such as dislocation engineering, high-density defect introduction via elevated-temperature preloading, severe plastic deformation, amorphous structuring, and eutectic microstructure refinement. These materials combine the traditional advantages of ceramics, such as high melting points, chemical inertness, wear resistance, and thermal stability, with metal-like plasticity, enabling reliable performance under complex thermomechanical loads, impact, vibration, and cyclic stresses. This unlocks broad engineering prospects across aero-engines, electronic devices, flexible wearable electronics, extreme-environment materials, nuclear energy, and deep-space applications, where conventional brittle ceramics often fail due to crack initiation and propagation.

7.1.1 Aero-engines

In aero-engines, advanced ceramic materials with enhanced plasticity or damage tolerance offer revolutionary potential for critical hot-section components, see **Fig. 27**, including turbine blades, vanes, nozzles, combustion liners, and thermal barrier coatings (TBCs) [213-215]. Their superior high-temperature stability, oxidation resistance, and mechanical reliability make them promising alternatives to conventional superalloys, particularly in next-generation engines operating under extreme conditions. Compared with currently deployed materials, particularly Ni-based superalloys,

advanced ceramics and ceramic-based systems offer several intrinsic advantages that are highly attractive for next-generation high-efficiency propulsion systems. While superalloys rely on complex cooling architectures to operate near their melting temperatures (~1100-1150 °C), ceramics such as oxide and non-oxide systems (e.g., SiC-based ceramic matrix composites) exhibit significantly higher temperature capability (>1300-1500 °C), enabling increased turbine inlet temperatures and thus improved thermodynamic efficiency [216].

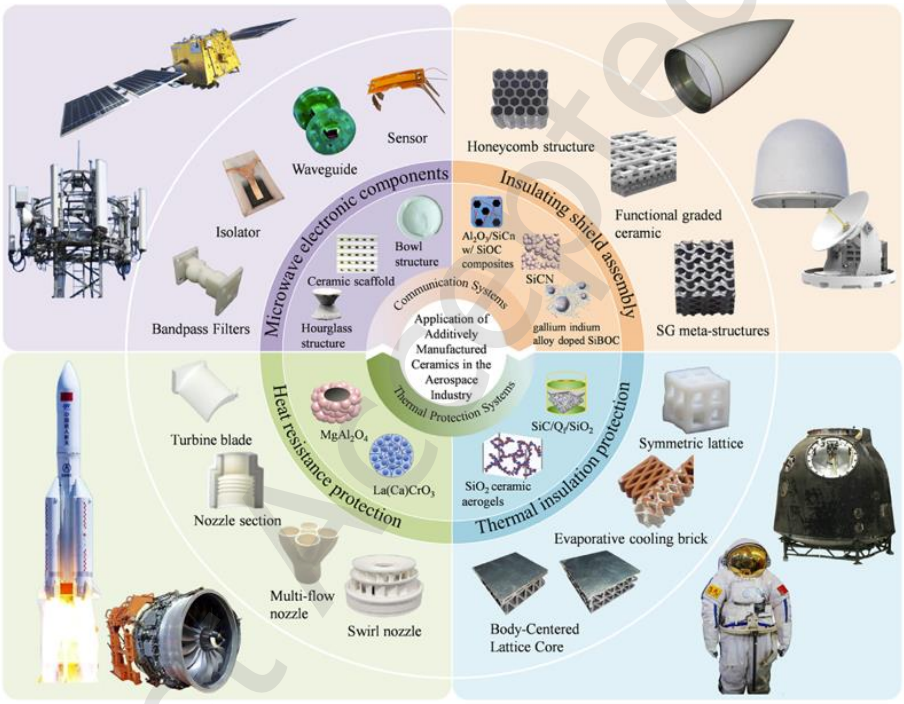

Fig. 27 Applications of additively manufactured ceramics in the aerospace industry. Reproduced with permission from Ref. [215], © KeAi 2026.

In addition, ceramics possess lower density (typically 2-4 g/cm^3) compared to superalloys (~8-9 g/cm^3), which can substantially reduce engine weight and enhance fuel efficiency. Furthermore, ceramics demonstrate superior oxidation and corrosion resistance under extreme environments, particularly in combustion atmospheres, reducing degradation and extending component lifetime [217]. Unlike metallic systems that suffer from creep and microstructural coarsening at elevated

temperatures, ceramics generally maintain phase stability and mechanical integrity over prolonged exposure [218].

Recent advances in plastic or damage-tolerant ceramics further mitigate their traditional brittleness, enabling non-catastrophic deformation, improved thermal shock resistance, and enhanced reliability under complex loading conditions. This emerging capability bridges the long-standing gap between ceramics and metals in terms of mechanical compliance, opening new opportunities for their application in turbine blades, vanes, combustion liners, and thermal barrier coatings. Plastic ceramics are increasingly viewed not only as high-temperature materials but also as structurally viable candidates for load-bearing components in advanced aero-engines. Enhanced RT and high-temperature plasticity improves resistance to thermal cycling, mechanical shock, and creep, reducing cooling requirements, boosting efficiency, and extending service life in extreme heat (< 1600 °C) and oxidative environments. Ceramic matrix composites (CMCs) incorporating ductile phases or defect-tuned matrices further enable lightweight, damage-tolerant components for next-generation jet engines and hypersonic vehicles, addressing the limitations of brittle failure in current ultra-high-temperature ceramics [219].

7.1.2 Extreme-environment materials

Extreme-environment materials benefit profoundly from plastic ceramics' ability to endure high temperature, corrosion, radiation, and mechanical abuse. Applications include seals, bearings, and structural components in petrochemical, metallurgical, or defense systems, where dislocation-mediated plasticity and shear-band formation (as in high-entropy or amorphous ceramics) provide energy dissipation mechanisms absent in brittle counterparts, enhancing reliability and lifespan [43].

Nuclear energy systems represent a critical domain: ductile ceramics can serve as advanced fuel pellets, cladding, structural components, or waste forms with improved radiation tolerance and resistance to swelling/cracking under neutron bombardment and high temperature gradients. Severe plastic deformation techniques (e.g., HPT-processed oxides or carbides [74]) yield nanograined structures with enhanced ion conductivity, thermomechanical stability, and defect annihilation, supporting safer, longer-life reactors and fusion components. Enormous technical progress has been made, but ceramic-based turbine components still have not found application in gas turbine engines, because of the problem of brittleness, should be overcome satisfactorily to achieve the utilization of ceramics in gas turbines [216, 220].

Deep-space applications, such as thermal protection systems, re-entry shields, satellite structures, radiators, and propulsion components, leverage plastic ceramics' lightweight nature, extreme thermal shock resistance, and plasticity for impact/vibration tolerance during launch, orbit, and planetary missions. Bioinspired high-entropy all-ceramics or dislocation-tuned variants retain strength up to 1300 ℃ while enabling complex geometries via additive manufacturing, critical for Mars missions, hypersonic vehicles, and long-duration spacecraft where failure is not an option [221].

7.1.3 Electronic devices, flexible wearable electronics

For electronic devices, plastic/ductile ceramics enable robust substrates, insulators, capacitors, and piezoelectric components with superior fracture toughness and formability [222]. Plastic deformability at RT facilitates integration into miniaturized, high-reliability systems (e.g., power electronics for electric vehicles or 5G/6G infrastructure) while maintaining dielectric stability and thermal management under operational stresses, vibrations, and thermal shocks, where traditional

ceramics suffer from microcracking. In flexible wearable electronics, the advent of RT tensile plasticity paves the way for thin-film or composite-based sensors, actuators, and interconnects that withstand repeated bending, stretching, and body-motion-induced strains without failure. These materials combine ceramic-level chemical stability and biocompatibility with polymer-like flexibility, enabling durable, skin-conformable devices for health monitoring, human-machine interfaces, and soft robotics in demanding environments.

Moreover, MAX phases possess tremendous potential for next-generation robust, stable and high-reliability flexible wearable electronic systems. Distinct from most brittle ceramic and rigid conductive materials, MAX phases achieve reversible interlayer slippage at RT under external deformation, which effectively releases mechanical strain and prevents structural damage and conductivity failure during cyclic bending, stretching and twisting. This exceptional RT plasticity endows MAX phases and their polymer composites with superior mechanical robustness and deformability, enabling their widespread use as flexible conductive electrodes, circuit interconnects and sensitive functional layers for wearable sensing devices. Meanwhile, their inherent thermal conduction and electromagnetic shielding performances resolve the heat accumulation and signal interference problems of highly integrated flexible electronics. Combined with favorable biocompatibility and sweat corrosion resistance, MAX-phase composites can be applied to epidermal sensors, flexible bioelectrodes and wearable self-powered triboelectric nanogenerators. Compared with conventional metallic nanomaterials and two-dimensional functional materials, MAX phases leverage stable RT plastic deformation to maintain consistent device performance under long-term mechanical cycling and harsh wearable service environments, avoiding material degradation and performance attenuation.

7.1.4 Biomedical Applications

Bioceramics have long been a cornerstone of biomedical engineering (e.g., dental restorations, implants, artificial joints, and synthetic bone substitutes) due to their exceptional biocompatibility, chemical stability, wear resistance, and similarity to bone mineral phases, such as hydroxyapatite (HA), Al_2O_3, ZrO_2, and silicate ceramics [223-226]. However, their intrinsic brittleness has historically limited performance in load-bearing applications such as orthopedic implants, dental prostheses, bone scaffolds, and tissue-engineering constructs, where cyclic mechanical stresses, impact, or surgical handling often induce catastrophic fracture. To address this limitation, various toughening strategies have been developed to introduce plasticity-related energy dissipation mechanisms, see **Fig. 28**, including crack-tip shielding, phase transformation, and composite reinforcement, which enable stress redistribution, crack deflection, and energy absorption, thereby mimicking the role of plastic deformation in metals while retaining ceramic-level bio-inertness or bioactivity [224]. These materials enable tougher, more reliable, and patient-specific implants that dissipate energy, and plastic deformation rather than brittle cleavage, significantly reducing failure rates in vivo and expanding the scope of bio-ceramic applications in regenerative medicine, dentistry, orthopedics, and soft-tissue interfaces.

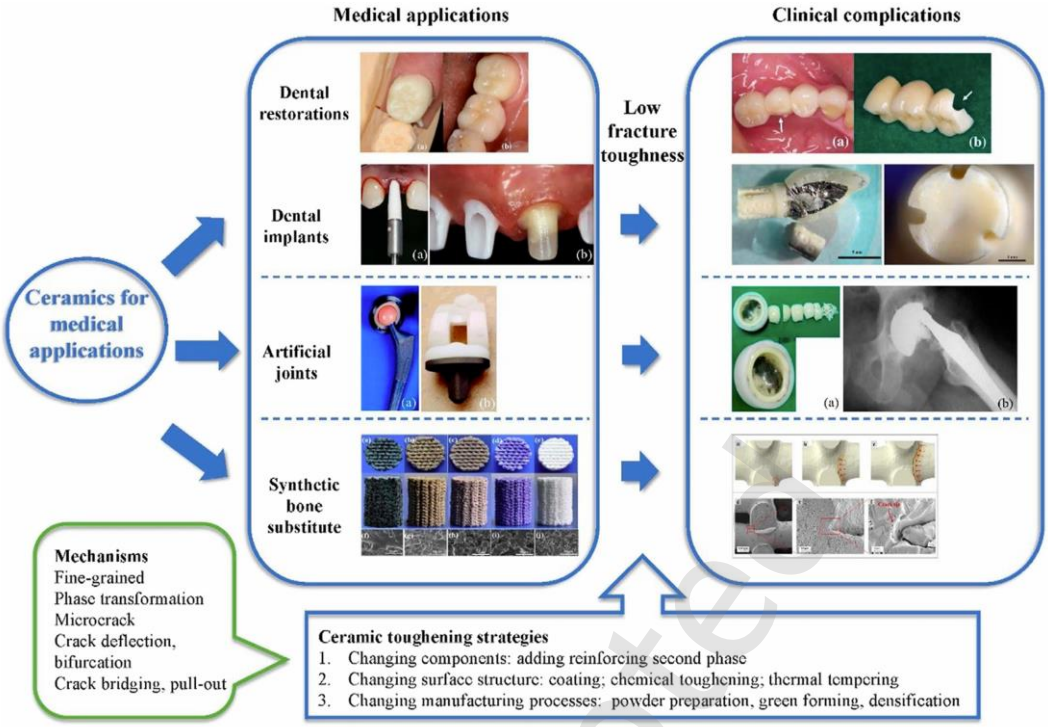

Fig. 28 Medical applications of ceramics, corresponding clinical complications due to the low fracture toughness of ceramics ,as well as toughening strategies and underlying mechanisms. Reproduced with permission from Ref. [224], © Frontiers Media 2022.

In orthopedic implants and bone repair, plastic ceramics offer transformative potential for hip/knee prostheses, spinal cages, and load-bearing scaffolds. Conventional ZrO_2 or Al_2O_3 components suffer from low fracture toughness (~3-6 $MPa \cdot m^{1/2}$) and are prone to chipping or cracking under physiological loads [225]. Then, dislocation-tuned or bioinspired high-entropy all-ceramics (e.g., HEC/Cr_7C_3 networks exhibiting ~12.5 $MPa \cdot m^{1/2}$ toughness and plastic shear bands [43]) can provide superior damage tolerance, fatigue resistance, and osseointegration. Patient-specific 3D-printed ductile bioceramic implants can better match bone elasticity, minimize stress shielding, and support complex geometries for personalized reconstruction after trauma or tumor resection [227]. Emerging projects such as ductile Ce- composites explicitly target patient-specific implants,

combining plasticity with bioactivity for enhanced long-term stability and reduced revision surgeries [228].

For dental restorations and maxillofacial applications, RT tensile plasticity revolutionizes crowns, bridges, implants, and abutments. Traditional all-ceramic systems fail via subsurface cracking during mastication; ductile variants enable thin, esthetic restorations with improved flexural strength (> 600 MPa) and quasi-ductile behavior under cyclic loading, while maintaining radiopacity, color stability, and biocompatibility. Additively manufactured ductile bio-ceramics further allow monolithic, multi-functional restorations with integrated antimicrobial or drug-release features, addressing peri-implantitis and improving clinical longevity [229]. Zhao *et al.* [230] demonstrated that ceramic quasi-plasticity can be achieved through multiscale structural and interfacial design. By integrating an amorphous ZrO_2 as intergranular phase, aligned nanowire architecture, and a confined polymer matrix, the material enables crack deflection, interfacial sliding, and viscoelastic energy dissipation. These features activate extrinsic toughening mechanisms such as crack bridging and pull-out, suppressing brittle fracture and producing enhanced strain tolerance.

In tissue engineering and regenerative scaffolds, plastic ceramics facilitate the design of highly porous, hierarchical structures that mimic trabecular bone or nacre while possessing intrinsic plasticity [231, 232]. Bioactive ductile ceramics (e.g., HA-based multiphase ceramics [233] or phosphate composites) promote osteoconduction/osteoinduction, vascularization, and controlled resorption without brittle fragmentation during implantation or remodeling. Their ability to undergo large plastic strains supports dynamic scaffolds for bone-tendon or neural interfaces, where mechanical mismatch with soft tissues has previously caused delamination or inflammation. Hybrid

organic-inorganic ductile systems (e.g., elastic ceramic-plastic hybrids inspired by biomineralization) extend applications to flexible bioelectronics or cartilage substitutes.

Additional biomedical niches include cardiovascular devices (e.g., heart-valve components requiring fatigue resistance) [234], drug-delivery carriers (porous ductile ceramics for sustained release under physiological stress) [229], and biosensors (piezoelectric ductile ceramics for implantable monitoring) [235]. Radiation tolerance and high-temperature stability of many plastic ceramics also suit sterilization processes and in vivo thermal management.

Scalable fabrication routes, such as flash sintering, mechanical dislocation seeding, cold sintering, or additive manufacturing, ensure biocompatibility while enabling cost-effective, customizable production. Challenges remain in optimizing degradation kinetics, surface biofunctionalization, and long-term in vivo plasticity retention, yet the synergy of plasticity with established bio-ceramic advantages positions plastic ceramics as next-generation biomaterials capable of meeting the demands of aging populations and personalized medicine.

7.2 Future research directions

The realization of RT plasticity in ceramics represents a paradigm shift in the long-standing perception of these materials as inherently brittle. Recent advances have demonstrated that, through various strategies such as tailored microstructural design and defect engineering, ceramics can exhibit significant plastic deformation under ambient conditions. These breakthroughs not only challenge classical theories of deformation in ionic and covalent solids but also open new opportunities for the application of ceramics in structurally demanding environments where both strength and damage tolerance are required. Despite this progress, the field remains at an early stage of development. Most

reported systems rely on carefully engineered extrinsic mechanisms, and their plasticity is often limited to small-scale specimens or specific loading conditions. Bridging the gap between fundamental discoveries and practical applications requires a more comprehensive understanding of deformation physics, as well as innovations in materials design and processing. Therefore, future research must move beyond proof-of-concept demonstrations toward the development of intrinsically ductile ceramic systems, scalable material architectures, and reliable manufacturing technologies.

7.2.1 Intrinsic plasticity design

Most current approaches rely on extrinsic defect engineering to introduce mobile dislocations post-synthesis. The next frontier lies in discovering or tailoring ceramic compositions and crystal structures that inherently possess low Peierls barriers, multiple independent slip systems, and facile dislocation glide or climb at RT without external intervention. This includes exploring new oxide, nitride, carbide, and high-entropy ceramic families where electronic structure, bonding character, and lattice symmetry naturally favor plasticity, moving beyond the limited set of perovskites (e.g., $SrTiO_3$, $KNbO_3$) or rock-salt oxides that currently exhibit bulk plasticity [30].

7.2.2 Synergistic plasticity design

Future advances are likely to arise from the synergistic interaction of multiple deformation mechanisms operating across different length scales. For example, transformation plasticity can effectively dissipate energy and shield crack tips through stress-induced phase transformations, while coherent interfaces may simultaneously facilitate defect-mediated deformation and suppress strain localization. Similarly, nanocrystalline grain-boundary networks can promote strain accommodation through grain-boundary-mediated processes, whereas interface engineering may improve the stability

and continuity of deformation. The cooperative operation of these mechanisms may significantly delay crack initiation and reduce the likelihood of catastrophic fracture.

Hierarchical architectures provide another promising platform for mechanism coupling. In such systems, different structural units may perform distinct mechanical functions. Interfaces can accommodate local strain, nanocrystalline regions may promote distributed plasticity, and transformation-capable phases can dissipate fracture energy. Consequently, crack propagation may be repeatedly deflected, blunted, or arrested across multiple length scales, resulting in enhanced damage tolerance.

Recent studies on borrowed-dislocation strategies, coherent-interface engineering, and multiphase ceramic systems collectively suggest that the simultaneous activation of multiple deformation pathways may provide a more effective route toward overcoming the traditional strength-toughness-plasticity trade-off. For instance, borrowed dislocations can reduce the barrier for dislocation nucleation and enhance local plasticity, while coherent interfaces promote strain accommodation through bond-switching and interface-mediated deformation. In multiphase systems, hard and soft constituents may cooperate through load redistribution, crack bridging, and interfacial energy dissipation, thereby improving both strength and damage tolerance.

Therefore, future ceramic design should move beyond the optimization of individual deformation mechanisms and instead focus on the deliberate integration of multiple plasticity pathways. Such synergistic plasticity design, combining defect engineering, interface engineering, transformation plasticity, and hierarchical architectures, is expected to become a key paradigm for the development of next-generation damage-tolerant ceramic materials.

7.2.3 Trade-off between ceramic plasticity and strength

A further fundamental issue that must be addressed is the strength-plasticity trade-off, which remains a central paradigm in the mechanical design of ceramics. Achieving an optimal balance between strength/hardness and plasticity demands systematic microstructure optimization. High dislocation densities or refined grains often enhance plasticity at the expense of hardness or ultimate strength. However, in most currently reported systems, the introduction of plasticity, induced by dislocation slip, GBS, or phase transformation, inevitably leads to a reduction in strength, hardness, or creep resistance. This trade-off arises because the same structural features that facilitate deformation (e.g., high defect densities, weak interfaces, or metastable phases) often act as stress concentrators or reduce resistance to crack initiation. Importantly, increasing evidence suggests that the strength-plasticity (or strength-toughness) trade-off in ceramics is not an immutable limitation, but rather a consequence of insufficient structural design across length scales.

One promising direction is the development of heterogeneous and hierarchical architectures, where regions optimized for plastic deformation are spatially integrated with domains that retain high strength and stiffness. For instance, nacre-mimetic anisotropic microstructural ceramics demonstrate that spatially organized hard/weak interfaces can simultaneously promote crack deflection and maintain load-bearing capability, thereby approaching the theoretical limits of strength and toughness by enabling plastic like-deformation [236]. Similarly, high-entropy all-ceramics incorporated a contiguous network of plastically deformable phases, showing that the introduction of localized plasticity via shear-band formation and defect accumulation can effectively dissipate energy while preserving high strength, offering a pathway to overcoming the traditional mutual exclusivity of these properties [43]. At smaller scales, engineered nano-heterogeneities and eutectic microstructures

further demonstrate that controlled phase distribution and interface density can activate multiple deformation mechanisms (e.g., dislocation glide, crack bridging, and phase-boundary sliding), enabling measurable plastic strain without catastrophic strength degradation [93, 237]. In parallel, architectured and interpenetrating-phase composites inspired by natural materials such as bone and nacre show that multiscale structural integration can significantly enhance both strength and energy absorption, primarily through synergistic mechanisms including crack deflection, interfacial debonding, and strain delocalization [238, 239].

These findings collectively indicate that the key to mitigating the strength-plasticity trade-off lies not in optimizing a single deformation mechanism, but in coordinating multiple mechanism across hierarchical structures. Future efforts should therefore focus on establishing quantitative structure-property relationships that link phase topology, interface chemistry, and defect dynamics to macroscopic mechanical performance. Such an approach will be essential for designing next-generation plastic ceramics that achieve both high strength and reliable deformation capability under practical service conditions. For instance, Sohail *et al.* [240] employed physics-guided machine learning to design strong yet ductile FeNiCoAlTa alloys by optimizing microstructures and work-hardening capacity, overcoming the strength-plasticity trade-off. Moreover, Wu *et al.* [172] achieved ultrahigh strength and large plasticity in a high-entropy MAX phase by introducing local chemical fluctuations through multicomponent alloying. These fluctuations strengthen the lattice while promoting distributed dislocation activity, thereby mitigating strain localization and overcoming the conventional strength–plasticity trade-off.

7.2.4 Reliability challenges and engineering feasibility

Although various plastic deformation mechanisms have been demonstrated in ceramics at the micro/nanoscale or under specific loading conditions, and remarkable progress has been achieved in improving the RT plastic deformability of ceramics, translating these progress into bulk, reproducible, and engineering-relevant ceramic components remains a major challenge. In addition to strength, hardness, and achievable plastic strain, engineering applications require systematic evaluation of long-term reliability under realistic service conditions. Another fundamental challenge is the stability and repeatability of plasticity itself. In many currently reported plastic ceramics, the measured deformation behavior is highly sensitive to sample dimensions, flaw population, grain size distribution, interface chemistry, local phase arrangement, loading configuration, and processing history. Consequently, plastic strain, yield-like behavior, and failure mode may vary substantially among nominally similar specimens or across different fabrication batches. Future studies should therefore establish quantitative processing-microstructure-plasticity relationships and evaluate the statistical reproducibility of deformation behavior using sufficiently large sample populations.

In particular, it is important to determine whether the plasticity-enhancing mechanisms remain active, stable, and controllable after repeated loading, prolonged thermal exposure, or service-induced microstructural evolution. Fatigue performance is critical issue because many ceramic components are subjected to cyclic mechanical or thermomechanical loading. Plastic deformation may relax local stress concentrations and delay catastrophic fracture, but repeated activation of dislocation motion, GBS, interfacial sliding, phase transformation, or amorphous flow may also induce accumulated damage, microcrack nucleation, interfacial degradation, or residual-stress redistribution. Therefore,

the fatigue life, cyclic deformation stability, and subcritical crack growth behavior of plastic ceramics should be carefully examined.

Moreover, crack initiation and propagation behavior must be understood in relation to plasticity mechanisms. For conventional brittle ceramics, failure is often governed by the rapid crack extension from pre-existing defects. In plastic ceramics, local plasticity may blunt crack tips, shield the crack driving force, and promote energy dissipation. However, if plasticity deformation is highly localized, it may instead generate shear bands, damaged grain boundaries, or weakened interfaces that accelerate crack propagation. Future studies should therefore combine fracture mechanics, *in-situ* characterization, and multiscale modeling to clarify how different plasticity mechanisms influence crack-tip shielding, crack deflection, bridging, and stable or unstable crack growth.

Then, high-temperature reliability is essential for structural, thermal-protection, aero-engine, and extreme-environment applications. Some strategies that promote RT plasticity, such as nanocrystalline structures, amorphous grain-boundary phases, or highly defective interfaces, may become vulnerable to creep, grain growth, interfacial diffusion, or structural relaxation at elevated temperatures. Thus, the resistance of plastic ceramics to high-temperature creep and thermomechanical degradation should be considered together with their RT deformability. A useful plastic ceramic for engineering applications should maintain a balance between plastic strain accommodation at RT and microstructural stability at service temperature.

On the other side, long-term environmental stability represents another key bottleneck. Plastic ceramics designed through defect engineering, multiphase composites, layered architectures, or amorphous-crystalline structures may contain chemically active deformation tolerance but may also reduce resistance to oxidation, corrosion, moisture-assisted degradation, irradiation damage, or

thermal cycling. Therefore, environmental durability tests in oxidizing, corrosive, humid, or radiation-containing environments are necessary to evaluate whether the plasticity-enhancing microstructures remain stable during long-term service.

The scale-up of plastic ceramics requires careful consideration of the process-performance-cost triangle. A central scientific challenge is whether the microstructures responsible for enhanced plasticity can be reproducibly retained during large-scale powder processing, shaping, densification, machining, and joining. Many currently reported plastic ceramic systems rely on small-scale samples, specialized microstructures, high-purity powders, severe plastic deformation, complex multilayer fabrication, or advanced sintering techniques. These approaches are valuable for revealing fundamental mechanisms but may face challenges in producing large, complex-shaped, and defect-controlled components at acceptable cost. In addition, scale-up may introduce microstructural gradients, residual stresses, porosity fluctuations, and a broader defect distribution, all of which can reduce the stability and repeatability of plastic deformation. Future engineering development should therefore focus on scalable powder processing, near-net-shape forming, reproducible microstructure control, nondestructive defect evaluation, and component-level mechanical testing. Many currently reported plastic ceramic systems rely on small-scale sample, specialized microstructures, high-purity powders, severe plastic deformation, complex multilayer fabrication, or advanced sintering techniques. These approaches are valuable for revealing fundamental mechanisms but may face challenges in producing large, complex-shaped, and defect-controlled components at acceptable cost. Future engineering development should therefore focus on scalable powder processing, near-net-shape forming, reproducible microstructure control, nondestructive defect evaluation, and component-level mechanical testing. Only by integrating plasticity design with reliability assessment

and manufacturability can plastic ceramics progress from laboratory materials to practical engineering components.

Achieving reliable, macroscopic plasticity in bulk ceramic components remains the ultimate engineering objective. However, the most promising route is unlikely to be universal. Rather than selecting a strategy solely according to the highest reported strain, future research should match the plasticity-design approach to the target application scenario and its required combination of temperature capability, strength, environmental stability, functional performance, and manufacturability. For structural components operating under extreme temperatures, high stresses, or aggressive environments, coherent-interface engineering appears particularly promising. Coherent-interface engineering offers significant potential because interfaces can provide strong load transfer while enabling interface-mediated deformation, crack deflection, and stress redistribution to remain structurally robust at elevated temperatures, offering a realistic pathway toward improving tensile reliability without sacrificing the thermal stability and load-bearing capability required for high-temperature ceramic applications [22, 31]. By contrast, applications such as flexible electronics, wearable devices, soft sensors, and deformable thermoelectrics prioritize RT deformability and functional retention over extreme-temperature structural stability. In these cases, Ag_2S-based intrinsically plastic semiconductors, together with composite and microstructural plasticity-design strategies, may be more advantageous. Their capacity for substantial deformation while maintaining electrical or thermoelectric functionality makes them attractive for mechanically compliant devices. Transformation plasticity appears attractive because stress-induced phase transformations can simultaneously accommodate strain, dissipate energy, and provide crack-tip shielding under complex stress states [122]. Similarly, Layered architectures, such as twist-stacked BN ceramics, may further

enhance fatigue resistance through interlayer sliding, kink-band formation, and distributed energy dissipation mechanisms [143, 144].

However, no individual mechanism is likely to provide sufficient reliability under all service conditions. Future breakthroughs will probably depend on the cooperative interaction of multiple deformation mechanisms operating across different length scales. For example, transformation plasticity may provide crack-tip shielding, while coherent interfaces facilitate defect-mediated plastic flow and nanocrystalline grain-boundary networks promote strain homogenization. Similarly, multiphase composite systems may combine dislocation-mediated deformation, interface sliding, crack bridging, and load redistribution to achieve simultaneous improvements in strength, toughness, fatigue resistance, and damage tolerance [25, 196, 197]. Therefore, the development of hierarchical and multi-mechanism ceramic systems capable of coordinating deformation, energy dissipation, and crack resistance across multiple length scales is expected to represent one of the most promising directions for achieving reliable RT plasticity in future engineering applications.

7.2.5 Data-driven and first-principles design of plasticity in ceramics

The integration of artificial intelligence (AI) with multiscale computational methods is emerging as a transformative pathway for understanding and designing plasticity in ceramics. Compared with conventional trial-and-error approaches, AI-enabled frameworks can significantly accelerate the exploration of composition-structure-property relationships, particularly for complex deformation phenomena that span multiple length scales. Computational design frameworks, density functional theory (DFT) calculations of slip barriers and Peierls stresses, phase-field modeling of dislocation dynamics and microstructure evolution, and machine-learning (ML) screening of vast

compositional spaces offer powerful tools for identifying promising candidates and optimizing processing parameters. Data-driven approaches have already begun to pinpoint key descriptors governing bulk RT plasticity [241], while neural-network potentials and deep-learning surrogates for phase-field simulations promise orders-of-magnitude reductions in computational cost [24], enabling high-throughput exploration of dislocation plasticity in complex ceramics.

For plasticity-oriented screening, however, the training and validation datasets must extend beyond equilibrium bulk structures to include deformation-relevant configurations, such as strained states along candidate slip paths, generalized stacking-fault energy surfaces, dislocation cores, point defects, free surfaces, grain boundaries, and relevant temperature-pressure conditions. This requirement is critical because a model that accurately reproduces bulk thermodynamic properties may still be unreliable for the highly distorted local environments governing dislocation nucleation, core reconstruction, and Peierls barriers. Machine-learning interatomic potentials (MLIPs), combined with uncertainty quantification and targeted retraining, therefore provide an important bridge between DFT-level accuracy and large-scale molecular-dynamics simulations of defect-mediated plasticity [242]. Recent work on dislocations in SiC further demonstrates the feasibility of developing MLIPs for ceramic defect environments that are difficult to access directly by DFT at large length scales [243]. Feng *et al.* [244] revealed that high-entropy carbide $(Zr_{0.2}Hf_{0.2}Ti_{0.2}Nb_{0.2}Ta_{0.2})C$ can undergo pronounced plastic deformation under shock loading, driven by hierarchical dislocation-mediated mechanisms activated at ultrahigh strain rates, see **Fig. 29**. Under extreme stress conditions (on the order of tens of GPa) and high strain rates ($\sim 10^5$-10^6 s^{-1}), the material exhibits the nucleation and rapid multiplication of dislocations, which subsequently organize into complex defect structures such as dislocation networks, cells, and sub-grains. The study further showed that the severe lattice

distortion inherent to the high-entropy composition lowers the energy barrier for dislocation activation while simultaneously impeding dislocation motion, leading to significant strain hardening. In addition, the formation of stacking faults and nanoscale deformation bands contributes to hierarchical strain accommodation, effectively delaying crack initiation and propagation. These coupled mechanisms enable measurable plastic strain under shock conditions while maintaining high strength, demonstrating that even ultrahard ceramics can exhibit dislocation slip-dominated plasticity when subjected to extreme loading environments.

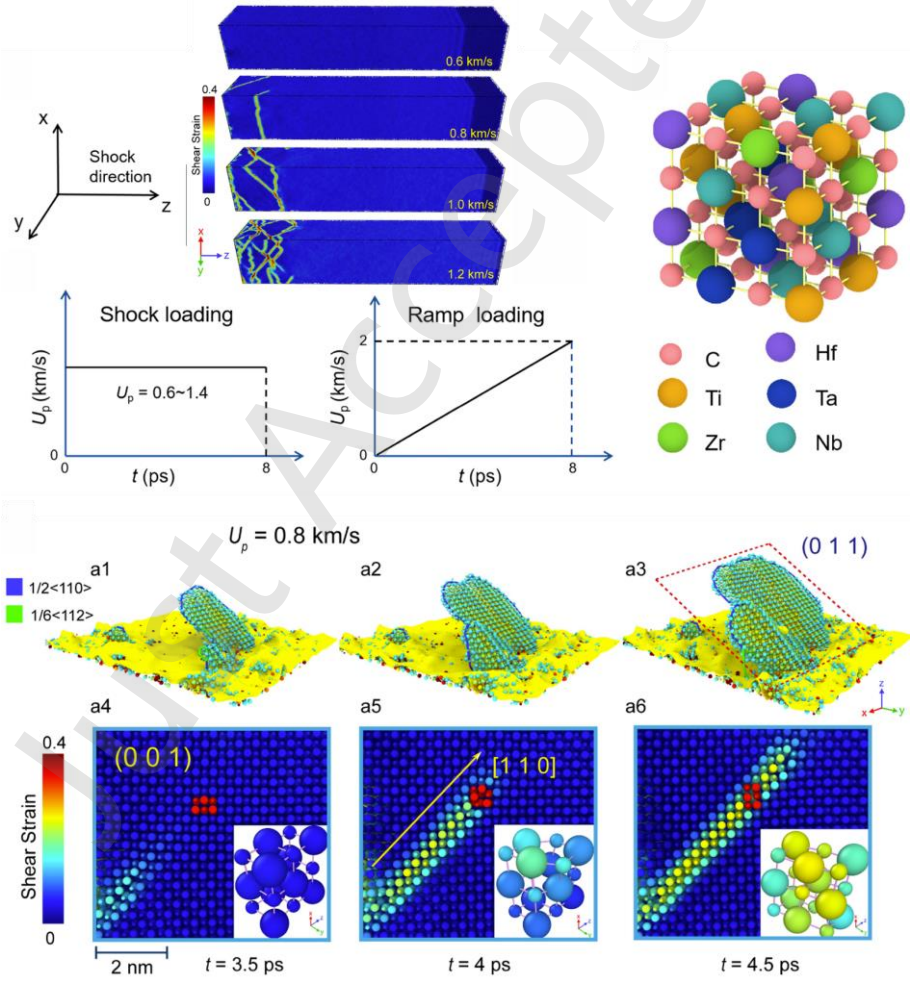

Fig. 29 Shock-induced hierarchical plastic deformations in high-entropy ceramics at high strain rate. Reproduced with permission from Ref. [244], © Elsevier Ltd. 2026.

AI-assisted computational design enables a shift from empirical discovery to data-driven and inverse design paradigms. By combining high-throughput simulations with machine learning (ML), it is now possible to rapidly predict mechanical properties and identify candidate materials with targeted plasticity. Integrating AI-driven materials design with Industry 4.0 enables closed-loop development of plastic ceramics. Digital twins of processing, combined with real-time sensing and machine learning, allow dynamic optimization of microstructure and defect states critical to plasticity. This data-centric framework links computational prediction, high-throughput experimentation, and scalable manufacturing, improving reproducibility and accelerating deployment. Such convergence is expected to establish autonomous materials innovation pipelines, bridging the gap between discovery and industrial application.

For plastic ceramics, the inverse-design objective should be explicitly multi-objective rather than based on an isolated plasticity-related descriptor. Candidate compositions should be simultaneously assessed for phase and processing stability, elastic stiffness, hardness, fracture resistance, environmental stability, and deformation-related descriptors, including generalized stacking-fault energies, ideal shear strengths, Peierls barriers, and predicted dislocation mobility. Such constraint-aware optimization is essential to avoid improving a nominal plasticity metric at the expense of phase stability or mechanical strength. Although fully autonomous development of plastic ceramics remains an emerging capability, uncertainty-aware active learning and digital-twin concepts provide a credible route toward closed-loop optimization: computational models identify informative composition-processing-microstructure experiments, experimental measurements update model uncertainty, and subsequent iterations refine both processing windows and defect-state targets [245-247]. Recent reviews highlight that AI can efficiently map structure-property relationships and

optimize material compositions under multiple constraints, thereby accelerating materials discovery beyond traditional approaches [248]. In particular, inverse design strategies based on generative models and optimization algorithms are increasingly used to propose new crystal structures or chemistries with enhanced deformability.

At the atomic scale, density functional theory (DFT) remains a cornerstone for quantifying the fundamental mechanisms governing plasticity, such as dislocation core structures, generalized stacking fault energies, and slip barriers. These quantities are critical descriptors of intrinsic plasticity in ceramics. However, the high computational cost of DFT limits its direct application to large compositional spaces. Recent efforts therefore combine DFT with ML surrogate models to retain quantum-mechanical accuracy while enabling high-throughput screening of deformation-related properties [249, 250]. Such hybrid approaches are particularly promising for identifying ceramic systems with reduced slip barriers and enhanced dislocation mobility. Beyond direct property regression, MLIPs make it computationally tractable to sample defect interactions, dislocation nucleation events, and thermally activated dislocation motion in simulation cells that are far larger than those accessible by conventional DFT. A robust multiscale workflow should therefore use DFT to generate and validate deformation-relevant quantities, use active learning to enrich the training set whenever model uncertainty increases, and subsequently transfer dislocation energetics and mobility laws to discrete-dislocation, phase-field, or crystal-plasticity models. This hierarchy makes the information flow across atomistic and mesoscale levels explicit, rather than treating DFT, molecular dynamics, and continuum modeling as independent screening tools [242, 243]. At the mesoscale, phase-field modeling provides a powerful framework for simulating microstructure evolution, strain localization, and defect interactions during plastic deformation. When coupled with AI techniques,

phase-field simulations can be significantly accelerated and extended to explore large parameter spaces. Moreover, physics-informed ML models are increasingly being integrated with phase-field methods to capture complex nonlinear behaviors and to establish quantitative links between microstructural features and macroscopic plasticity. Recent ML surrogate and physics-embedded graph-network approaches have demonstrated substantial acceleration of phase-field microstructure simulations while retaining physically constrained model representations [251, 252]. Although many such demonstrations have not yet focused specifically on dislocation plasticity in ceramics, they provide transferable computational strategies for accelerating the exploration of microstructure-sensitive deformation mechanisms. This multiscale coupling is essential for bridging atomistic insights and engineering-scale performance.

ML has become a key tool for high-throughput screening of candidate ceramic materials with potential plasticity. ML models trained on DFT or experimental datasets can predict mechanical properties such as elastic moduli, hardness, and even plasticity-related descriptors with high efficiency [248]. For example, ML-guided discovery has already been successfully applied to complex ceramic systems such as high-entropy carbides, enabling rapid identification of stable compositions and phase structures [253]. More specifically, ML has been used to identify candidate high-entropy ceramic compositions, construct single-phase probability maps for equiatomic and non-equiatomic carbides, and perform active-learning-guided exploration of substantially expanded high-entropy ceramic composition spaces [253, 254]. These studies provide a direct ceramic-specific foundation for future plasticity-oriented screening. The next step is to augment phase-stability datasets with deformation-sensitive labels, including generalized stacking-fault energy landscapes, ideal shear strengths, Peierls stresses, dislocation mobilities, defect formation energies, and crack-

tip/slip competition metrics, thereby allowing phase stability and plasticity to be co-optimized rather than evaluated sequentially. More broadly, integrated workflows combining DFT, ML, and kinetic modeling have demonstrated the ability to predict composition, stability, and long-term performance of ceramic materials in a unified framework [249]. Future research should therefore focus on developing physics-informed AI models, active learning strategies, and autonomous experimentation platforms to iteratively refine predictions. Equally important, uncertainty estimates and targeted experimental validation should accompany predicted deformation properties, particularly when models are extrapolated to high-pressure, high-strain-rate, or chemically disordered ceramic systems. Ultimately, the synergy between AI and multiscale modeling is expected to play a pivotal role in discovering intrinsically plastically deformable ceramics and in overcoming long-standing limitations such as the strength-plasticity trade-off.

8. Conclusions

This review has systematically summarized the fundamental theory, material systems, plastic deformation mechanisms, and engineering strategies associated with RT plasticity in ceramics. Traditionally regarded as inherently brittle due to strong ionic/covalent bonding, ceramics have long been excluded from applications requiring mechanical reliability under complex stress conditions. However, recent advances have demonstrated that plasticity in ceramics can be activated under carefully designed strategies, fundamentally reshaping our understanding of the mechanical deformation behaviors.

From a mechanistic perspective, multiple deformation pathways (e.g., dislocation, GBS, twinning, phase transformation, amorphous flow, and interface sliding) have been identified as viable

contributors to plastic deformation of ceramics. It is worth to noting that the observed plasticity in practical ceramic systems response is commonly determined by the coupled activation, accommodation, and competition of multiple mechanisms at atomic, interfacial, grain, and microstructural length scales. These mechanisms often operate synergistically depending on composition, crystal structure, defect state, and loading conditions. Importantly, the activation of these mechanisms is closely tied to the competition between dislocation mobility and fracture, which remains the central governing principle for achieving RT plasticity in ceramics. In terms of material systems, a diverse range of ceramics (e.g., including oxides, non-oxides, inorganic thermoelectric materials, amorphous ceramics, HECs, and MAX phases) have exhibited varying degrees of RT plasticity. While early studies emphasized deformation at reduced length scales, increasing evidence suggests that plasticity can also be realized in bulk or architected ceramics through material-design strategies, which highlights the importance of moving beyond size-constrained effects toward intrinsically deformable material systems.

Significant progress has been achieved through engineering strategies aimed at promoting plastic deformation. Dislocation engineering approaches, such as pre-deformation, dislocation seeding, and high-temperature preloading, effectively reduce the barriers for dislocation nucleation and motion. Structural design strategies (e.g., nanocrystalline architectures, coherent interfaces, layered structures, defect engineering, and multiphase composites) enhance deformation compatibility and suppress catastrophic crack propagation. In addition, amorphous-crystalline composite designs provide alternative pathways for strain accommodation. External field regulation further offers a promising route to dynamically tailor defect activity and local stress states. Advances in experimental characterization techniques have played a critical role in these developments. The

combination of *in-situ* mechanical testing with high-resolution imaging has enabled direct observation of deformation processes, while improved methods for measuring small strains have facilitated more accurate assessment of plasticity. These tools have significantly deepened our understanding of the interplay between microstructure, defects, and mechanical response across different length scales.

Despite these achievements, several key challenges remain. The translation of plasticity from controlled experimental conditions to reliable macroscopic performance is still limited. And, the development of intrinsically plastic ceramic systems that do not rely on extreme geometrical constraints or complex architectures remains in its early stages. Moreover, the trade-off between plasticity and strength continues to constrain practical applications. In addition, scalable fabrication techniques and reproducibility of mechanical performance are critical barriers to engineering implementation.

Future research should focus on the design of intrinsically RT plastic ceramic compositions and crystal structures, bridging the gap between fundamental mechanisms and bulk-scale material behavior, developing scalable processing and manufacturing strategies, optimizing the balance between strength and plasticity, and leveraging data-driven and artificial intelligence approaches to accelerate microstructure design and property prediction. In summary, the emerging understanding of RT plasticity in ceramics marks a paradigm shift in ceramic materials science. By integrating advances in theory, materials design, and characterization, it is increasingly feasible to develop ceramics that combine high strength with appreciable plasticity. Such progress is expected to unlock new opportunities for ceramics in structural, electronic, and extreme-environment applications, ultimately transforming them from brittle materials into damage-tolerant engineering systems.

Funding

This work was supported by the National Key Research and Development Program of China (No.2025YFF0520903), the National Natural Science Foundation of China (No.U23A20566 and No.52531005), Natural Science Foundation of Zhejiang Province (No.LZYQ25E020001 and No.LD26E010002), "Pioneer" and "Leading Goose" R & D Program of Zhejiang (Grant No.2024SSYS0051), Young Scientists Innovation Team of Zhejiang Province (Grant No.2025TD2072), the Young Elite Scientists Sponsorship Program by China Association for Science and Technology (CAST) (Grant No. 2024QNRC001).

Author contributions

Zhitong xu: Conceptualization, Data curation, Investigation, Methodology, Resources, Validation, Visualization, Writing-original draft, Writing - review & editing.

Jie Zhang: Conceptualization, Data curation, Funding acquisition, Investigation, Methodology, Resources, Supervision, Validation, Visualization, Writing - original draft, Writing - review & editing.

Liran Dong: Conceptualization, Data curation, Funding acquisition, Investigation, Methodology, Resources, Supervision, Validation, Visualization, Writing - original draft, Writing - review & editing.

Yuanwei Chao: Writing-original draft, Writing-review & editing.

Guanghua Liu: Data curation, Investigation, Validation, Writing - review & editing.

Kexin Chen: Conceptualization, Funding acquisition, Supervision, Writing - review & editing.

Availability of data and materials

The data that support the findings of this study are available from the corresponding author upon reasonable request.

Competing interests

The authors have no competing interests to declare that are relevant to the content of this article.

References

[1] Brook R J, Superhard ceramics. *Nature* 1999, **400**: 312-313.

[2] Wang K, Zhang Y, Ma G*, et al.*, Exceptional mechanical properties of $(Ti_{1-x}Zr_x)_2AlC$ MAX phase coatings with amorphous-nanocrystalline oxidation layers. *J Adv Ceram* 2026, **15**: 9221201.

[3] Zhao Z, Xie W, Xiang H*, et al.*, Single-phase high-entropy (TiZrNbMoW)C ceramic: A potential high-temperature anti-wear material. *Ceram Int* 2026, **52**: 11989-12000.

[4] Xu L, Lin J, Yang Y*, et al.*, Ultrahigh thermal stability and piezoelectricity of lead-free KNN-based texture piezoceramics. *Nat Commun* 2024, **15**: 9018.

[5] Zeng Y, Wang D, Xiong X*, et al.*, Ablation-resistant carbide $Zr_{0.8}Ti_{0.2}C_{0.74}B_{0.26}$ for oxidizing environments up to 3, 000 ℃. *Nat Commun* 2017, **8**: 15836.

[6] Liu S, Deng J, Zhao H*, et al.*, Tooth enamel-inspired ceramic coating on metal surface for enhanced mechanical properties and corrosion resistance. *Nat Commun* 2025, **16**: 5980.

[7] Zheng Y, Sun J, Ning S*, et al.*, Determination of optimal graphene configuration on the mechanical responses and machining performance of ceramic cutting tool. *Ceram Int* 2025, **51**: 60542-60554.

[8] Wang L, He L, Xu Z*, et al.*, Erosion behavior of YSZ, LZC, and LZC/YSZ double-ceramic-layers thermal barrier coatings by EB-PVD under high-temperature gas streams with entrained solid particles. *Surf Interfaces* 2026, **87**: 109073.

[9] Wang K, Guo L, Yuan X*, et al.*, First principles insights into solid solution mechanisms of doped $Gd_2Zr_2O_7$ and guides to develop novel thermal barrier coating materials. *J Adv Ceram* 2026, **15**: 9221295.

[10] Cheng J, Wang H, Xu X*, et al.*, Negative thermal expansion ScF_3 ceramic for electronic packaging applications. *J Materiomics* 2026, **12**: 101126.

[11] An X, Dong K, Cao K*, et al.*, Engineering high-stability ceramic core of turbine blade by controllable additive manufacturing and microstructural synergy. *J Manuf Processes* 2026, **167**: 221-236.

[12] Carter C B and Norton M G, *Ceramic materials: Science and engineering*. New York: Springer, 2013.

[13] Chokshi A H, Diffusion creep in oxide ceramics. *J Eur Ceram Soc* 2002, **22**: 2469-2478.

[14] Ruano O A, Wadsworth J and Sherby O D, Deformation of fine-grained alumina by grain boundary sliding accommodated by slip. *Acta Mater* 2003, **51**: 3617-3634.

[15] Feng B, Wang Z, Fan Y*, et al.*, Creep deformation behavior during densification of ZrB_2-SiBCN ceramics with ZrO_2 additive. *J Adv Ceram* 2020, **9**: 544-557.

[16] Kawasaki M, Figueiredo R B and Langdon T G, A review of the role of grain boundary sliding in creep deformation. *Mater High Temp* 2026, **43**: 3-16.

[17] Jian J, Lee J H, Liu Y*, et al.*, Plastic deformation in nanocrystalline TiN at ultra-low stress: An *in situ* nanoindentation study. *Mater Sci Eng A* 2016, **650**: 445-453.

[18] Frisch A, Okafor C, Preuß O*, et al.*, Room-temperature dislocation plasticity in ceramics: Methods, materials, and mechanisms. *J Am Ceram Soc* 2025, **108**: e20575.

[19] Fang X, Lu W, Zhang J*, et al.*, Harvesting room-temperature plasticity in ceramics by mechanically seeded dislocations. *Mater Today* 2025, **82**: 81-91.

[20] Wu Y, Zhang Y, Wang X*, et al.*, Twisted-layer boron nitride ceramic with high deformability and strength. *Nature* 2024, **626**: 779-784.

[21] Shen C, Li J, Niu T*, et al.*, Achieving room temperature plasticity in brittle ceramics through elevated temperature preloading. *Sci Adv* 2024, **10**: eadj4079.

[22] Liu L, An X, Gu X*, et al.*, Nanotwinned CrN ceramics with enhanced plasticity. *Nat Commun* 2025, **16**: 5934.

[23] Wu W, Shao L, Li N*, et al.*, Superior plastic flow stability of self-patterned carbide – amorphous ceramic nanostructures. *Mater Res Lett* 2025, **13**: 719-728.

[24] Zhang S, Li Y, Suzuki S*, et al.*, Neural network potential for dislocation plasticity in ceramics. *npj Comput Mater* 2024, **10**: 266.

[25] Dong L R, Zhang J, Li Y Z*, et al.*, Borrowed dislocations for ductility in ceramics. *Science* 2024, **385**: 422-427.

[26] Liu M and Xu Z, Micromechanical characterization of microwave dielectric ceramic BaO-Sm_2O_3-$5TiO_2$ by indentation and scratch methods. *J Adv Ceram* 2023, **12**: 1136-1165.

[27] Bu Y, Su Z, Huang J*, et al.*, Activating deformation twinning in cubic boron nitride. *Nat Mater* 2025, **24**: 361-368.

[28] Deforming brittle materials. *Nat Mater* 2023, **22**: 1161-1161.

[29] Fan M, Wen T, Chen S*, et al.*, Perspectives toward damage-tolerant nanostructure ceramics. *Adv Sci* 2024, **11**: 2309834.

[30] Li Y, Liu X, Zhang P*, et al.*, Theoretical insights into the Peierls plasticity in $SrTiO_3$ ceramics via dislocation remodelling. *Nat Commun* 2022, **13**: 6925.

[31] Zhang J, Liu G, Cui W*, et al.*, Plastic deformation in silicon nitride ceramics via bond switching at coherent interfaces. *Science* 2022, **378**: 371-376.

[32] Tao Z, Zheng P, Dong G*, et al.*, The mechanical behaviors in oxides: Beyond brittleness. *Adv Mater* 2026, e15834.

[33] Zhao J, Xu Z, Yan Z*, et al.*, Stacking faults toughened SiC ceramics formed by FSPS induced grain deformation. *J Eur Ceram Soc* 2025, **45**: 117499.

[34] Goel S, Yan J, Luo X*, et al.*, Incipient plasticity in 4H-SiC during quasistatic nanoindentation. *J Mech Behav Biomed Mater* 2014, **34**: 330-337.

[35] Tomastik J, Ctvrtlik R, Ingr T*, et al.*, Effect of nitrogen doping and temperature on mechanical durability of silicon carbide thin films. *Sci Rep* 2018, **8**: 10428.

[36] An Q and Goddard W A, Atomistic origin of brittle failure of boron carbide from large-scale reactive dynamics simulations: Suggestions toward improved ductility. *Phys Rev Lett* 2015, **115**: 105501.

[37] Qu R T and Zhang Z F, A universal fracture criterion for high-strength materials. *Sci Rep* 2013, **3**: 1117.

[38] Qiang S, Wu F, Liu H*, et al.*, Integration of high strength, flexibility, and room-temperature plasticity in ceramic nanofibers. *Nat Commun* 2025, **16**: 3265.

[39] Li J, Wang X, Guo S*, et al.*, Recent progress in the fabrication strategies and toughening mechanism of flexible ceramics and their applications. *J Mater Chem C* 2024, **12**: 17742-17788.

[40] C1421-18 A, Standard test methods for determination of fracture toughness of advanced ceramics at ambient temperature, ASTM International, West Conshohocken, PA, USA, 2025.

[41] Gavalda-Diaz O, Saiz E, Chevalier J*, et al.*, Toughening of ceramics and ceramic composites through microstructure engineering: A review. *Int Mater Rev* 2025, **70**: 3-30.

[42] Hu J, Yang Q, Zhu S*, et al.*, Superhard bulk high-entropy carbides with enhanced toughness via metastable in-situ particles. *Nat Commun* 2023, **14**: 5717.

[43] Zhu Z, Liu Y, Qin Y*, et al.*, Tough and strong bioinspired high-entropy all-ceramics with a contiguous network structure. *Nat Commun* 2025, **16**: 4587.

[44] Yang Z, Zhang X, Jin J*, et al.*, Embedding two dimensional Al_2O_3 platelets array into YSZ ceramics for high-temperature applications. *Nat Commun* 2026, **17**: 2988.

[45] Huang Y and Jiang J, A critical review of von Mises criterion for compatible deformation of polycrystalline materials. *Crystals* 2023, **13**: 244.

[46] Gilman J J and Johnston W G, Observations of dislocation glide and climb in lithium fluoride crystals. *J Appl Phys* 1956, **27**: 1018-1022.

[47] Johnston W G and Gilman J J, Dislocation velocities, dislocation densities, and plastic flow in lithium fluoride crystals. *J Appl Phys* 1959, **30**: 129-144.

[48] Amodeo J, Merkel S, Tromas C*, et al.*, Dislocations and plastic deformation in MgO crystals: A review. *Crystals* 2018, **8**: 240.

[49] Brunner D, Taeri-Baghbadrani S, Sigle W*, et al.*, Surprising results of a study on the plasticity in strontium titanate. *J Am Ceram Soc* 2001, **84**: 1161-1163.

[50] Stich S, Ding K, Muhammad Q K*, et al.*, Room-temperature dislocation plasticity in $SrTiO_3$ tuned by defect chemistry. *J Am Ceram Soc* 2022, **105**: 1318-1329.

[51] Liu T S and Li C H, Plasticity of barium fluoride single crystals. *J Appl Phys* 1964, **35**: 3325-3330.

[52] Fang X, Preuß O, Breckner P*, et al.*, Engineering dislocation-rich plastic zones in ceramics via room-temperature scratching. *J Am Ceram Soc* 2023, **106**: 4540-4545.

[53] Salamania J, Sangiovanni D G, Kraych A*, et al.*, Elucidating dislocation core structures in titanium nitride through high-resolution imaging and atomistic simulations. *Mater Des* 2022, **224**: 111327.

[54] Li P and Howe J M, Dislocation reactions in ZrN. *Acta Mater* 2002, **50**: 4231-4239.

[55] Weng S, Yue X, Fu T*, et al.*, Incipient plasticity and dislocation loop evolution in rock-salt vanadium nitride. *Ceram Int* 2020, **46**: 11169-11178.

[56] Hoo C M, Men D, Taherabadi L*, et al.*, Grain-boundary sliding in a superplastic three-phase alumina-zirconia-mullite ceramic composite. *J Am Ceram Soc* 2011, **94**: 2171-2180.

[57] Wakai F, Sakaguchi S and Matsuno Y, Superplasticity of yttria-stabilized tetragonal ZrO_2 polycrystals. *Adv Ceram Mater* 1986, **1**: 259-263.

[58] Nieh T G, McNally C M and Wadsworth J, Superplastic properties of a fine-grained yttria-stabilized tetragonal polycrystal of zirconia. *Scr Metall* 1988, **22**: 1297-1300.

[59] Ashby M F, Boundary defects, and atomistic aspects of boundary sliding and diffusional creep. *Surf Sci* 1972, **31**: 498-542.

[60] Clarisse L, Bataille A, Pennec Y*, et al.*, Investigation of grain boundary sliding during superplastic deformation of a fine-grained alumina by atomic force microscopy. *Ceram Int* 1999, **25**: 389-394.

[61] Addad A, Crampon J, Guinebretière R*, et al.*, Grain boundary sliding-induced deformation in a 30 wt% zirconia–spinel composite: Influence of stress. *J Eur Ceram Soc* 2000, **20**: 2063-2068.

[62] Flacher O and Blandin J J, Grain boundary sliding contribution to superplastic deformation in alumina–zirconia composites. *J Mater Sci* 1997, **32**: 3451-3456.

[63] Dusza J, Kovalčík J, Hvizdoš P*, et al.*, Creep behavior of a carbon-derived Si_3N_4/SiC nanocomposite. *J Eur Ceram Soc* 2004, **24**: 3307-3315.

[64] Langdon T G, Grain-boundary sliding in ceramics. *J Am Ceram Soc* 1972, **55**: 430-430.

[65] Bell R L and Thompson N B W, Grain-boundary sliding. *Nature* 1962, **193**: 363-364.

[66] Yang G and Park S-J, Deformation of single crystals, polycrystalline materials, and thin films: A review. *Materials* 2019, **12**: 2003.

[67] Liu S, Kent D, Doan N*, et al.*, Effects of deformation twinning on the mechanical properties of biodegradable Zn-Mg alloys. *Bioact Mater* 2019, **4**: 8-16.

[68] Scott W D, Deformation twinning in ceramics, in *Deformation of Ceramic Materials II*, Springer US, Boston, MA, 1984, pp. 235-249.

[69] Scott W D and Orr K K, Rhombohedral twinning in alumina. *J Am Ceram Soc* 1983, **66**: 27-32.

[70] Zhang H, Gu H, Jetter J*, et al.*, Size-dependence of zirconia-based ceramics via deformation twinning. *Extreme Mech Lett* 2021, **42**: 101124.

[71] Masuda H and Yoshida H, Surface plasticity and dislocation structures in oxide ceramics subjected to shot peening. *Materialia* 2026, **46**: 102728.

[72] Huang C, Yang B, Peng X*, et al.*, Plastic deformation and hardening mechanisms of a nano-twinned cubic boron nitride ceramic. *ACS Appl Mater Interfaces* 2020, **12**: 50161-50175.

[73] Tromas C, Parent S, Sylvain W*, et al.*, Nanoindentation-induced deformation twinning in MAX phase Ti_2AlN. *Acta Mater* 2022, **227**: 117665.

[74] Edalati K, Hidalgo-Jiménez J, Nguyen T T*, et al.*, Severe plastic deformation of ceramics by high-pressure torsion: Review of principles and applications. *Annu Rev Mater Res* 2025, **55**: 89-124.

[75] Tavakoli K S and Mirzadeh H, A simple kinetics model for strain-induced martensitic transformation in metastable austenitic stainless steels. *J Mater Res Technol* 2026, **41**: 5216-5222.

[76] Garvie R C, Hannink R H and Pascoe R T, Ceramic steel? *Nature* 1975, **258**: 703-704.

[77] Liens A, Reveron H, Douillard T*, et al.*, Phase transformation induces plasticity with negligible damage in ceria-stabilized zirconia-based ceramics. *Acta Mater* 2020, **183**: 261-273.

[78] Zheng W, Shi Y, Zhao L*, et al.*, Realizing reversible phase transformation of shape memory ceramics constrained in aluminum. *Nat Commun* 2023, **14**: 7103.

[79] Li J, Zhang Y, Fu Y*, et al.*, Twin toughening-driven martensitic transformation strategy synergistic improvement for plasticity-thermal shock resistance of (Hf─Zr─Ti)C ceramic coating in severe thermal environments. *Adv Sci* 2025, **12**: 2503226.

[80] Falk M L and Langer J S, Deformation and failure of amorphous, solidlike materials. *Annu Rev Condens Matter Phys* 2011, **2**: 353-373.

[81] Tanguy A, Elasto-plastic behavior of amorphous materials: A brief review. *C R Phys* 2021, **22**: 117-133.

[82] Lacroix R, Kermouche G, Teisseire J*, et al.*, Plastic deformation and residual stresses in amorphous silica pillars under uniaxial loading. *Acta Mater* 2012, **60**: 5555-5566.

[83] Lee K, Yang Y, Ding L*, et al.*, Plasticity of borosilicate glasses under uniaxial tension. *J Am Ceram Soc* 2020, **103**: 4295-4303.

[84] Zehnder C, Bruns S, Peltzer J-N*, et al.*, Influence of cooling rate on cracking and plastic deformation during impact and indentation of borosilicate glasses. *Front Mater* 2017, **4**: 5.

[85] Simmons J H, Ochoa R, Simmons K D*, et al.*, Non-Newtonian viscous flow in soda-lime-silica glass at forming and annealing temperatures. *J Non-Cryst Solids* 1988, **105**: 313-322.

[86] Janakiraman N and Aldinger F, Indentation analysis of elastic and plastic deformation of precursor-derived Si–C–N ceramics. *J Eur Ceram Soc* 2010, **30**: 775-785.

[87] Wang J, Wang S, Yang Y*, et al.*, Nanostructured amorphous Al_2O_3-ZrO_2 (La_2O_3) ceramics with plastic deformation via interface inducing hierarchical shear bands. *Int J Plast* 2024, **181**: 104103.

[88] Tang H, Cheng Y, Yuan X*, et al.*, Toughening oxide glasses through paracrystallization. *Nat Mater* 2023, **22**: 1189-1195.

[89] Barsoum M W, Farber L and El-Raghy T, Dislocations, kink bands, and room-temperature plasticity of Ti_3SiC_2. *Metall Mater Trans A* 1999, **30**: 1727-1738.

[90] Barsoum M W, Zhen T, Kalidindi S R*, et al.*, Fully reversible, dislocation-based compressive deformation of Ti_3SiC_2 to 1 GPa. *Nat Mater* 2003, **2**: 107-111.

[91] Li S and Zhai H, A Soft Ceramic Ti_3SiC_2 with Microscale Plasticity at Room Temperature. *Key Eng Mater* 2007, **280-283**: 1343-1346.

[92] Xu H, Ji W, Jiang J*, et al.*, Contribution of boundary non-stoichiometry to the lower-temperature plasticity in high-pressure sintered boron carbide. *Nat Commun* 2023, **14**: 4889.

[93] Aoki Y, Masuda H, Tochigi E*, et al.*, Overcoming the intrinsic brittleness of high-strength Al_2O_3–$GdAlO_3$ ceramics through refined eutectic microstructure. *Nat Commun* 2024, **15**: 8700.

[94] Gao X X, Liu C, Gu X*, et al.*, Creating high plasticity in hard ceramics via coherent twin boundary migration-driven detwinning. *Nano Lett* 2026, **26**: 7655-7664.

[95] Zhao L, Guan W, Xu J*, et al.*, Atomistic investigation of effect of twin boundary on machinability in diamond cutting of nanocrystalline 3C-SiC. *AIMS Mater Sci* 2024, **11**: 1149-1164.

[96] Kondo S, Shibata N, Mitsuma T*, et al.*, Dynamic observations of dislocation behavior in $SrTiO_3$ by in situ nanoindentation in a transmission electron microscope. *Appl Phys Lett* 2012, **100**: 181906.

[97] Fang X, Ding K, Janocha S*, et al.*, Nanoscale to microscale reversal in room-temperature plasticity in $SrTiO_3$ by tuning defect concentration. *Scr Mater* 2020, **188**: 228-232.

[98] Coble R L, A model for boundary diffusion controlled creep in polycrystalline materials. *J Appl Phys* 1963, **34**: 1679-1682.

[99] Ashby M F and Verrall R A, Diffusion-accommodated flow and superplasticity. *Acta Metall* 1973, **21**: 149-163.

[100] Lagerlof K P D, Mitchell T E and Heuer A H, Deformation and Diffusion in Sapphire(α-Al_2O_3), in *Deformation of Ceramic Materials II*, Springer US, Boston, MA, 1984, pp. 199-212.

[101] Chen M, McCauley J W and Hemker K J, Shock-induced localized amorphization in boron carbide. *Science* 2003, **299**: 1563-1566.

[102] An Q and Goddard W A, III, Nanotwins soften boron-rich boron carbide ($B_{13}C_2$). *Appl Phys Lett* 2017, **110**: 111902.

[103] Reddy K M, Guo D, Song S*, et al.*, Dislocation-mediated shear amorphization in boron carbide. *Sci Adv* 2021, **7**: eabc6714.

[104] Li J, Luo K and An Q, Activating mobile dislocation in boron carbide at room temperature via Al doping. *Phys Rev Lett* 2023, **130**: 116104.

[105] Fujita S, Maeda K and Hyodo S, Dislocation glide motion in 6H SiC single crystals subjected to high-temperature deformation. *Philos Mag A* 1987, **55**: 203-215.

[106] Nixon R D and Davis R F, Diffusion-accommodated grain boundary sliding and dislocation glide in the creep of sintered alpha silicon carbide. *J Am Ceram Soc* 1992, **75**: 1786-1795.

[107] Matsumoto M, Huang H, Harada H*, et al.*, On the phase transformation of single-crystal 4H–SiC during nanoindentation. *J Phys D: Appl Phys* 2017, **50**: 265303.

[108] Lankford J, Page R A and Rabenberg L, Deformation mechanisms in yttria-stabilized zirconia. *J Mater Sci* 1988, **23**: 4144-4156.

[109] Zhang N and Asle Zaeem M, Competing mechanisms between dislocation and phase transformation in plastic deformation of single crystalline yttria-stabilized tetragonal zirconia nanopillars. *Acta Mater* 2016, **120**: 337-347.

[110] Cho J, Li Q, Wang H*, et al.*, High temperature deformability of ductile flash-sintered ceramics via in-situ compression. *Nat Commun* 2018, **9**: 2063.

[111] Frankberg E J, Lambai A, Zhang J*, et al.*, Exceptional microscale plasticity in amorphous aluminum oxide at room temperature. *Adv Mater* 2023, **35**: 2303142.

[112] Shahbeyk S, Voyiadjis G Z, Habibi V*, et al.*, Review of size effects during micropillar compression test: Experiments and atomistic simulations. *Crystals* 2019, **9**: 591.

[113] Liu X D, Nagumo M and Umemoto M, The Hall-Petch relationship in nanocrystalline materials. *Mater Trans JIM* 1997, **38**: 1033-1039.

[114] Shibutani Y, Matsunaka D and Tarumi R, Plastic strain and temperature dependences of Hall-Petch effect. *J Soc Mater Sci, Jpn* 2024, **61**: 724-729.

[115] Tian Y, Xu B, Yu D*, et al.*, Ultrahard nanotwinned cubic boron nitride. *Nature* 2013, **493**: 385-388.

[116] Ryou H, Drazin J W, Wahl K J*, et al.*, Below the Hall-Petch limit in nanocrystalline ceramics. *ACS Nano* 2018, **12**: 3083-3094.

[117] Zhou S, Yuan J, Wu H*, et al.*, Size-dependent uniform deformation transitions enabling hardness and toughness enhancement of nanocrystalline Cr_2AlC MAX phase. *J Mater Sci Technol* 2025, **232**: 170-180.

[118] Yuan J, Zhou S, Wu H*, et al.*, Ultrahigh strength-ductility of nanocrystalline Cr_2AlC coating under micropillar compression. *Scr Mater* 2023, **235**: 115594.

[119] Camposilvan E and Anglada M, Size and plasticity effects in zirconia micropillars compression. *Acta Mater* 2016, **103**: 882-892.

[120] Zhu T T, Bushby A J and Dunstan D J, Size effect in the initiation of plasticity for ceramics in nanoindentation. *J Mech Phys Solids* 2008, **56**: 1170-1185.

[121] Yilmaz H and Derby B, Unifying the size effect observed in micropillar compression experiments. *Philos Mag* 2024, **104**: 482-498.

[122] Ussui V, Lazar D, Lima N*, et al.*, Room temperature plasticity of zirconia-yttria-titania ceramics: Experimental indications and structural modelling. *Process Appl Ceram* 2022, **16**: 367-373.

[123] Zhang S, Li Y, Tochigi E*, et al.*, Formation of a one-dimensional dislocation loop array in wurtzite zinc oxide at ambient temperature. *J Mater Sci Technol* 2026, **269**: 173-182.

[124] Tanabe M, Tatami J, Iijima M*, et al.*, Deformation behaviors and fracture strength of β-Si_3N_4 single crystals. *J Am Ceram Soc* 2023, **106**: 5431-5439.

[125] Piao Y, Li C, Hu Y*, et al.*, Nanoindentation induced anisotropy of deformation and damage behaviors of MgF_2 crystals. *J Mater Res Technol* 2024, **28**: 4615-4625.

[126] Kadota N, Taniguchi K, Kishida K*, et al.*, Room-temperature plastic deformation of single crystals of high-purity β-silicon nitride investigated by micropillar compression. *J Am Ceram Soc* 2025, **108**: e70161.

[127] Pan X, Zhu Y and Wu H, Twist-activated universal kink deformations enabling high plasticity in layered boron nitride ceramic. *ACS Appl Mater Interfaces* 2025, **17**: 64006-64014.

[128] Han X D, Zhang Y F, Zheng K*, et al.*, Low-temperature in situ large strain plasticity of ceramic SiC nanowires and its atomic-scale mechanism. *Nano Lett* 2007, **7**: 452-457.

[129] Fang X, Nakamura A and Rödel J, Deform to perform: Dislocation-tuned properties of ceramics. *Am Ceram Soc Bull* 2023, **102**: 24-29.

[130] Oshima Y, Nakamura A and Matsunaga K, Extraordinary plasticity of an inorganic semiconductor in darkness. *Science* 2018, **360**: 772-774.

[131] Ji C, Chen Q, Hu Z*, et al.*, Research on plastic deformation and machinability of zone-melted N-type bismuth telluride thermoelectric materials. *Scr Mater* 2025, **261**: 116630.

[132] Shi X, Chen H, Hao F*, et al.*, Room-temperature ductile inorganic semiconductor. *Nat Mater* 2018, **17**: 421-426.

[133] Wei T, Jin M, Wang Y*, et al.*, Exceptional plasticity in the bulk single-crystalline van der Waals semiconductor InSe. *Science* 2020, **369**: 542-545.

[134] Sun Y, Ma Y, Zhang J*, et al.*, Van der Waals semiconductor InSe plastifies by martensitic transformation. *Sci Adv* 2024, **10**: eado9593.

[135] Deng T, Gao Z, Qiu P*, et al.*, Plastic/ductile bulk 2D van der Waals single-crystalline $SnSe_2$ for flexible thermoelectrics. *Adv Sci* 2022, **9**: 2203436.

[136] Yang Q, Yang S, Qiu P*, et al.*, Flexible thermoelectrics based on ductile semiconductors. *Science* 2022, **377**: 854-858.

[137] Deng T, Gao Z, Li Z*, et al.*, Room-temperature exceptional plasticity in defective Bi_2Te_3-based bulk thermoelectric crystals. *Science* 2024, **386**: 1112-1117.

[138] Li Z, Deng T, Qiu P*, et al.*, Plasticity of Bi_2Te_3-family thermoelectric crystals. *Nat Commun* 2025, **16**: 5190.

[139] Wu X and Mori T, Sub-lattice amorphization as a new driver of room temperature plasticity in inorganic semiconductors. *The Innovation* 2025, **6**: 100891.

[140] Gao Z, Yang S, Ma Y*, et al.*, Warm metalworking for plastic manufacturing in brittle semiconductors. *Nat Mater* 2025, **24**: 1538-1544.

[141] Gao Z, Wei T, Deng T*, et al.*, High-throughput screening of 2D van der Waals crystals with plastic deformability. *Nat Commun* 2022, **13**: 7491.

[142] Peng L, Yang S, Wei T-R*, et al.*, Phase-modulated mechanical and thermoelectric properties of $Ag_2S_{1-x}Te_x$ ductile semiconductors. *J Materiomics* 2022, **8**: 656-661.

[143] Yang S, Gao Z, Qiu P*, et al.*, Ductile $Ag_{20}S_7Te_3$ with excellent shape-conformability and high thermoelectric performance. *Adv Mater* 2021, **33**: 2007681.

[144] Gao Z, Yang Q, Qiu P*, et al.*, p-type plastic inorganic thermoelectric materials. *Adv Energy Mater* 2021, **11**: 2100883.

[145] Liang J, Liu J, Qiu P*, et al.*, Modulation of the morphotropic phase boundary for high-performance ductile thermoelectric materials. *Nat Commun* 2023, **14**: 8442.

[146] Qiu P, Deng T, Chen L*, et al.*, Plastic inorganic thermoelectric materials. *Joule* 2024, **8**: 622-634.

[147] Bouchbinder E, Langer J S and Procaccia I, Athermal shear-transformation-zone theory of amorphous plastic deformation. I. Basic principles. *Phys Rev E* 2007, **75**: 036107.

[148] Csanádi T, Castle E, Reece M J*, et al.*, Strength enhancement and slip behaviour of high-entropy carbide grains during micro-compression. *Sci Rep* 2019, **9**: 10200.

[149] Sangiovanni D G, Mellor W, Harrington T*, et al.*, Enhancing plasticity in high-entropy refractory ceramics via tailoring valence electron concentration. *Mater Des* 2021, **209**: 109932.

[150] Han Y, Liu X, Zhang Q*, et al.*, Ultra-dense dislocations stabilized in high entropy oxide ceramics. *Nat Commun* 2022, **13**: 2871.

[151] Wang X, Cortez J, Dupuy A D*, et al.*, High entropy oxide (Co,Cu,Mg,Ni,Zn)O exhibits grain size dependent room temperature deformation. *Mater Res Lett* 2023, **11**: 196-204.

[152] Bian H, He Q, Luan J*, et al.*, Liquefaction-induced plasticity from entropy-boosted amorphous ceramics. *Applied Materials Today* 2021, **23**: 101011.

[153] Zhang X, Zeng Z, Zeng X*, et al.*, Hardening mechanism and plastic deformation behavior in super-hard AlCrNbSiTiN high-entropy nitride nanocomposite coatings. *Mater Res Lett* 2025, **13**: 103-112.

[154] Barsoum M, *MAX phases: Properties of machinable ternary carbides and nitrides*. John Wiley & Sons., 2013.

[155] Barsoum M W, The $M_{N+1}AX_N$ phases: A new class of solids: Thermodynamically stable nanolaminates. *Prog Solid State Chem* 2000, **28**: 201-281.

[156] Ion A, Sallot P, Badea V*, et al.*, The dual character of MAX phase nano-layered structure highlighted by supersonic particles deposition. *Coatings* 2021, **11**: 1038.

[157] Zhang Z, Duan X, Jia D*, et al.*, On the formation mechanisms and properties of MAX phases: A review. *J Eur Ceram Soc* 2021, **41**: 3851-3878.

[158] Radovic M and Barsoum M W, MAX phases: Bridging the gap between metals and ceramics, 2013, pp. 20-27.

[159] Barsoum M W and Radovic M, Elastic and mechanical properties of the MAX phases. *Annu Rev Mater Res* 2011, **41**: 195-227.

[160] Alam M S, Chowdhury M A, Khandaker T*, et al.*, Advancements in MAX phase materials: Structure, properties, and novel applications. *RSC Adv* 2024, **14**: 26995-27041.

[161] Barsoum M W and El-Raghy T, Synthesis and characterization of a remarkable ceramic: Ti_3SiC_2. *J Am Ceram Soc* 1996, **79**: 1953-1956.

[162] Zhang Z F, Sun Z M, Zhang H*, et al.*, Micron-scale deformation and damage mechanisms of Ti_3SiC_2 crystals induced by indentation. *Adv Eng Mater* 2004, **6**: 980-983.

[163] Clarkin D, Naik Parrikar P and Shukla A, Dynamic response of TI_2AlC under radial confinement at high temperature. *J Dyn Behav Mater* 2017, **3**: 461-473.

[164] Hossain R and Ogata S, Unveiling kink band formation mechanism in MAX phases. *Commun Mater* 2025, **6**: 51.

[165] Lei X W and Nakatani A, Analysis of kink deformation and delamination behavior in layered ceramics. *J Eur Ceram Soc* 2016, **36**: 2311-2317.

[166] Gavalda-Diaz O, Lyons J, Wang S*, et al.*, Basal plane delamination energy measurement in a Ti_3SiC_2 MAX phase. *JOM* 2021, **73**: 1582-1588.

[167] Tang Z, Zhu L, Hua D*, et al.*, Achieving cryogenic wear resistance of MoS_2 beyond conventional lubricity: An atomistic simulation study. *Tribol Int* 2026, **221**: 112053.

[168] Ye W, Li S, Li Y*, et al.*, Bioinspired design of extraordinary wear-resistant graphene/CoCrNi multi-principal element alloy composites. *cMat* 2026, **3**: e70034.

[169] Jia Q, Li J, Zhou Z*, et al.*, Nanowear of Zr-based metallic glasses regulated by cooling rate-induced heterogeneity. *Int J Mech Sci* 2026, **321**: 111666.

[170] Zhang Z, Yang B, Chen L*, et al.*, Oxygen vacancy-induced strengthening and toughening in $(K,Na)NbO_3$-based piezoceramics revealed via nanoindentation. *Nat Commun* 2025, **16**: 7015.

[171] Khan S A, Ahmed T, Park H W*, et al.*, Effects of B- and A/B-sites codoping on lattice distortion and defect concentration for high electromechanical response of lead-free piezoelectrics. *Acta Mater* 2024, **278**: 120262.

[172] Wu Z, Zhu X, Shen Y*, et al.*, High-entropy MAX phase with ultrahigh strength and large plasticity mediated by local chemical fluctuations. *Mater Today* 2024, **80**: 61-73.

[173] Dash A, Liu Y-c, Yoshida H*, et al.*, Electroplasticity of metals and ceramics: Current status. *Annu Rev Mater Res* 2025, **55**: 151-174.

[174] Pan S, Shao G, He H*, et al.*, Effects of strain rate and current density on plastic deformation of zirconia ceramics under a high electric field. *Ceram Int* 2023, **49**: 27758-27763.

[175] Shen Z, Peng H and Nygren M, Formidable increase in the superplasticity of ceramics in the presence of an electric field. *Adv Mater* 2003, **15**: 1006-1009.

[176] Luo J, Xi C, Gu Y*, et al.*, Superplastic forging for sialon-based nanocomposite at ultralow temperature in the electric field. *Sci Rep* 2019, **9**: 2452.

[177] Domínguez-Rodríguez A, Gómez-García D, Castillo-Rodríguez M*, et al.*, Superplasticity in nanocrystalline ceramics: pure grain boundary phenomena or not? *Int J Mater Res* 2010, **101**: 1215-1221.

[178] Winnubst A J A, Boutz M M R, He Y J*, et al.*, Plasticity of nanocrystalline zirconia ceramics and composites. *Ceram Int* 1997, **23**: 215-221.

[179] Castro R H R, On the thermodynamic stability of nanocrystalline ceramics. *Mater Lett* 2013, **96**: 45-56.

[180] Wu Y, Zhang Y, Zhang S*, et al.*, The rise of plastic deformation in boron nitride ceramics. *Sci China Mater* 2021, **64**: 46-51.

[181] Kumar S and Le Ferrand H, Nacre-like ceramic–metal composites: State-of-the-art, challenges, and opportunities. *J Am Ceram Soc* 2025, **108**: e20623.

[182] Shen X, Nie B, Tang H*, et al.*, Nacre-inspired Si_3N_4/h-BN layered ceramics with enhanced tribological performance. *Mater Lett* 2026, **402**: 139203.

[183] Zhang C, Cao K, Luo J*, et al.*, Unveiling the microscopic origins of dual-phase $HfTaC_2$/W ceramics with enhanced plasticity. *Sci China Technol Sci* 2026, **69**: 1320204.

[184] Awaji H, Choi S-M and Yagi E, Mechanisms of toughening and strengthening in ceramic-based nanocomposites. *Mech Mater* 2002, **34**: 411-422.

[185] Huang Y, Chen Z, Meindlhumer M*, et al.*, Harvesting superior intrinsic plasticity in nitride ceramics with negative stacking fault energy. *Acta Mater* 2025, **286**: 120774.

[186] Lorentzon M, Sangiovanni D G, Takata N*, et al.*, Metal-like ductility and high hardness in nitrogen-rich HfN thin films by point defect superstructuring. *Commun Mater* 2025, **6**: 46.

[187] Rahimizadeh A, Yazdani Sarvestani H, Li L*, et al.*, Engineering toughening mechanisms in architectured ceramic-based bioinspired materials. *Mater Des* 2021, **198**: 109375.

[188] Wei B, Li L, Shao L*, et al.*, Crystalline–amorphous nanostructures: microstructure, property and modelling. *Materials* 2023, **16**: 2874.

[189] Cui Y, Huang P, Wang F*, et al.*, The hardness and related deformation mechanisms in nanoscale crystalline–amorphous multilayers. *Thin Solid Films* 2015, **584**: 270-276.

[190] Yang C, Liang Y, Zhou L*, et al.*, Strengthening mechanism and plasticity deformation of crystalline/amorphous Cu_3Fe/Fe_3Cu nanolayered composite. *Physica B: Condensed Matter* 2023, **668**: 415269.

[191] Zhang J Y, Liu G and Sun J, Crystallization-aided extraordinary plastic deformation in nanolayered crystalline Cu/amorphous Cu-Zr micropillars. *Sci Rep* 2013, **3**: 2324.

[192] Maehara Y and Langdon T G, Superplasticity in ceramics. *J Mater Sci* 1990, **25**: 2275-2286.

[193] Gust M, Goo G, Wolfenstine J*, et al.*, Influence of amorphous grain boundary phases on the superplastic behavior of 3-mol%-yttria-stabilized tetragonal zirconia polycrystals (3Y-TZP). *J Am Ceram Soc* 1993, **76**: 1681-1690.

[194] Dou L, Yang B, Ye X*, et al.*, Flexible high-entropy functional ceramics. *Nat Commun* 2025, **16**: 5915.

[195] Janus F, Kinoshita R, Li R*, et al.*, A nanoindentation study on the room-temperature plasticity in titanium dioxide bicrystals. *J Am Ceram Soc* 2025, **108**: e20593.

[196] Li P, Li J, Feng Q*, et al.*, Unveiling high ductility in boron carbide crystal at room temperature. *Sci Adv* 2025, **11**: eadr4648.

[197] Huang J, Chen Y, Su Z*, et al.*, Size-dependent plasticity in titanium carbide mediated by dislocation at room temperature. *J Alloys Compd* 2025, **1018**: 179259.

[198] Fang X, Porz L, Ding K*, et al.*, Bridging the gap between bulk compression and indentation test on room-temperature plasticity in oxides: Case study on $SrTiO_3$. *Crystals* 2020, **10**: 933.

[199] Li J, Cho J, Ding J*, et al.*, Nanoscale stacking fault–assisted room temperature plasticity in flash-sintered TiO_2. *Sci Adv* 2019, **5**: eaaw5519.

[200] Wang C, Li Z, Cheng Y*, et al.*, Reversible shuffle twinning yields anisotropic tensile superelasticity in ceramic GeSe. *Nat Nanotechnol* 2025, **20**: 732-739.

[201] Huang J Y, Zhong L, Wang C M*, et al.*, In situ observation of the electrochemical lithiation of a single SnO_2 nanowire electrode. *Science* 2010, **330**: 1515-1520.

[202] Kushima A, Huang J Y and Li J, Quantitative fracture strength and plasticity measurements of lithiated silicon nanowires by *in situ* TEM tensile experiments. *ACS Nano* 2012, **6**: 9425-9432.

[203] Korte-Kerzel S, Microcompression of brittle and anisotropic crystals: recent advances and current challenges in studying plasticity in hard materials. *MRS Commun* 2017, **7**: 109-120.

[204] Uchic M D, Dimiduk D M, Florando J N*, et al.*, Sample dimensions influence strength and crystal plasticity. *Science* 2004, **305**: 986-989.

[205] El-Awady J A, Woodward C, Dimiduk D M*, et al.*, Effects of focused ion beam induced damage on the plasticity of micropillars. *Phys.l Rev. B* 2009, **80**: 104104.

[206] Greer J R and De Hosson J T M, Plasticity in small-sized metallic systems: Intrinsic versus extrinsic size effect. *Prog Mater Sci* 2011, **56**: 654-724.

[207] Oliver W C and Pharr G M, An improved technique for determining hardness and elastic modulus using load and displacement sensing indentation experiments. *J Mater Res* 1992, **7**: 1564-1583.

[208] Nix W D and Gao H, Indentation size effects in crystalline materials: A law for strain gradient plasticity. *J Mech Phys Solids* 1998, **46**: 411-425.

[209] Fang X, Bishara H, Ding K*, et al.*, Nanoindentation pop-in in oxides at room temperature: Dislocation activation or crack formation? *J Am Ceram Soc* 2021, **104**: 4728-4741.

[210] C1161-18 A, Standard test method for flexural strength of advanced ceramics at ambient temperature, ASTM International, 2018.

[211] C1273-18 A, Standard test method for tensile strength of monolithic advanced ceramics at ambient temperatures, ASTM International, 2018.

[212] C1683-10 A, Standard practice for size scaling of tensile strengths using Weibull statistics for advanced ceramics, ASTM International, 2024.

[213] Ni D, Cheng Y, Zhang J*, et al.*, Advances in ultra-high temperature ceramics, composites, and coatings. *J Adv Ceram* 2022, **11**: 1-56.

[214] Zhang S, Zhang J, Wang X*, et al.*, Preparation, mechanical, and thermal properties of $CrNbO_4$: A novel dual-functional scale to protect RHEAs from oxidation and thermal attack. *J Adv Ceram* 2025, **14**: 9221100.

[215] Bai L, Gao X, Li Y*, et al.*, A deep insight into the additively manufactured ceramics for aerospace applications. *ChemPhysMater* 2026, **5**: 1-21.

[216] Muktinutalapati N R, Materials for gas turbines – An overview, in *Advances in Gas Turbine Technology*, IntechOpen, London, 2011.

[217] Clarke D R and Levi C G, Materials design for the next generation thermal barrier coatings. *Annu Rev Mater Res* 2003, **33**: 383-417.

[218] Naslain R, Design, preparation and properties of non-oxide CMCs for application in engines and nuclear reactors: An overview. *Compos Sci Technol* 2004, **64**: 155-170.

[219] Zok F W, Ceramic-matrix composites enable revolutionary gains in turbine engine efficiency. *Am Ceram Soc Bull* 2016, **95**: 22-28.

[220] Richerson D W, Historical review of addressing the challenges of use of ceramic components in gas turbine engines, ASME Turbo Expo 2006: Power for Land, Sea, and Air, 2006, pp. 241-254.

[221] Shvydyuk K O, Lanceros-Mendez S and Silva A P, Advanced ceramics in aerospace and defense: The interrelationship between traditional and additive manufacturing approaches. *Adv Mater Technol-US* 2026, **11**: e01012.

[222] Yan Z, Gao Y and Zhang H, Materials development and potential applications of ceramics: New opportunities and challenges. *Appl Sci* 2023, **13**: 10957.

[223] Launey M E and Ritchie R O, On the fracture toughness of advanced materials. *Adv Mater* 2009, **21**: 2103-2110.

[224] Bai R, Sun Q, He Y*, et al.*, Ceramic toughening strategies for biomedical applications. *Fron. bioeng biotechnol* 2022, **10**: 840372.

[225] Shi H Y, Pang R, Yang J*, et al.*, Overview of several typical ceramic materials for restorative dentistry. *Biomed Res Int* 2022, **2022**: 8451445.

[226] Vaiani L, Boccaccio A, Uva A E*, et al.*, Ceramic materials for biomedical applications: An overview on properties and fabrication processes. *J Funct Biomater* 2023, **14**: 146.

[227] Budharaju H, Suresh S, Sekar M P*, et al.*, Ceramic materials for 3D printing of biomimetic bone scaffolds – Current state-of-the-art & future perspectives. *Mater Des* 2023, **231**: 112064.

[228] Yu C S and Shetty D K, Transformation yielding, plasticity and crack-growth-resistance (R-curve) behaviour of CeO_2-TZP. *J Mater Sci* 1990, **25**: 2025-2035.

[229] Bose S and Tarafder S, Calcium phosphate ceramic systems in growth factor and drug delivery for bone tissue engineering: A review. *Acta Biomater* 2012, **8**: 1401-1421.

[230] Zhao H, Liu S, Wei Y*, et al.*, Multiscale engineered artificial tooth enamel. *Science* 2022, **375**: 551-556.

[231] Bouville F, Maire E, Meille S*, et al.*, Strong, tough and stiff bioinspired ceramics from brittle constituents. *Nat Mater* 2014, **13**: 508-514.

[232] Wegst U G K, Bai H, Saiz E*, et al.*, Bioinspired structural materials. *Nat Mater* 2015, **14**: 23-36.

[233] George S M, Nayak C, Singh I*, et al.*, Multifunctional hydroxyapatite composites for orthopedic applications: A review. *ACS Biomater-Sci Eng* 2022, **8**: 3162-3186.

[234] Oveissi F, Naficy S, Lee A*, et al.*, Materials and manufacturing perspectives in engineering heart valves: A review. *Materials Today Bio* 2020, **5**: 100038.

[235] Wang R, Sui J and Wang X, Natural piezoelectric biomaterials: A biocompatible and sustainable building block for biomedical devices. *ACS Nano* 2022, **16**: 17708-17728.

[236] He Z, Behera R P, Gao H*, et al.*, Achieving strength and toughness limits of anisotropic microstructured alumina ceramics through interface engineering. *Mater Horiz* 2026, **13**: 2022-2034.

[237] Ming K, Gu C, Su Q*, et al.*, Strength and plasticity of amorphous ceramics with self-patterned nano-heterogeneities. *Int J Plast* 2020, **134**: 102837.

[238] Kang J, Yu M, Wu Y*, et al.*, Mechanical properties regulation of high-strength and high-toughness ceramic/polymer composites with interpenetrating phase. *Compos Part B: Eng* 2026, **314**: 113443.

[239] Azad E, Yazdani Sarvestani H, Rahmat M*, et al.*, Bioinspired programmable multi-scale surface architectures for toughening ceramic-polymer composites. *Compos Part B: Eng* 2026, **309**: 113049.

[240] Sohail Y, Zhang C, Xue D*, et al.*, Machine-learning design of ductile FeNiCoAlTa alloys with high strength. *Nature* 2025, **643**: 119-124.

[241] Słodczyk I, Frisch A, Fang X*, et al.*, A data-driven quest for room-temperature bulk plastically deformable ceramics. *J Am Ceram Soc* 2026, **109**: e70577.

[242] Freitas R and Cao Y, Machine-learning potentials for crystal defects. *MRS Commun* 2022, **12**: 510-520.

[243] Cheng M, Jiang X, Zhang H*, et al.*, Revealing phonon signature of dislocations in silicon carbide using machine-learning interatomic potential. *Appl Phys Lett* 2025, **127**: 242102.

[244] Feng L, Li W, Tang W*, et al.*, Shock-induced hierarchical plastic deformations in high entropy $(Zr_{0.2}Hf_{0.2}Ti_{0.2}Nb_{0.2}Ta_{0.2})C$ at high strain rate. *Int J Plast* 2026, **196**: 104543.

[245] Lookman T, Balachandran P V, Xue D*, et al.*, Active learning in materials science with emphasis on adaptive sampling using uncertainties for targeted design. *npj Comput Mater* 2019, **5**: 21.

[246] Ament S, Amsler M, Sutherland D R*, et al.*, Autonomous materials synthesis via hierarchical active learning of nonequilibrium phase diagrams. *Sci Adv* 2021, **7**: eabg4930.

[247] Deagen M E, Brinson L C, Vaia R A*, et al.*, The materials tetrahedron has a "digital twin". *MRS Bulletin* 2022, **47**: 379-388.

[248] Papadimitriou I, Gialampoukidis I, Vrochidis S*, et al.*, AI methods in materials design, discovery and manufacturing: A review. *Comput Mater Sci* 2024, **235**: 112793.

[249] Wang J, Ghosh D B and Zhang Z, Computational materials design for ceramic nuclear waste forms using machine learning, first-principles calculations, and kinetics rate theory. *Materials* 2023, **16**: 4985.

[250] Cheng M, Fu C, Okabe R*, et al.*, AI-driven materials design: a mini-review. *arXiv preprint arXiv:2502.02905* 2025,

[251] Montes de Oca Zapiain D, Stewart J A and Dingreville R, Accelerating phase-field-based microstructure evolution predictions via surrogate models trained by machine learning methods. *npj Comput Mater* 2021, **7**: 3.

[252] Xue T, Gan Z, Liao S*, et al.*, Physics-embedded graph network for accelerating phase-field simulation of microstructure evolution in additive manufacturing. *npj Comput Mater* 2022, **8**: 201.

[253] Zhang J, Xu B, Xiong Y*, et al.*, Design high-entropy carbide ceramics from machine learning. *npj Comput Mater* 2022, **8**: 5.

[254] Leverant C J and Harvey J A, Accelerating the discovery of new, single phase high entropy ceramics via active learning. *Chem Mater* 2024, **36**: 10994-11003.